Е.В. Валеева

Academic Reading for Physicists and Electricians

Северск, 2024

МИНИСТЕРСТВО НАУКИ И ВЫСШЕГО ОБРАЗОВАНИЯ РОССИЙСКОЙ ФЕДЕРАЦИИ
ФЕДЕРАЛЬНОЕ ГОСУДАРСТВЕННОЕ АВТОНОМНОЕ ОБРАЗОВАТЕЛЬНОЕ УЧРЕЖДЕНИЕ ВЫСШЕГО ОБРАЗОВАНИЯ
«Национальный исследовательский ядерный университет «МИФИ»
Северский технологический институт –
филиал федерального государственного автономного образовательного учреждения высшего образования «Национальный исследовательский ядерный университет «МИФИ»
(СТИ НИЯУ МИФИ)

УТВЕРЖДАЮ
И.о. зав. кафедрой иностранных
языков, канд. филол. наук, доцент
________________ Т.Ю. Казанцева
«____»________________2024 г.

Е.В. Валеева

Academic Reading for Physicists and Electricians

Практическое руководство

по курсу «Иностранный язык»
для студентов технических направлений и специальностей

Северск 2024

УДК 811(Англ)
ББК 81.2Англ
В 29

Автор:

Валеева Е. В. – старший преподаватель кафедры «Иностранный язык» СТИ НИЯУ МИФИ;

Рецензент:

Казанцева Т. Ю. – кандидат филологических наук, доцент кафедры «Иностранный язык» СТИ НИЯУ МИФИ

Валеева Е. В.

В 29 Academic Reading for Physicists and Electricians: практическое руководство /Е. В. Валеева; Северский технологический институт НИЯУ МИФИ – Северск: Издательство СТИ НИЯУ МИФИ, 2024. – 174 с. – Текст: электронный

Данное практическое руководство ставит своей задачей обучение чтению и переводу технической литературы на английском языке. С этой целью предлагаются современные статьи по физике и электротехнике, рассматриваются особенности перевода научных статей вместе с элементами анализа. Также имеются таблицы единиц измерений, терминологических сокращений и чтения математических и химических формул и уравнений Ркуоводство предназначено для студентов бакалавриата и магистратуры, а также аспирантов.

Руководство рассмотрено и одобрено на заседании кафедры иностранных языков и рекомендовано к изданию (протокол № 2 от 29 октября 2024 г.).

Издается в соответствии с планом выпуска учебно-методической литературы на 2024 г., утвержденным Ученым Советом СТИ НИЯУ МИФИ.

Рег. № 14/24 от 25.11.2024 г. Редактор М. В. Ворожейкина

Содержание

Введение

В связи с ускоряющимся научно-техническим прогрессом все более востребованным становится перевод технической литературы, такой как сопроводительная техническая документация, инструкции, статьи для международных научных журналов, доклады и презентации выступлений. Поэтому можно уверенно утверждать, что умение переводить технические тексты является необходимым для будущего специалиста.

Наше практическое руководство предназначено для студентов и аспирантов, которые проводят исследовательскую работу в области физики и электротехники, в качестве пособия для чтения специальной научной литературы на английском языке.

Перевод научно-технического текста с английского языка на русский – задача повышенного уровня сложности. Существует множество нюансов, касающихся понмания структуры предложения в англоязычных научно-технических текстах вообще и перевода терминов и сокращений конкретного направления исследований в частности. Тем более нельзя полностью полагаться на программы-переводчики. Как правило, они не учитывают специфическую терминологию технического контекста. Требуется не только знать язык, но и разбираться в вопросах тематики исследования. Поэтому студентам и аспирантам, придется браться за дело самостоятельно, чтобы избежать грубых ошибок и досадных погрешностей. Ведь никто лучше автора не знает специфику своей работы.

В данном практическом руководстве рассматриваются некоторые вопросы технического перевода, таких как учитывание многозначности терминов и приемов словообразования, а также умение определить грамматическую основу проедложения и распознать наиболее употребительные семантические структуры. Основная часть отводится нучным материалам по физике и электричеству, написанным многочисленными исследователями за рубежом. В приведенных текстах статей встречаются графики, диаграммы и таблицы, используются физические и электрические термины, числительные, уравнения, а также распространенные знаки, условные обозначения и терминологические сокращения, принятые в иностранной технической литературе. В связи с этим приводятся правила и таблицы их чтения и произношения.

Выбор содержания статей и их источников обусловлен желанием предоставить наиболее современные международные исследования, чтрбы заинтересовать обучаемых и расширить их кругозор, а также приблизить к культуре самостоятельного написания подобных научных работ.

Создание руководства такого рода является первым опытом, так как планируется обновление статей, чтобы поддержать интерес к постоянно возрастающему уровню современной науки.

Автор будет благодарен читателям за все замечания и пожелания и просит направлять их по адресу: г. Северск, пр. Коммунистический, д 65, кафедра иностранных языков СТИ НИЯУ МИФИ.

1 Особенности перевода научно-технического текста

Для грамотного перевода технической статьи на английский язык необходимо обратить вниание на особенности его перевода, которые состоят состоят в следующем:

1) текст содержит большое количество специальных терминов. Многие технические термины образуются из широко употребляемых слов, но приобретают совершенно другой смысл. Более того, в разных отраслях науки и техники одно и тоже слово может иметь разное значение и переводиться по-разному. Сочетание слов часто меняет их исходное значение;

2) активное развитие науки приводит к тому, что постоянно появляются новые термины. Они отсутствуют в словарях и образуют своеобразный сленг, понятный только для специалистов;

3) сокращения и аббревиатуры могут выглядеть по-другому или отсутствовать в иностранном языке;

4) общепринятые термины нельзя заменять синонимами. Формулировки не допускают вольного трактования. В техническом тексте не должно быть разночтений или двойных смыслов.

Важнейший признак научного исследования – воспроизводимость. Смысл статьи должен быть ясным и однозначным, чтобы ученые любой другой лаборатории могли повторить эксперимент и получить непротиворечивые результаты.

2 Технические термины в английском языке

Основная особенность научно-технических текстов – насыщенность терминами. Многие из них используются только в определенной узкой области или меняют смысл в другой отрасли науки и техники.

Чаще всего используются термины латинского происхождения. При этом слова, заимствованные из латыни без изменений, подчиняются правилам исходного языка:
e.g. *analysis* – анализ, *analyzes* – анализы.

Различают три основные категории технических терминов в английском языке:

- простые – состоящие из одного слова:

e.g. *oxygen* – кислород, *resistance* – сопротивление, *velocity* – скорость, частота, *switch* – выключатель;

- сложные – состоящие из двух или нескольких слов:

e.g. *crossmembers* – поперечины, *lifeline* – жизненно-важные коммуникации.

При этом может происходить редукция одного или всех слов:
e.g. *escalator = escalating + elevator* (эскалатор = рост + подъемник).

Некоторые сложные термины пишутся через дефис:

e.g. *half-way* – на пол-оборота (на 180^0), *doubling-overtest* – испытание на сгиб.

Литерные термины образуются с использованием буквы:
e.g. *V-typeengine* – V-образный двигатель, *X-rays* – рентгеновские лучи.

Словосочетания:
e.g. *in full blast* – полной тягой, c*hamber combustion* – камера сгорания, w*ing-box* – крыло с топливным баком (кессон), a*utomatic switch* – автоматический выключатель, *high-speed circuit breaker* – быстродействующий выключатель.

Хорошо знакомые и распространенные слова в техническом тексте могут приобретать другой смысл и становиться терминами или профессиональным сленгом:
e.g. *man of war* – морской корабль, *no play to admitted* – , люфт не допускается, *shoe* – колодка в тормозной системе, лыжа токоприемника в электропоезде, звено гусеницы, *dead* – обесточенный в электромеханике, глухой или несквозной в машиностроении и строительстве.

Встречаются следующие варианты перевода технических терминов на английский:

- некоторые термины переводятся путем транслитерации, так как были заимствованы из английского или других романо-германских языков: e.g. *generator* – генератор;
- часть терминов имеет прямые соответствия в английском языке: e.g. *voltage* – напряжение;
- термины, которые калькируются, то есть передаются словами, дословно воспроизводящими исходное выражение: e.g *program code* – программный код;
- иногда в русском языке используется описательный перевод англоязычного термина, это надо учитывать при обратном переводе на английский: e.g. *video-gain* – регулировка яркости отметок от отраженных сигналов, *workhorse* – рабочий механизм, а также средство, выполняющее большую часть работы или наиболее надежное в эксплуатации.

Многозначность терминов – отдельная проблема. При переводе с русского на английский она сводится к тому, что переводчик должен знать, каким словом обозначается тот или иной термин в английском: e.g. *seal* – изоляция, перемычка, обтюратор, впай, герметик, заваривание; *spring* – весна, горячий источник, рессора, пружина; *face* – лицо, поверхность, грань, фасад, облицовка, забой, лава.

Важная особенность английского языка – употребление одних и тех же слов в роли существительных или глаголов. Рассмотренное выше слово '*face'* имеет общеупотребительное значение "стоять напротив чего-либо", в металлообработке означает "шлифовать", в строительстве – "отделывать, облицовывать, покрывать".

В таких случаях помните о порядке слов и грамматике: не пропускайте окончания глаголов третьего лица; используйте служебные слова, если это необходимо; предлоги для связи сказуемого с дополнением.

3 Приемы словообразования в английском языке

При переводе научно-технических текстов на английский важно понимать основные принципы словообразования. Довольно часто образование терминов в английском языке происходит путем присоединения приставок и суффиксов.

Например, берем корень *use* – польза;
прибавление отрицательного суффикса – *less* приводит к образованию прилагательного – *useless* – бесполезный;
суффикс существительного – *ness* позволяет получить существительное *uselessness* — бесполезность, ненужность.

В научно-технических терминах английского языка часто используются приставки:

- *bi-* или *di-* в значении “два”: *bivalent* – двухвалентный, *dipole* – диполь;
- *dis-* в значении “расстройство, нарушение, разделение, отрицание”: *disable* – запрещать, делать непригодным;
- *re-* в значении повторения: *reusable* – многоразовый, *to reinstall* – переустанавливать;
- *over-* в значении “над, сверх, свыше”: *overheat* – перегрев;
- *de-* в значении отхода, устранения, обратных процессов: *debugging* – отладка, доводка аппаратуры;
- *en-* в значении “вводить в определенное состояние, окружать, наделять чем-то”: *to enlarge* – увеличивать, укрупнять, расширять, распространяться;
- *inter-* в значении “между, среди чего-то, взаимодействие”: *to interlock* – сцепляться, смыкаться, блокировать, *interconnection* – взаимосвязь;
- *under-* в значении “под” или “недо”: *to underline* – подчеркивание, пояснение под чертежом, объяснительная надпись;
- *un-* – отрицательная приставка, меняющая значение на противоположное: *undue* – неподходящий, несвоевременный;
- *im-* в значении “не” или “без”: *immobile* – неподвижный;
- *after-* в значении “после”: *afterburner* – форсаж, форсажная камера и др.

Суффиксы в английских технических терминах часто закрепляют определенные группы понятий:

- суффиксы *-ine, -in, -yne, -ium* и др. наиболее часто встречаются в химических названиях – *amine, -florine* (-амин, -флорин);
- суффиксы *-er, -or* образуют слова, обозначающие работника, специалиста – *operator* (рабочий, радист, механик, телефонист), *driver*

(водитель, ведущее колесо). Эти же суффиксы дают названия новых машин, механизмов, приборов – *sensor* (датчик), *trailer* (прицеп);

- отвлеченные понятия, как правило, образуются при помощи суффиксов:

-ing: splicing – сращивание;

-(t)ion: depression – снижение, углубление, разрежение; *tension* – растяжение, давление, упругость;

-ty: veriety – разнообразие, множество, ряд;

-ness: weakness – слабость, слабое место, неубедительность;

-hood: likelyhood – вероятность;

-ment: statement – утверждение, формулировка, сообщение;

-ence (-ance): dependence – зависимость, *resistance* – сопротивление;

-ite: satellite – спутник;

-ize: memorize – помнить, *characterize* – характеризовать;

-ee: nominee – кандидат, *employee* – сотрудник, trainee – стажер;

-ism: constructivism – конструктивизм;

-ant: resistant – стойкий, прочный;

-ing: researching – исследование и др.

Окончание (флексия) множественного числа в технических терминах английского языка может образовывать новое существительное:
e.g. *control* – управление, *control**s*** – органы управления.

В научно-технических текстах определительные придаточные предложения могут быть заменены прилагательными с суффиксами *-able* или *-ive*:
e. g. *The materials available show excellent properties never before attainable*. – Доступные материалы с отличными свойствами недостижимыми прежде.

Обратите внимание, что вместо слов англо-саксонского происхождения в технических статьях принято использовать термины с латинскими корнями:

- вместо ~~*to clean*~~ (для очистки) – *to purify;*
- вместо ~~*to say*~~ (сказать) – *to state* (настаивать), *to assert* (утверждать), *to reply* (объявлять).

Поскольку образование технических терминов в английском языке не подчиняется единым правилам, даже большой опыт не гарантирует избежать ошибки. При переводе технических терминов на английский может помочь:

1) Обычный словарь. Распространенные и давно употребляемые термины в нем, как правило, есть. Фразовые глаголы и некоторые устойчивые конструкции также можно найти в словаре.

2) Специальные словари технических терминов на английском. Без них невозможно перевести технический текст, так как количество специальных терминов в каждой узкой области науки и техники очень велико.

3) Учебники и монографии по отрасли. В них можно найти доступные объяснения терминов и устойчивые конструкции с этими терминами.

4) ГОСТы дают определения терминов и понятий, применяемых в науке, технике и производстве с эквивалентами на английском языке.

Систематическое изучение англоязычной литературы по своей специальности поможет говорить на одном языке с коллегами и не совершать ошибок.

4 Сокращения в технических текстах на английском языке

В научно-технических текстах используется два основных вида сокращений:

1) Авторские. Они встречаются только в пределах данной статьи и расшифровываются в самой статье.

2) Общепринятые. Входят в лексическую систему языка и фиксируются в специальных справочниках. Такие сокращения подразделяются на аббревиатуры и акронимы.

Аббревиатуры чаще всего образуются из начальных букв ключевого понятия:

WWW — World Wide Web — всемирная паутина.

Иногда сокращается только часть слов в словосочетании:

D.C. amplifier — direct current amplifier — усилитель постоянного тока.

Акроним представляет собой сокращение, которое выглядит и используется как слово:

laser — light amplification by stimulated emission of radiation — лазер.

Такие сокращения чаще всего подчиняются правилам языка, на котором используются.

Важно: в английском языке присутствуют сокращения, которых нет в русском и наоборот. Без учета таких особенностей статья будет выглядеть странно и непонятно для англоязычного читателя. Например:

AC 800 kV — переменный ток 800 кВ.

HVDC 600 kV — постоянный ток высокого напряжения 600 кВ.

Некоторые сокращения выглядят не так, как русские аббревиатуры с тем же смыслом:

emt — ЭДС (электродвижущая сила).

5 Конверсия слов в английском языке

При переводе научно-технических текстов на английский нужно учитывать конверсию – явление, которое в чистом виде не встречается в русском языке. В английском разные части речи могут выражаться одним и тем же словом. Например, слово *water* можно использовать в качестве:

1) Существительного:

Water is necessary for life. — Вода необходима для жизни.

2) Глагола:

Water the flower-bed, please. — Полей, пожалуйста, клумбу.

3) Прилагательного:

Water mills served a source of energy. — Водяные мельницы служили источником энергии.

4) Частью сложного слова:

Water-supply system — система водоснабжения

Water-proof watch — водонепроницаемые часы

В таких случаях помните, что в английском предложении твердый порядок слов. Положение слова зависит от того, в каком качестве вы его используете: подлежащего, сказуемого, дополнения или определения. Это поможет избежать ошибок при переводе научно-технического текста.

6 Структура предложения в англоязычных научно-технических текстах

В англоязычной научно-технической литературе часто используются сложносочиненные и сложноподчиненные предложения. **Части сложного предложения и логические конструкции соединяются предлогами и союзами**, например: *on, upon, about besides, instead of, in preference to* и др.**:**

*Equations are obtained for the dependences of the magnetic moment and Curie t° **on** the concentration of nonmagnetic cations.* — Получены уравнения для зависимостей магнитного момента и температуры Кюри от концентрации немагнитных катионов.

*Importance may depend **upon** some matters* — значимость зависит от нескольких факторов.

*Atmospheric oxidation reactions are also important in particle formation, **besides** ozone*. — **Помимо** озона, важную роль в образовании частиц также играют реакции окисления в атмосфере.

*Most assessments were qualitative, and used expert judgement **instead of** quantitative studies*. — Большинство оценок носят качественный характер и основаны на экспертных заключениях, а не на результатах количественных исследований.

*Google uses Google Neural Machine Translation (GNMT) **in preference to** its previous statistical methods*. — Google использует нейронный машинный перевод Google (GNMT) вместо ранее используемых статистических методов.

Особое место в техническом переводе с русского на английский занимают причастные конструкции, которые вводятся предлогом *with*:

***With** the steam cut off, it became possible to start repairs*. — После того, как был отключен пар, появилась возможность приступить к ремонту.

В последнее время в текстах технического характера на английском языке стали все чаще встречаться цепочки слов, не связанных предлогами:

overload prevention device — устройство для предотвращения перезагрузки

X-ray thickness gauge — рентгеновский толщинометр

two-stage single-cylinder air-cooled reciprocating compressor — двухступенчатый одноцилиндровый компрессор с возвратно-поступательным движением поршня и с воздушным охлаждением

В логических рассуждениях часто используются наречия however, thus, alternatively, on the other hand:

*It noted **however** that progress in this area is often constrained by limited resources.* — **Однако**, отмечается, что прогресс в этой области часто сдерживается ограниченностью ресурсов.

*This would infinitely increase the network density and **thus** lead to unacceptable costs*. — Это повлекло бы за собой бесконечное увеличение плотности сети, и **тем самым**, привело бы к неприемлемым издержкам.

*The series of temperatures within square brackets may **alternatively** be used.* — **В качестве альтернативы** могут использоваться температурные ряды, заключенные в квадратные скобки.

*This view may **on the one hand** explore possible motivations for the present method, and **on the other hand** highlight some of its deficiencies*. — Такой подход может, **с одной стороны**, открыть потенциальные преимущества нынешнего метода, а **с другой стороны**, выявить некоторые его недостатки.

Использование страдательного залога также характерная особенность научно-технического текста:

Brakes are used to slow or to stop the car. — Тормозная система используется для того, чтобы замедлять ход автомобиля, или останавливать его.

Часто встречаются безличные или неопределенно-личные конструкции типа:

it was decided — было решено

it is necessary — необходимо

В функции определения нередко используется инфинитив:

the properties to be expected — ожидаемые свойств.

В англоязычных научно-технических статьях **действие часто выражается не глаголом, а глагольно-именным сочетанием**:

study — изучать, *make a study* — проводить исследование;

measure — измерять, *make measurements* — делать измерения.

Например: *The phenomenon of absorption was studied*. — Исследовалось явление поглощения.

A study was made of the absorption spectra of fluorine centers. — Проведено исследование спектров поглощения фторовых центров.

В предложениях типа *a study is made* предмет изучения вводится предлогом ***of***:

Measurements were made ***of*** *the substance density*. — Измерялась плотность вещества.

Материал вводится предлогом ***on***:

Measurements were made **on** *purified samples*. — Измерения проводились на очищенных образцах.

Сказуемое в английском языке может стоять как после подлежащего, так и после группы подлежащего, оказываясь при этом в конце предложения:

A short description ***is given*** *of some species of ciliates. = A short description of some species of ciliates* ***is given***. — Дается краткое описание некоторых видов инфузорий.

Обратите внимание, что при переводе с русского языка на английский грамматическая структура предложения должна соответствовать языку перевода, а не быть калькой с русского. Помните, что в английском сказуемое должно присутствовать:

Объект исследования – свинцово-цинковая сульфидная руда одного из месторождений Красноярского края. — ~~*Object of research – lead-zinc sulphidic ore of one of Krasnoyarsk Territory's entrails*~~. — *An object of research* **is** *the lead-zinc sulphidic ore of one of Krasnoyarsk Territory's entrails*.

Используйте **предлоги** так, как это принято в английском языке:

Проведен отбор штаммов микроорганизмов (бактерий) по способности к росту на дизельном топливе. — ~~*The selection of strains of microorganisms* ***on ability to growth on*** *diesel fuel is made*~~. — *The selection of bacterial strains* ***based on growth*** *ability* ***in*** *diesel fuel*.

Один из признаков хорошего владения языком при переводе научно-технического текста — умение использовать **устойчивые языковые конструкции**:

на материале — *based on* или *case study of;*

в рамках — *as part of;*

предложено использование — *suggests using;*

во втором разделе обсуждается — *Section II discusses;*

на рисунке 1 показано — *Fig. 1 shows;*

в результате эксперимента было выявлено — *the experiment has revealed.*

Проблема обсуждается в статье — ~~*The problem is discussed in the article*~~ — *The articles suggests…, The article discusses…, The article discloses…*

Частой ошибкой при переводе на английский является **пропуск артикля**. Однако, в технических текстах отсутствующий артикль — скорее норма:

5General view is that… — общее представление — это…

Характерно отсутствие артикля перед названием конкретной детали:

lever assembly are stainless steel — рычаг сделан из нержавеющей стали

7 Алгоритм работы с текстом

Алгоритм работы с текстом при переводе с английского языка на русский следующий:

- прочитывается весь текст;
- текст размечается;
- выделяются непонятные термины и словосочетания;
- выделяются сокращения, англо-американские не метрические меры переводятся в метрические;
- после этого делается полный перевод в письменном или устном виде в зависимости от задания.

8 Тексты по физике

TEXT 8.1

Implementing topologically ordered time crystals on quantum processors/
Реализация топологически упорядоченных временных кристаллов на квантовых процессорах

NOVEMBER 10, 2024.by Tejasri Gururaj (7360)

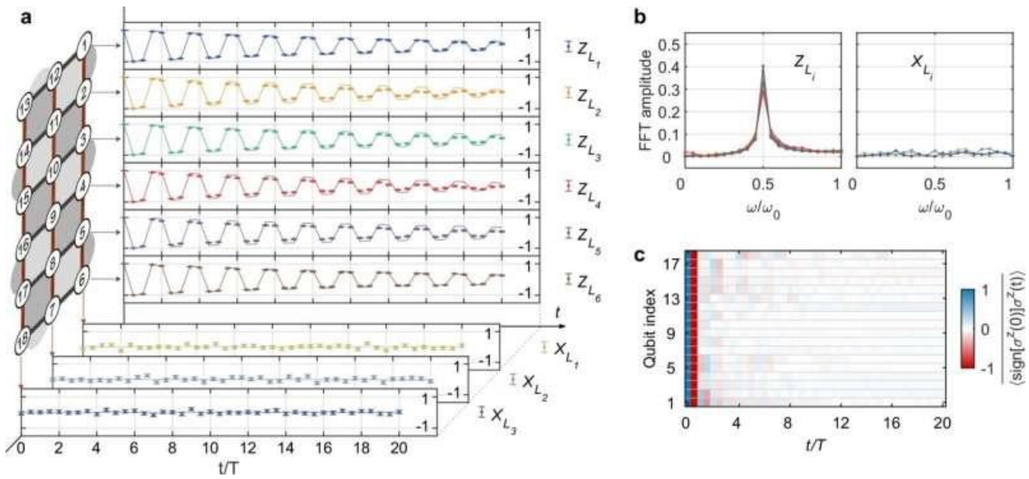

Time-translation symmetry breaking. Credit: *Nature Communications* (2024). DOI: 10.1038/s41467-024-53077-9

In a new study published in *Nature Communications*, scientists have implemented the topologically ordered time crystal on a quantum processor for the first time.

This marks a new era for quantum technology, since time crystals have been traditionally challenging to combine with topological order. However, achieving this combination adds stability and robustness to the system, a requirement for quantum computing applications.

Time crystals are a recent introduction to science, with the idea first proposed in 2012 by Nobel laureate Frank Wilczek. It is a quantum system that can naturally oscillate between states without the need for a continuous external energy source.

In simple terms, time crystals are a type of material in which the atoms are arranged periodically in time, rather than space, which is how ordinary crystals (like diamonds) are.

The system always remains in the lowest energy state during oscillations, which is the ground level. Time crystals were experimentally confirmed in 2017 and have potential applications in various quantum technologies.

Achieving topological order, or global order, in time crystals can be challenging due to their dynamic nature. The research team aimed to bridge this gap by demonstrating a topologically ordered time crystal.

Phys.org spoke to some of the researchers behind the study, including Dr. Liang Xiang, Wenjie Jiang, Zehang Bao, Assistant Prof. Qiujiang Guo, and Prof. Haohua Wang from Zhejiang University and Associate Prof. Dong-Ling Deng from Tsinghua University.

Speaking of the process of bringing topologically ordered time crystals to life, the researchers said, "The collaboration between theoretical physicists and the experimental team makes this beautiful project happen. The goal is to push forward the understanding of topological order in periodically driven systems."

The uniqueness of time crystals

Time crystals exhibit something called time-translation symmetry breaking. Time translation is a property of systems wherein the system's state does not change over time.

In the case of time crystals, this symmetry is broken since time crystals periodically oscillate between different states. What makes time crystals unique is that they can exhibit periodic motion in time without energy dissipation.

However, they do not violate conservation laws.

After being given an initial push, the system starts oscillating at a frequency lower than the driving force. The oscillations are self-sustained due to many-body interactions, creating collective, synchronized oscillations.

Their lack of equilibrium allows them to maintain motion indefinitely, even in their ground state. This symmetry breaking is a form of non-equilibrium matter which brings out the uniqueness of time crystals.

Topological order

A system can be characterized via two types of properties—local and global.

Local properties are those that depend on a specific environment or position within a system—for example, the spin of an atom or its magnetic moment.

Global properties, on the other hand, depend on the whole system at large. These properties are long-ranged compared to local properties, which are short-ranged. An example of a global property is superconductivity.

Topological order is a type of global property of a system not described by local disturbances or noise. It emerges as a result of long-range entanglement within a system, meaning that changes in one part of the system can affect another part of the system.

Quantum computers are very prone to errors or noise from the environment. These can interact with the system, leading to a loss of coherence. This means the system can no longer maintain superposition and entanglement, which are the core features of a quantum system.

Since topological order is stable against local disturbances, it is of interest for topological quantum computing.

The challenge with introducing topological order in time crystals is their dynamic nature. Topological order requires stability and equilibrium states, which time crystals do not exhibit.

Programmable superconducting qubits

The researchers set up their processor using 18 programmable superconducting transmon qubits arranged in a two-dimensional square lattice. These qubits are more stable than other ones.

The square lattice facilitates qubit interactions, which helps generate the entanglement needed for quantum algorithms and error correction (noise reduction).

The researchers highlighted a key feature of their setup, the surface code.

"The surface code is not only one of the most successful models for quantum error correction, but it also supports exotic topologically ordered phases. The quantum processor developed by the experimental team at Zhejiang University naturally fit the surface code model."

"This makes it an ideal testbed for exploring these elusive topologically ordered states and potentially expanding their boundaries from equilibrium systems to non-equilibrium ones," they explained.

Their processor has a depth of 700 circuit layers and can run 2,300 single-qubit gates and 1,400 two-qubit gates. This demonstrates its ability to handle large and complex computations.

The platform can also simulate four-body interactions, which are needed for modeling complex systems. Further, a neuroevolution algorithm was used to find optimal configurations for quantum circuits, which can improve the efficiency and effectiveness of the computations.

The researchers added, "To meet the stringent requirements of observing the long-lived topological time crystal dynamics, we have made a huge amount of effort to improve the performance of our processor, which has state-of-the-art gate fidelities and qubit coherence times now."

Robust and stable topological time crystal order

The researchers found that the system could maintain stable behavior at a fractional frequency of the driving force, even when dealing with noise, demonstrating its stability. The system also stabilized after being disturbed without any unwanted oscillations.

The system also remained stable under small fluctuations, meaning it can function in noisy environments. When faced with stronger disturbances, the system loses its time-crystal-like behavior.

The team found that the system's topological entanglement matched the one made by theoretical predictions, suggesting its properties are robust and well-defined.

For four-body qubit interactions, the system could successfully measure the interactions with high accuracy. The system could also create and verify quantum states driven periodically, supporting its time-periodic behavior.

The researchers commented on the potential of their system, saying, "We believe that with the growth of the system size, control accuracy, and coherence time, superconducting processors will allow scientists to explore more exotic non-equilibrium phases of matter that are not accessible in natural materials."

They also mention that their experiment has demonstrated all necessary building blocks for implementing Floquet-enriched topological order that hosts dynamical anyon permutation and emergent non-Abelian anyons.

"An observation of such an unconventional phenomenon would also mark an important step in deepening our understanding of exotic non-equilibrium phases," they remarked.

TEXT 8.2

Ultrafast imaging technique reveals how ozone-damaging molecule reacts to light/ Сверхбыстрый метод визуализации показывает, как молекулы, разрушающие озон, реагируют на свет

NOVEMBER 1, 2024.by Rachel Berkowitz, Lawrence Berkeley National Laboratory (3768)

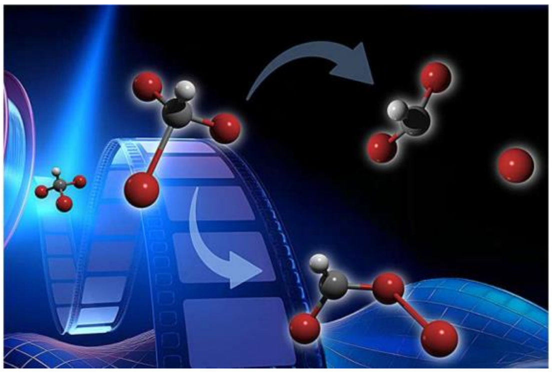

A long-predicted ultrafast pathway in the UV photochemistry of bromoform is visualized for the first time by femtosecond time-resolved electron diffraction. Credit: Melody Li, Debadarshini Mishra, and Lars Hoffmann

For the first time, researchers have observed how bromoform rearranges its atoms in less than a trillionth of a second after it gets hit by an ultraviolet (UV) pulse. The imaging technique captured a long-predicted pathway by which the ozone-layer-damaging molecule transforms its structure upon interaction with light.

Energy from the sun's UV rays induces many chemical processes on Earth. To understand, use, or mitigate damage from these often ultrafast chemical reactions, it's vital to understand how they work at the atomic level.

"How do the electrons and atoms talk to each other to make a certain chemical reaction happen? Bromoform is a prominent model system for answering these questions," said Oliver Gessner, a senior scientist at the Department of Energy's Lawrence Berkeley National Laboratory (Berkeley Lab).

Chemists around the world have studied the UV photochemistry of bromoform for decades. The natural compound breaks down ozone in Earth's atmosphere, and is naturally produced by phytoplankton and seaweeds in the oceans.

Theory says that it undergoes two different processes under UV exposure: in dissociation, one bromine atom breaks away from the rest of the molecule; in isomerization, the atoms rearrange into a different configuration or isomer.

"Some claim to have observed signatures of this isomer, but it was too short-lived to prove," said Gessner, who leads the Atomic, Molecular, and Optical

Sciences Program in the Chemical Sciences Division at Berkeley Lab. Moreover, different theories have widely different predictions of the proportion of bromoform that follows each pathway.

In a study published in the *Journal of the American Chemical Society*, Gessner and his colleagues developed an experiment that not only confirmed this isomer formation but determined what proportion of bromoform molecules undergo dissociation and what proportion form isomers.

The researchers first excited bromoform gas molecules with an ultrafast burst of UV light (267 nanometer wavelength), then imaged the excited molecules with ultrashort electron pulses using the relativistic ultrafast electron diffraction instrument at the SLAC National Accelerator Laboratory. The instrument is part of the Linac Coherent Light Source at SLAC, a Department of Energy Office of Science user facility.

"The molecules decide within a few hundred femtoseconds which way they go, so we had to be faster than that," said Gessner.

From the electron images, the researchers could measure the distances between atoms within the bromoform molecules and track how these distances changed over time. The analysis showed that approximately 60% of bromoform molecules underwent isomerization within the first 200 femtoseconds of excitation and persisted for the duration of the 1.1-picosecond-long experiment.

"It was really exciting to see exactly the configuration that some people had predicted for this isomer," Gessner said. The other 40% of the bromoform underwent direct dissociation.

The result is an important step toward understanding bromoform photochemistry, and UV-induced photochemistry in general. "The sequence of chemical pathways impacts the final chemical products," said Gessner.

The benchmark measurement for a long debated isomer formation rate makes it possible to refine theories that predict these reactions and their products. Moreover, the study demonstrates that the ultrafast technique is good for providing clear-cut answers to questions about how fast isomers populate and how long they live. That, said Gessner, is a very powerful tool.

TEXT 8.3

Transforming polyethylene: From functionalization to antibacterial properties for sustainable applications/ Преобразование полиэтилена: от функционализации к антибактериальным свойствам для устойчивого применения

by Saeed Ataie (5697)

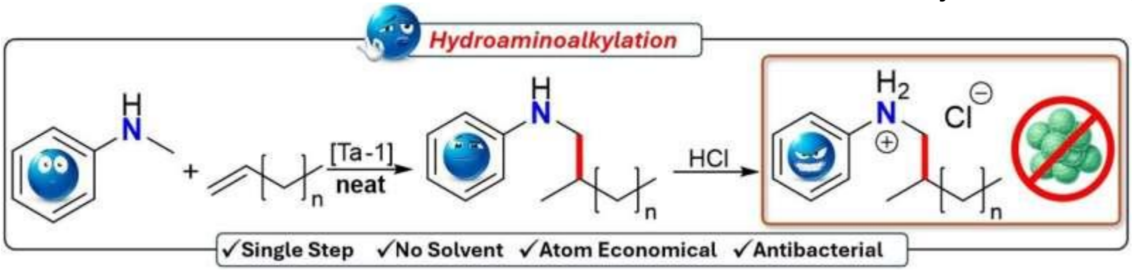

Hydroaminoalkylation enables efficient amine group incorporation into polyethylene, with subsequent conversion to antibacterial ammonium groups. Credit: Saeed Ataie

Polyethylene (PE) is one of the most widely used and versatile plastic materials globally, prized for its cost-effectiveness, lightweight properties and ease of formability. These characteristics make PE indispensable across a broad spectrum of applications, from packaging materials to structural plastics.

However, despite its widespread utility, PE's inherent chemical inertness limits its functionality in advanced applications, holding back its potential for more innovative uses.

To unlock this potential, it's essential to introduce polar functional groups into PE, which can significantly enhance its properties and open doors to new applications. This challenge has become a major focus in polymer chemistry, where developing efficient methods to modify PE has drawn increasing interest.

One of the primary obstacles in modifying PE is its chemical resistance, which makes it difficult to functionalize using conventional methods. This inertness also contributes to the buildup of PE waste in landfills, posing a severe environmental challenge. As plastic pollution continues to threaten ecosystems worldwide, finding ways to recycle or upcycle PE into valuable products is imperative.

Although some approaches exist for modifying PE, they often lack scalability or efficiency, underscoring the need for innovative solutions that balance environmental impact with functional benefits for this ubiquitous plastic.

Among the various strategies available, amination has emerged as one of the most promising methods for modifying PE.

But why focus on amines?

Amines are nitrogen-based groups with one or more hydrogen atoms attached in the form of N-H bonds. These N-H groups can engage in hydrogen bonding, enabling interactions between polymer chains. This not only enhances the polymer's chemical reactivity but also improves its performance across a variety of applications, from adhesives to coatings.

However, achieving efficient functionalization of PE with amines has been a significant challenge; most methods require multiple, energy-intensive steps or risk degrading the polymer's properties.

Consequently, progress toward a scalable, effective method for aminating PE has been limited. Notably, converting the N-H groups in aminated PE into other species could further broaden PE's range of applications.

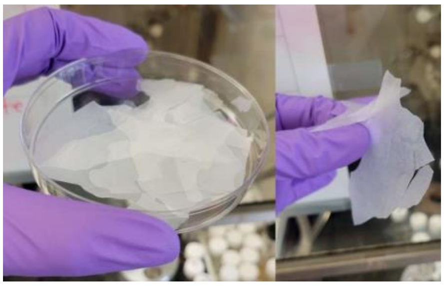

Thin films of polyethylene functionalized with antibacterial ammonium groups. Credit: Saeed Ataie

This is where my research, as a postdoctoral fellow in the Schafer group at the University of British Columbia, makes a bold leap forward.

Through extensive exploration, I focused on a catalytic process called hydroaminoalkylation to aminate PE efficiently. Previously used in modifying polypropylene, this technique showed promise in transforming PE through a simple, one-step reaction.

The work is published in the journal *Angewandte Chemie International Edition*.

The strength of this method lies in its efficiency: It works under mild, solvent-free conditions and avoids the radical-induced degradation seen in conventional methods. By applying this approach to vinyl-terminated polyethylene (VTPE), generously provided by my industrial partner NOVA Chemicals, I successfully created amine-functionalized PE with minimal reaction steps, enhancing scalability and cost-effectiveness.

At the University of British Columbia, my colleagues in the Hatzikiriakos group conducted rheological and mechanical tests on my aminated PE. They found that introducing amine groups not only modified the chemical properties of PE but also impacted its physical characteristics.

For instance, the crystallization temperature of the modified PE increased, indicating stronger intermolecular interactions within the polymer due to the amine groups. The amine groups also increased the material's hydrophilicity (or attraction to water), as the N-H bonds can form hydrogen bonds with water molecules.

Traditionally, recycling PE has been challenging due to its chemical inertness, but this new approach allows us to upcycle PE waste into valuable resources. Aminating waste PE holds significant promise for sustainability, making it possible to reuse and repurpose it for various applications.

Now, imagine a world where you don't need to sanitize your hands every time you touch a surface, a common concern during the COVID-19 pandemic. This is the problem I aimed to address in my study.

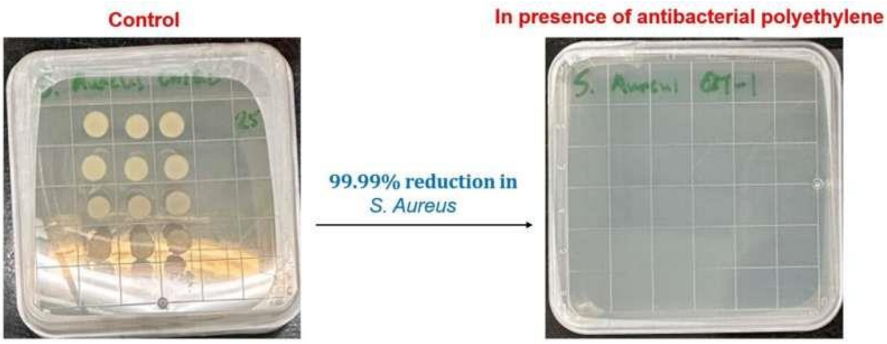

Complete reduction of Staphylococcus aureus bacteria in the presence of antibacterial polyethylene. Credit: Saeed Ataie

Here's how amination can lead to an antibacterial effect: I converted the amine groups in the polymer into positively charged ammonium groups by treating the aminated PE with a hydrochloride solution. Since bacteria have negatively charged cell membranes, they are naturally attracted to the positively charged ammonium groups.

This electrostatic interaction disrupts the bacterial cell membrane, ultimately killing the bacteria. After this transformation, my collaborators at the University of Calgary, the Heyne team, exposed the modified polymer to Staphylococcus aureus bacteria. The polymer killed all the bacteria in a short exposure time.

In essence, I developed an antibacterial polymer that holds potential for use as a coating on everyday surfaces, offering a way to prevent the spread of germs without the need for constant sanitizing.

TEXT 8.4

Can unknown physics be seen in interactions between Higgs bosons?/
Можно ли увидеть неизвестную физику во взаимодействиях между бозонами Хиггса?

NOVEMBER 7, 2024? by Polish Academy of Sciences (4780)

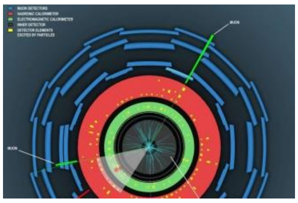

Secondary particle tracks recorded during a proton collision inside the ATLAS detector, indicating the presence of a single Higgs boson in the event. Credit: IFJ PAN / CERN / ATLAS Experiment

Since the launch of the Large Hadron Collider, there has been ongoing research there into Higgs bosons and a search for traces of physics beyond the existing model of elementary particles. Scientists working at the ATLAS detector have combined both goals: with the latest analysis it has been possible to expand our knowledge of the interactions of Higgs bosons with each other, and stronger constraints on the phenomena of "new physics" have been found.

An undisputed success of the Large Hardon Collider (LHC) is the discovery of the last missing element of the Standard Model: the Higgs boson, responsible for the origin of the mass of elementary particles. There is also a disappointment: the persistent absence of any trace of physics beyond this model.

Scientists at the facility of the European Organization for Nuclear Research (CERN) in Geneva are therefore trying to conduct their current research in such a way as to combine more precise measurements of the properties of the Higgs boson with further searches for "new physics."

The study just published in the *Journal of High Energy Physics* is an example of this approach. In it, physicists from the ATLAS experiment focused on events leading to the creation of two Higgs bosons, which would then decay into multiple particles of the lepton family (mainly electrons and muons).

The production of Higgs boson pairs can occur within the Standard Model itself. It is such a rare process here that it has not been possible to observe it in the data collected so far. There are, however, theoretical models describing phenomena beyond the Standard Model, predicting the production of Higgs boson pairs with a higher probability.

Observing instances of this sort of production using data already collected would confirm the existence of a hitherto unknown class of physical phenomena. It is therefore not surprising that for the scientists in the ATLAS experiment, this very process became the starting point for the analysis described above.

"Experimental studies of the interactions of Higgs bosons with each other encounter a fundamental problem. It is this: in proton collisions at the LHC, Higgs bosons appear so infrequently that so far not a single event of Higgs boson pair production has been detected, which at first glance seems absolutely necessary if we want to look at interactions between these particles. How, then, can we study a phenomenon that has not yet been observed?" asks Dr. Bartlomiej Zabinski, a physicist at the Institute of Physics of the Polish Academy of Sciences (IPJ PAN) who coordinated the international team responsible for this analysis.

Within the Standard Model, increasingly precise predictions can be made about the probabilities of various known processes. A rationale for suggesting unexpected properties of Higgs bosons or the existence of new physics would be a discrepancy between theoretical predictions and actual data from the LHC detectors.

Operating solely within the framework of the Standard Model, the physicists in the ATLAS experiment therefore simulated (together with the background) the signals that should appear in the detectors in the event of two Higgs boson phenomena, and then normalized the results according to the expected amount of data coming from their detector. The final step was to compare the values thus obtained with those derived from previous observations. The use of machine learning based on decision trees helped in the search for these rare processes.

"Our analysis of double Higgs boson production events in the final state with multiple leptons complements the studies already carried out on other final states. So far, we have not noticed anything in the data from our detectors that disagrees with the Standard Model. However, this result does not rule out the possibility of the existence of 'new physics' phenomena, but only informs us that their possible influence on the production of Higgs boson pairs remains too weak to be seen in the data collected so far," concludes Dr. Zabinski.

In the coming years, the LHC is to undergo a major upgrade. The intensity of the beams will then increase tenfold, resulting in a significant increase in the number of recorded proton collisions.

The limitations imposed by the current analysis on the production and parameters describing the interactions of Higgs bosons allow physicists to hope that perhaps already at the beginning of the next decade it will be possible to select the first events of double Higgs production from more data and to verify today's predictions in direct observations of the phenomenon.

TEXT 8.5

Scientists use high-energy heavy ion collisions as a new tool to reveal subtleties of nuclear structure/ Ученые используют высокоэнергетические столкновения тяжелых ионов в качестве нового инструмента для выявления тонкостей ядерной структуры

NOVEMBER 6, 2024.by Brookhaven National Laboratory (11369)

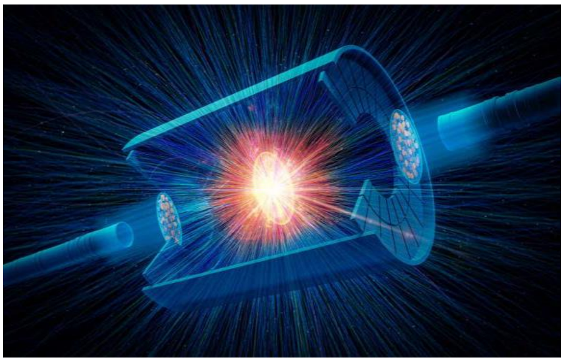

An artistic representation of charged particle tracks streaming from a collision of two uranium nuclei overlaid on a sketch of the STAR detector at the Relativistic Heavy Ion Collider (RHIC). The incoming uranium nuclei, exaggerated in size, are shown contracted along the beam direction, illustrating the effects of traveling close to the speed of light. By analyzing particle flow patterns from many such collisions scientists can reconstruct the shape of the original colliding nuclei. Credit: Chunjian Zhang/Fudan University and Jiangyong Jia/Stony Brook University

Scientists have demonstrated a new way to use high-energy particle smashups at the Relativistic Heavy Ion Collider (RHIC)—a U.S. Department of Energy (DOE) Office of Science user facility for nuclear physics research at DOE's Brookhaven National Laboratory—to reveal subtle details about the shapes of atomic nuclei.

The method, described in a paper published in *Nature*, is complementary to lower energy techniques for determining nuclear structure. It will add depth to scientists' understanding of the nuclei that make up the bulk of visible matter.

"In this new measurement, we not only quantify the overall shape of the nucleus—whether it's elongated like a football or squashed down like a tangerine—but also the subtle triaxiality, the relative differences among its three principle axes that characterize a shape in between the 'football' and 'tangerine,'" said Jiangyong Jia, a professor at Stony Brook University (SBU) who has a joint appointment at Brookhaven Lab and is one of the principal authors on the STAR Collaboration publication.

Deciphering nuclear shapes has relevance to a wide range of physics questions, including which atoms are most likely to split in nuclear fission, how heavy atomic elements form in collisions of neutron stars, and which nuclei could point the way to exotic particle decay discoveries.

Leveraging improved knowledge of nuclear shapes will also deepen scientists' understanding of the initial conditions of a particle soup that mimics the early universe, which is created in RHIC's energetic particle smashups.

The method can be applied to analyzing additional data from RHIC as well as data collected from nuclear collisions at Europe's Large Hadron Collider (LHC). It will also have relevance to future explorations of nuclei at the Electron-Ion Collider, a nuclear physics facility in the design stage at Brookhaven Lab.

Ultimately, since 99.9% of the visible matter that people and all the stars and planets of the cosmos are made of resides in the nuclei at the center of atoms, understanding these nuclear building blocks is at the heart of understanding who we are.

"The best way to demonstrate the robustness of nuclear physics knowledge gained at RHIC is to show that we can apply the technology and physics insights to other fields," Jia said. "Now that we've demonstrated a robust way to image nuclear structure, there will be many applications."

From long exposure to freeze-frame snapshots

For decades, scientists used low-energy experiments to infer nuclear shapes—for example, by exciting the nuclei and observing photons, or particles of light, emitted as the nuclei decay back to the ground state. This method probes the overall spatial arrangement of the protons inside the nucleus, but only at a relatively long time scale.

"In low-energy experiments, it's like taking a long-exposure picture," said Chun Shen, a theorist at Wayne State University whose calculations were used in the new analysis.

Because the exposure time is long, the low-energy methods do not capture all the subtle variations in the arrangement of protons that can occur inside a nucleus at very fast timescales. And because most of these methods use electromagnetic interactions, they can't directly "see" the uncharged neutrons in the nucleus.

"You only get an average of the whole system," said Dean Lee, a low-energy theorist at the Facility for Rare Isotope Beams, a DOE Office of Science user facility at Michigan State University. Though Lee and Shen are not co-authors on the study, they and other theorists have contributed to developing this new nuclear imaging method.

"The high-energy imaging method, which captures many freeze-frame snapshots that reveal information about both the protons and neutrons, is orders of magnitude faster," said Chunjian Zhang, a former SBU postdoctoral fellow, now a junior faculty member at Fudan University, who co-led the STAR analysis.

Importantly, the snapshots taken by RHIC's STAR detector all come from different collision events.

"You cannot image the same nuclei again and again because you destroy them in the collision," Jia noted. But by looking at the whole collection of images from many different collisions, scientists can reconstruct the subtle properties of the 3D structure of the smashed nuclei.

As Lee explained, "In each collision, you freeze time for a moment and look at where all the protons and neutrons are. And every time you do this, it's a different distribution due to the quantum nature of atomic nuclei. So, the high-energy method captures a ton of information, a ton of complexity that we do not probe in low-energy experiments."

Reconstructing shapes from debris

How exactly does STAR see that complexity if the nuclei get destroyed? By tracking how particles fly out—and how fast—from the most central, head-on nuclear smashups.

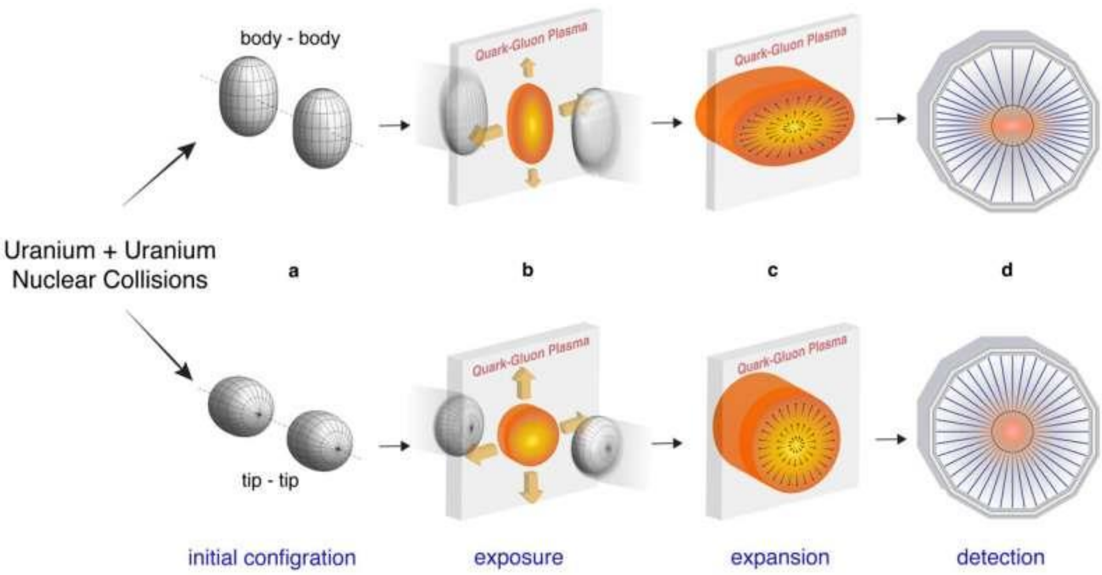

Head-on collisions of oblong uranium nuclei can take orientations between body-body and tip-tip (a) to produce a quark-gluon plasma (QGP) with varying shapes and sizes (b). These QGP characteristics drive distinct expansion patterns (c), leading to different distributions of emitted particles (d). By measuring the variation in these "flow" patterns from collision to collision and comparing them to collisions of near-spherical gold nuclei, scientists can extract the shape of the uranium nuclei. Credit: Jiangyong Jia/Stony Brook University
As the STAR scientists note in their *Nature* paper, "In an ironic twist, this effectively realizes [famous physicist] Richard Feynman's analogy of the seemingly impossible task of 'figuring out a pocket watch by smashing two together and observing the flying debris.'"

From years of experiments at RHIC, the scientists know that high energy nuclear collisions melt the protons and neutrons of the nuclei to set free their inner building blocks, quarks and gluons. The shape and expansion of each hot blob of this melted nuclear matter, known as a quark-gluon plasma (QGP), is determined by the shape of the colliding nuclei.

The shape and size of each QGP blob directly affect pressure gradients generated in that blob of plasma, which in turn influence the collective flow and momentum of particles emitted as the QGP cools.

The STAR scientists reasoned they could "reverse engineer" this relationship to derive information about nuclear structure. They analyzed the flow and momentum of particles emerging from collisions and compared them with models of hydrodynamic expansion for different QGP shapes to arrive at the shapes of the originally colliding nuclei.

To show their method worked, they compared central collisions of gold nuclei—which are believed, from low energy studies, to be close to spherical—with central collisions of uranium nuclei, which have a pronounced elongated football-like shape. Because the gold nuclei are nearly spherical, there shouldn't be much variation from collision to collision in the flow patterns of emitted particles.

"Central collisions of gold nuclei produce a circular, fixed size QGP that expands evenly in all directions," said Shengli Huang, a SBU research scientist who co-led the STAR analysis.

"The oblong uranium nuclei, on the other hand, can collide in a wide range of orientations, generating droplets of QGP with various shapes and sizes," he said. So, the scientists expected central collisions of uranium to exhibit much more variability in the flow patterns.

By comparing measurements between uranium-uranium and gold-gold collisions—and fitting those results to hydrodynamic models that have successfully described other characteristics of the QGP—the scientists were able to infer a quantitative description of the shape of the uranium nucleus. The results also include a first determination of the relative lengths of the three principal axes of the oblong uranium nucleus.

Computing tools

Obtaining precision predictions from various hydrodynamic models, including Shen's model, posed significant computational challenges. Accomplishing this task took over a year, with Zhang running calculations on the Open Science Grid. Zhang used more than 20 million central processing unit (CPU) hours to produce more than ten million collision events from hydrodynamic models, which were then fitted to the experimental data.

"Many features in the STAR data are indicative of the significant differences in the shape between the uranium and gold nuclei, but the computational data-model comparisons certainly helped us to more precisely quantify the nuclear shapes," Zhang said.

Though this study aimed to establish a new nuclear imaging method, the data did reveal some new information about uranium nuclei. Instead of observing distortion in just the one principal axis that leads to "prolate" elongation, the scientists found differences in all three axes, suggesting that uranium nuclei are more complex than previously thought.

Expanded impacts

As noted, the new method will improve physicists' understanding of the initial conditions in heavy ion collisions that generate QGP at both RHIC and the LHC. Nuclear structures derived from low-energy experiments were essential in analyses that linked those initial conditions with hydrodynamic flow patterns to establish that the QGP created in these collisions is a nearly perfect liquid.

Scientists can now use the new method to check the consistency with low-energy approaches using nuclei like uranium where the structure is relatively well known. This will further reduce uncertainties about initial state conditions to improve the determination of QGP properties.

The method can also be used to determine shapes of other nuclei, especially those where the low-energy experiments yielded limited understanding. One example would be to apply the method to so-called isobar nuclei—nuclei with the same total number of protons and neutrons (nucleons), but different proportions of each type.

Such pairs are involved when two neutrons in a higher-neutron-number "parent" nucleus transform into protons via a nuclear weak decay process to create the lower-neutron-number "daughter"—a process known as double beta decay. Knowing the shape differences between parent and daughter nuclei could help reduce model uncertainties in experiments searching for an unseen type of decay known as neutrinoless double beta decay.

"There are many interdisciplinary aspects of this research," Jia explained. "Nuclear physics has many subfields. Usually, each community uses its own tools—theory and experiments. But because of these results, the low-energy nuclear structure and nuclear reaction communities around the world have taken notice.

"Several workshops, meetings, and conferences were organized to explore the connections between the high-energy and low-energy frontiers in nuclear physics, which allowed us to understand each other better," he said.

TEXT 8.6

Improving detector sensitivity to neutrinos and dark matter: Latest experimental setup yields 50% higher ionization/ Повышение чувствительности детектора к нейтрино и темной материи: новейшая экспериментальная установка обеспечивает повышение ионизации на 50%.

NOVEMBER 1, 2024.by Patricia DeLacey, University of Michigan College of Engineering (4644)

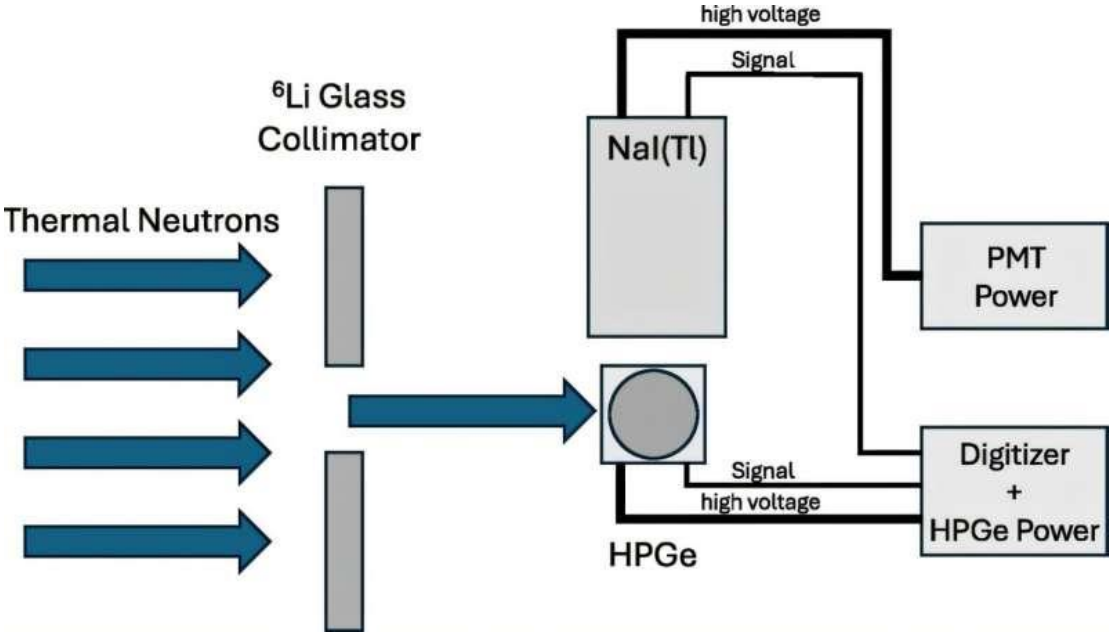

Simplified diagram of the experimental setup. A HPGe detector was placed within the collimated neutron beam, and a NaI(Tl) detector was placed to the side outside the neutron beam. Credit: *Physical Review D* (2024). DOI: 10.1103/PhysRevD.110.083043

Fine tuning an experimental setup improved a detector's sensitivity to neutrinos and perhaps eventually dark matter—two difficult-to-measure forms of matter which hold great importance for understanding particle physics and experimental cosmology. The University-of-Michigan-led study is published in *Physical Review D*.

The trouble with detecting neutrinos and dark matter lies in their weak interaction with other forms of matter.

Neutrinos—tiny, subatomic particles produced in nuclear reactions in the stars and by radioactive decay—only rarely interact with other matter through weak nuclear forces. Typically, neutrinos pass straight through visible matter, earning the nickname "ghost particles." These neutrally charged particles do not interact with electromagnetic forces, and they only weakly interact with gravity as their mass is around ten million times less than an electron.

Neutrinos can be detected through nuclear recoil. When trillions of neutrinos are directed at atoms, a rare collision between a neutrino and an atom can occur. This causes the nucleus to recoil and pushes electrons of nearby atoms out of orbit. Applying a voltage across the detector and recording ionization energy reveals neutrino collisions.

Similarly elusive, dark matter exerts gravitational force upon visible matter but does not absorb, reflect or emit light. Researchers are actively working to create and detect dark matter, thought to be the "glue" holding galaxies together, to better understand the formation of the universe.

Although dark matter has not yet been detected on earth, hypothetical particles called Weakly Interacting Massive Particles (WIMPs) are expected to cause nuclear recoil similar to neutrinos.

Once only able to be detected in massive underground facilities, commercially available high purity germanium detectors, or HPGe detectors, just a few inches long are now able to detect weak nuclear recoils. These compact detectors leverage the heavy metal's large nucleus to increase the probability of collisions while cooling the detector to 77 Kelvin (about -196 °C) to minimize signal noise from atomic vibrations.

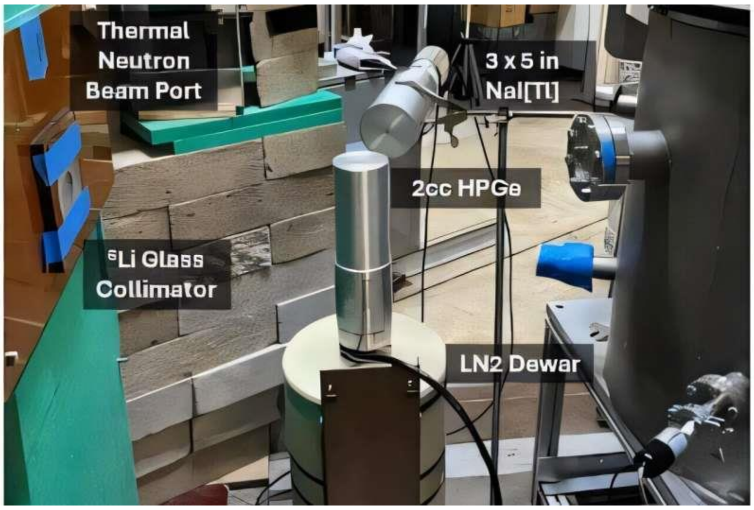

Experimental set up at The Ohio State University Nuclear Reactor Laboratory. The high purity germanium detector (HPGe) is within the path of a neutron beam while the sodium iodide (NaI) scintillation detector is placed to the side of the beam. Credit: Applied Nuclear Science Group (Prof. Jovanovic).

To accurately detect these tiny disturbances, detectors must first measure and understand nuclear recoils under a neutron beam to ensure proper calibration.

"Radiation is the means by which we observe the universe, be it in the Large Hadron Collider, dark matter experiments or nuclear experiments. Understanding how that radiation interacts with matter greatly impacts our ability to interpret measured results," said Igor Jovanovic, a U-M professor of nuclear engineering and radiological sciences and senior author of the study.

The research team performed an experiment measuring the response of germanium nuclei to 254 electron volt (eV) nuclear recoils, or about one fourth of a keV, as nuclear recoils to lower energy neutron beams are poorly understood. Two previous experiments measuring nuclear recoil at the same energy had conflicting ionization yields.

The experimental setup used a two cubic centimeter HPGe detector and an external sodium iodide (NaI) scintillation detector to measure ionizing radiation from nuclear recoils. To reconcile previous experimental differences, the researchers saved the raw output from both the HPGe and NaI detector using improved digital electronic recording devices.

Using the raw output improved shaping analysis, removing any signal processing biases, and allowed the same data to be analyzed using multiple algorithms to find the optimal method.

Results yielded a 50% higher ionization yield compared to a previously established theory, dramatically increasing the sensitivity of high purity germanium detectors to dark matter or neutrino detection.

"Our results could greatly improve the sensitivity of commercially available detector technologies for neutrino detection and impact the results of several ongoing neutrino experiments," said Alexander Kavner, a U-M doctoral graduate in the Applied Physics Program and lead author of the study.

Experimentation was conducted at The Ohio State University Nuclear Reactor

TEXT 8.7

Successful experiment paves the way for discovery of a new element/
Успешный эксперимент открывает путь к открытию нового элемента

NOVEMBER 3, 2024.by Lund University (2390)

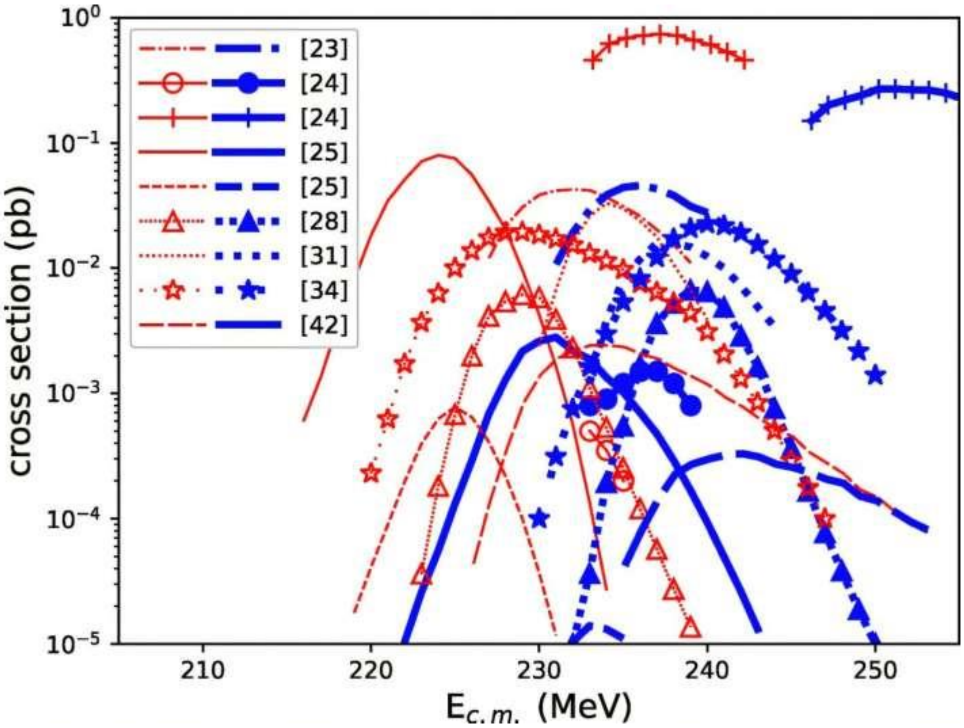

Theoretical predictions of cross sections for the production of element Z=120. Credit: *Physical Review Letters* (2024). DOI: 10.1103/PhysRevLett.133.172502

The search for new elements comes from the dream of finding a variant that is sufficiently stable to be long-lived and not prone to immediate decay. There is a theory in nuclear physics about an island of stability of superheavy elements. This is a potential zone in the upper part of the periodic table of as-yet-undiscovered elements that could remain stable for longer than just a few seconds. The aim is to explore the limits of stability of atomic nuclei.

In a study involving Lund University, Sweden, researchers have tested a new method for observing the element livermorium, which has 116 protons in its atomic nucleus. The research shows that the new method is a promising step forward for embarking on the mission to produce element 120, which would be the heaviest element to date. The work is published in the journal *Physical Review Letters*.

"We were able to register a livermorium nucleus in our detector just eight days into the experiment, which shows that we had chosen pretty good settings from the start," says Dirk Rudolph, one of the researchers from Lund University engaged in the new study.

The experiment campaign was conducted at the Berkeley Lab in the United States. For Dirk Rudolph and his Lund colleagues, it is a feather in their cap to have been entrusted with supplying the new detector system for the extensive experiments at Berkeley. The detector from Lund, called SHREC, was flown to the United States in the researchers' hand luggage. The heart of the detector is a small box containing 14 customized silicon wafers.

Research on superheavy elements first requires an accelerator to deliver an intense ion beam, which is then focused onto a target. The target consists of a thin layer of an element heavier than uranium. The product formed during the fusion reaction can be registered in a detector system after an efficient separation.

"I'm very proud that SHREC performed like clockwork in the experimental setup right after we brought it with us from Lund," says Pavel Golubev, the detector expert in the Lund team.

The livermorium experiment will continue for the rest of the year, after which the researchers plan to start work on trying to produce element number 120, which could take several years.

TEXT 8.8

New technique enhances precision in measuring short-lived atomic nuclei/ Новая методика повышает точность измерений короткоживущих атомных ядер

OCTOBER 17, 2024.by Nuclear Science and Techniques (4066)

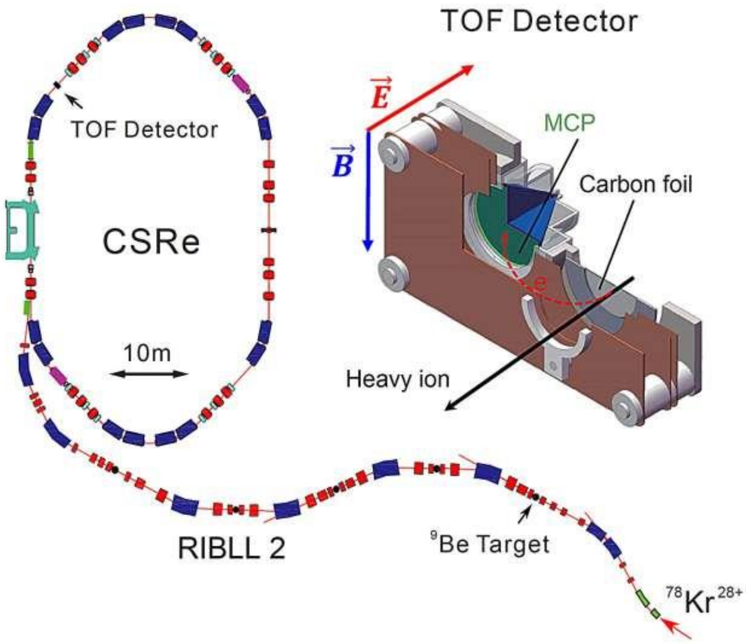

Layout of the experimental Cooler Storage Ring of the Heavy Ion Research Facility in Lanzhou, together with a schematic diagram of the TOF detector. Credit: Han-Yu Deng

Researchers at the Heavy Ion Research Facility in Lanzhou (HIRFL-CSR) have introduced a technique, Tune-IMS, designed to improve the precision of isochronous mass spectrometry (IMS) in measuring short-lived atomic nuclei. The development offers refined data for nuclear structure studies and could have potential applications in astrophysics, nuclear energy, and medicine.

The Tune-IMS technique has proven its capability to enhance the mass precision of certain short-lived nuclei, such as ^{63}Ge, ^{65}As, ^{67}Se, and ^{71}Kr. Compared with the previous IMS method, it additionally utilizes betatron oscillation of the ions to further reduce the mass errors, which is particularly important for short-lived nuclides.

"Our method can achieve higher precision for isotopes that have been challenging to measure," said Prof. Meng Wang, lead researcher on the project. "This may benefit ongoing studies in nuclear physics and related fields."

The findings are published in the journal *Nuclear Science and Techniques*.

The improved precision provided by Tune-IMS may offer more reliable data for researchers studying nuclear reactions, which are important for understanding processes such as stellar evolution and the formation of elements in stars. More accurate mass measurements could also contribute to nuclear energy research, where precise data can enhance the efficiency of reactors and improve safety protocols.

In addition, the advancement may assist in nuclear medicine, where isotopes used in diagnostic imaging and therapeutic treatments require accurate mass data for stability and effectiveness.

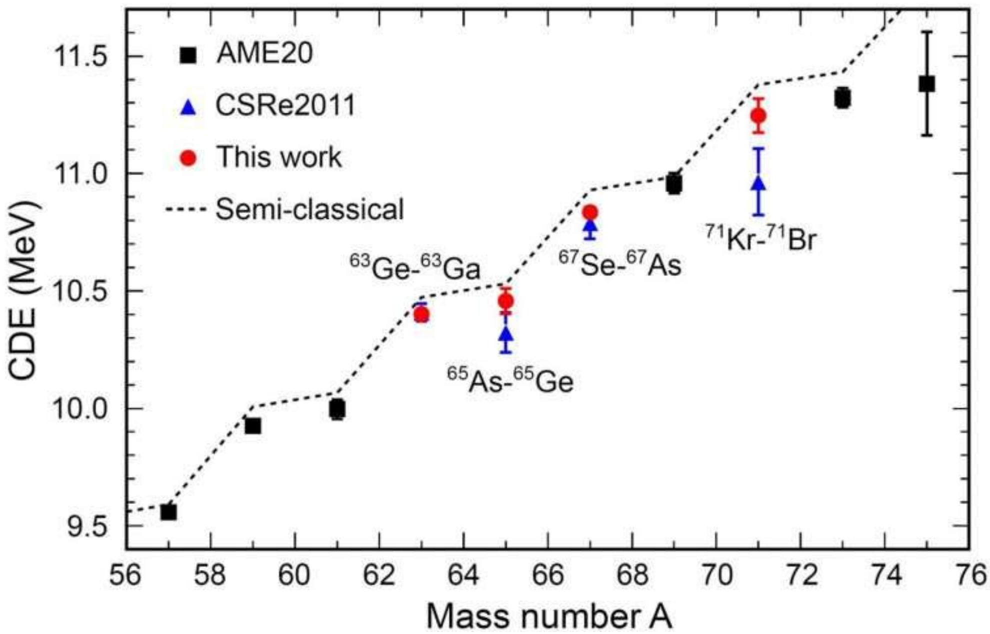

The comparison of CDEs for TZ = ±1/2 mirror pairs obtained by using experimental masses from AME20, CSRe2011, and this work. The dotted line denotes the result from a semi-classical approach. Credit: Han-Yu Deng

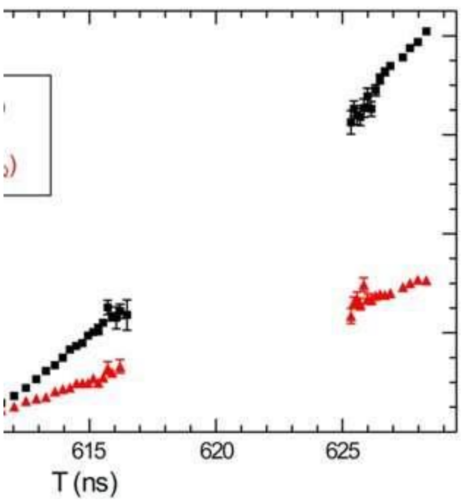

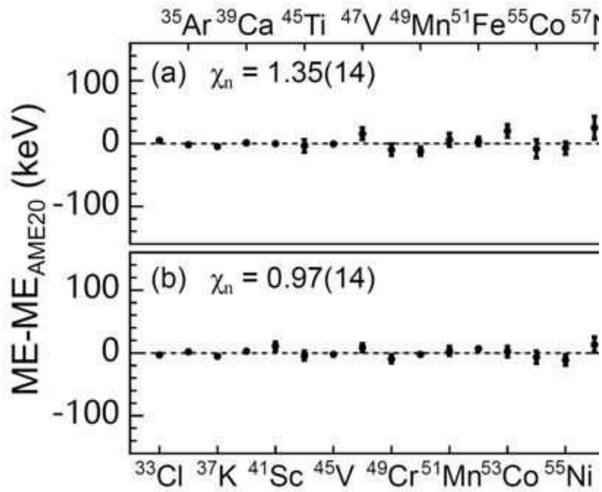

Left: The standard deviation of the revolution time with (red filled triangles) and without (black filled squares) the new technology. Right: The comparison of the re-determined mass values for the reference nuclides with (a) and without (b) the new technology. Credit: Han-Yu Deng

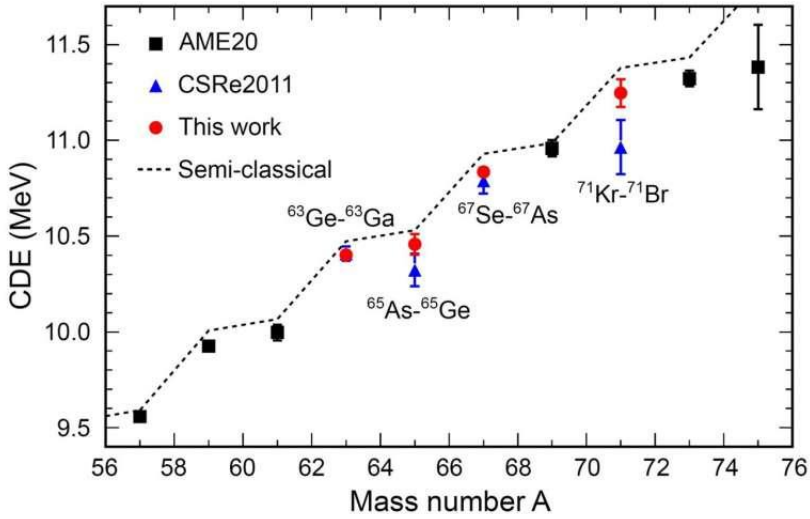

The comparison of CDEs for TZ = ±1/2 mirror pairs obtained by using experimental masses from AME20, CSRe2011, and this work. The dotted line denotes the result from a semi-classical approach. Credit: Han-Yu Deng

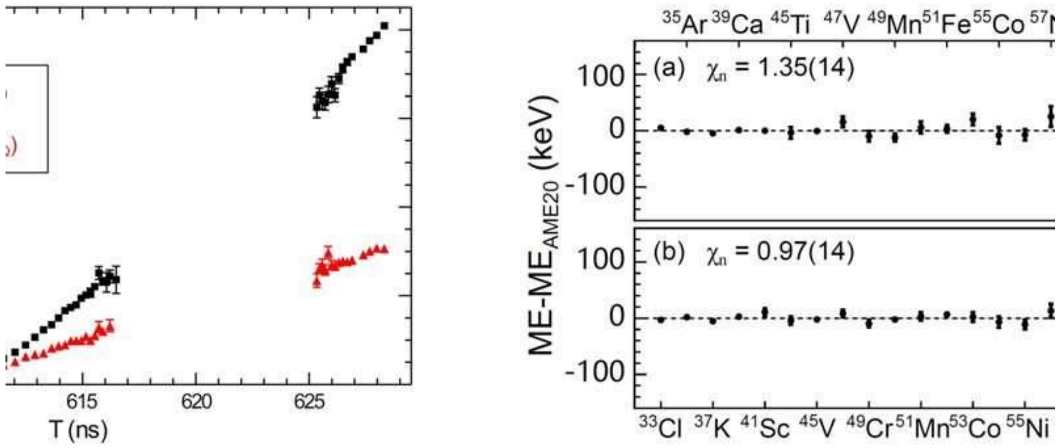

Left: The standard deviation of the revolution time with (red filled triangles) and without (black filled squares) the new technology. Right: The comparison of the re-determined mass values for the reference nuclides with (a) and without (b) the

Conventional isochronous mass spectrometry (IMS) has faced challenges in achieving high accuracy, particularly with short-lived nuclei. These limitations have been tied to the spread of magnetic rigidity in ions, which can affect the resolution of mass measurements.

The Tune-IMS technique addresses this issue by utilizing betatron oscillations, which reduce the spread in revolution times and thus improve measurement precision. This method has been successfully tested on several nuclides and has compared favorably with established IMS methods.

While Tune-IMS offers improvements, the current method requires the selection of specific oscillation values, which limits the number of ions available for analysis. The research team is developing a new time-of-flight detector with positional sensitivity to address this limitation, aiming to increase the method's efficiency and applicability.

"By improving the sensitivity of our detectors, we hope to expand the range of nuclei that can be studied with Tune-IMS," Prof. Wang noted.

The Tune-IMS technique represents a refinement in the precision of mass measurements for short-lived atomic nuclei, with potential applications in both fundamental nuclear research and practical fields like nuclear energy and medicine. Researchers at HIRFL-CSR plan to continue developing the technology to broaden its scope.

TEXT 8.9

A new tool for faster, more in-depth analysis of nuclear properties and mass data/ Новый инструмент для более быстрого и углубленного анализа ядерных свойств и данных о массе

OCTOBER 25, 2024.by Nuclear Science and Techniques (3873)

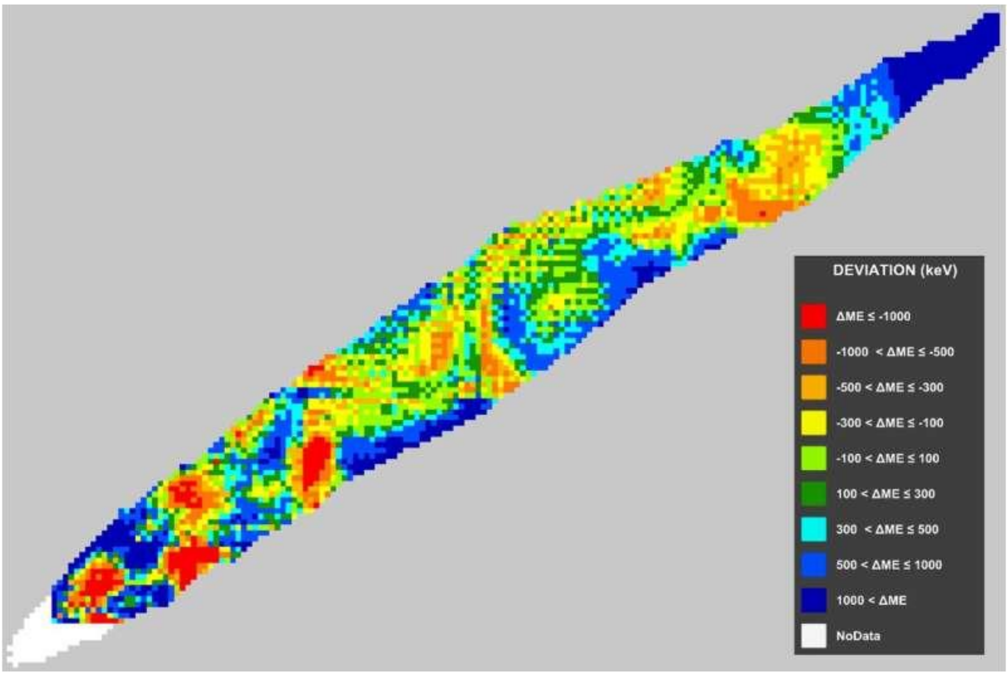

Mass-excess value differences between experimental data from AME2020 and predictions from mass model FRDM12. Credit: Wenjia Huang

A significant advancement in nuclear-data analysis has been achieved, which is relevant for several key areas, ranging from particle and nuclear physics to clean energy and health care. Researchers have developed a new tool to process nuclear data in a faster and more transparent way, helping to advance technologies that rely on nuclear science. The study is published in the journal *Nuclear Science and Techniques*.

Nuclear data is crucial for advancing our understanding of particle and nuclear physics, as it provides essential information on the properties and interactions of various nuclei and particles. Accurate nuclear data allows researchers to validate theoretical models, leading to more precise descriptions and predictions of nuclear phenomena.

By compiling and regularly updating nuclear data, scientists can enhance their ability to decipher fundamental questions about the universe's building blocks and the forces that govern their behavior, ultimately paving the way for new technological innovations and discoveries.

This development may also contribute to clean energy initiatives, particularly in advancing nuclear fusion research. Innovations in this area could help address energy needs while minimizing impacts on the environment.

In health care, enhanced nuclear data could refine medical imaging and treatment methods such as radiation therapy, offering more effective options for diagnosing and treating complex diseases.

Top Nuclear properties of 127Sn for the ground and isomeric states in order of excitation energies. (Bottom) Example illustrating the new features of mass lineage in Nuclues++: the mass of the primary nuclide 127Sn is determined from a Penning-trap mass measurement and three beta-decay end-point energy measurements. Credit: Wenjia Huang

The software, Nucleus++, developed by the Chinese Academy of Sciences and Advanced Energy Science and Technology Guangdong Laboratory, in collaboration with Université Paris-Saclay and Argonne National Laboratory, integrates nuclear mass data from the AME and nuclear physics properties from NUBASE, providing faster and more in-depth analysis for researchers worldwide.

With collaboration among leading international research institutions, this improved approach for nuclear data analysis will help efforts in energy, health care, and space exploration, benefiting people around the world.

TEXT 8.10

Accelerator lab provides detailed data on the 'magic' N=50 neutron shell closure/ Лаборатория ускорителей предоставляет подробные данные о "волшебном" закрытии нейтронной оболочки N=50

NOVEMBER 7, 2024.by University of Jyväskylä (4425)

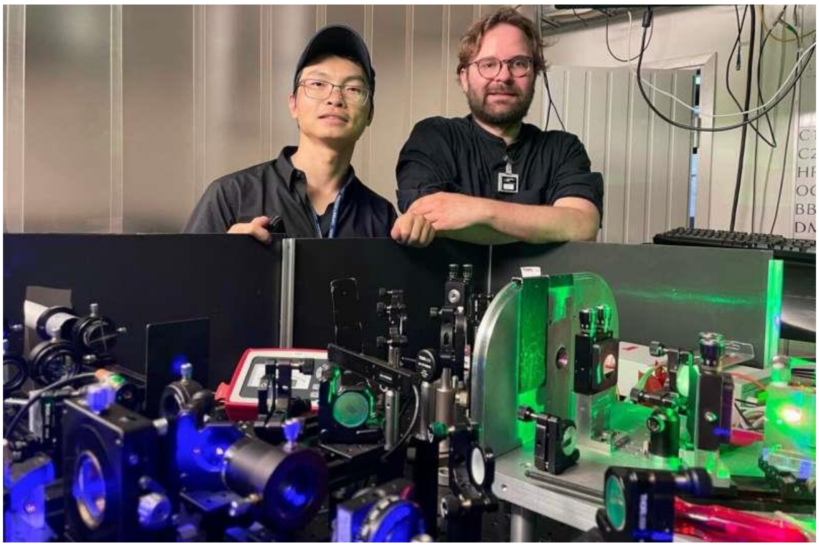

Researchers Mikael Reponen and Zhuang Ge from the Department of Physics of the University of Jyväskylä has measured more detailed data on the "magic" N=50 neutron shell closure. Credit: University of Jyväskylä

Researchers from the Department of Physics of the University of Jyväskylä (Finland) have found new information about the strength of the so-called magic neutron number 50 shell closure in the silver isotope chain.

The new more detailed information on the properties of the nuclei will contribute crucial information for refining our understanding of nuclear forces. The research improves state-of-the-art theoretical models and thus benefits the global description of the atomic nucleus.

Nuclear physicists have focused their attention at the area below tin-100 (^{100}Sn) on the nuclear chart. The area near tin-100, the heaviest doubly magic self-conjugate nucleus, exhibits diverse nuclear structure phenomena.

Essential nuclear properties, such as the binding energies of exotic nuclei in this region, are vital for assessing shell closure stability and the evolution of single-particle energies. Additionally, these properties aid in studying the proton–neutron interaction on long-lived isomers and the proximity of the proton drip line.

"Furthermore, binding energies offer essential data for accurately describing astrophysical processes like rapid proton capture. Precise nuclear data serve as a critical benchmark for theoretical predictions in nuclear physics, ensuring the accuracy and reliability of theoretical models.

"The charge radii behavior observed in our breakthrough work supported the magicity of N=50 in the silver isotopic chain," explains Staff Scientist, docent, Mikael Reponen from University of Jyväskylä.

The study has been published in *Physical Review Letters* and is also a direct follow-up to the researchers' previous publication in *Nature Communications*.

New technology for more detailed data

In the latest work, researchers have utilized an efficient hot-cavity catcher laser ion source coupled with a Penning trap mass spectrometer employing a state-of-the-art phase-imaging ion-cyclotron resonance (PI-ICR) technique. This has allowed the investigation of the magic N = 50 neutron shell closure in exotic silver isotopes in even more detail.

"The use of novel production methods for exotic nuclei, combined with high precision mass measurement techniques enabled the ground state masses of silver- 95−97 nuclei and the isomeric state in silver-96 to be probed with a precision of about 1 keV/c^2 even with yields as low as one event every 10 minutes," says Academy Research Fellow Zhuang Ge from the University of Jyväskylä.

These new mass values quantify the robustness of the N = 50 shell closure in the silver isotopic chain and benchmark state-of-the-art nuclear ab initio, density functional theory, and shell model calculations near the N = Z line, continues Ge.

Theorists must replicate experimental results

The precise excitation energy of the silver-96 isomer serves as a benchmark for ab initio predictions of nuclear properties beyond the ground state, especially for odd-odd nuclei close to the proton dripline near tin-100.

Moreover, the first precise measurement of the excitation energy of the isomer of silver-96, as a possible astrophysical nuclear isomer, enables the ground state and isomer of silver-96 to be treated as separate species in astrophysical modeling.

"All applied theoretical approaches face challenges in reproducing the trend of nuclear ground-state properties across the N = 50 neutron shell and towards the proton dripline. Our measurements thus contribute crucial information for refining the nuclear forces to improve these theoretical models and thus benefit the global description of the atomic nucleus," says Ge.

More detailed isotope measurements

This work highlights the scientific capabilities of the new experimental method employed for the first time at the IGISOL facility of the Accelerator Laboratory. The coupling of the phase-imaging Penning-trap mass spectrometer technique with the hot-cavity catcher laser ion source provides remarkably high sensitivity that enables high-precision mass measurements of exotic isotopes with exceedingly low yields.

"Ongoing studies, based on the achievements of this work, will shed light on the ground- state properties along the N=Z line in the immediate region below tin-100 in the near-future," says Reponen.

TEXT 8.11

New insights into exotic nuclei creation using Langevin equation model/ Новое понимание создания экзотических ядер с использованием модели уравнения Ланжевена

OCTOBER 11, 2024.by Nuclear Science and Techniques (3935)

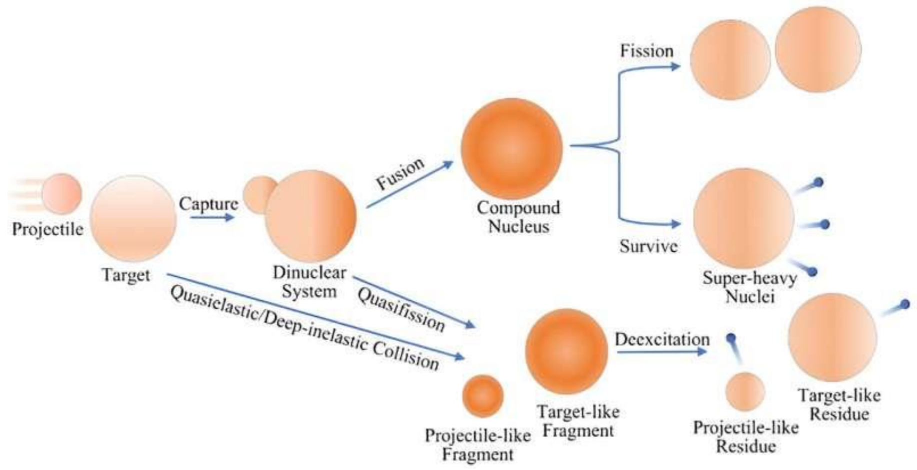

Evolution of nuclear system in fusion and MNT reactions. MNT reactions encompass quasi-elastic (QE), deep inelastic (DI), and quasi-fission (QF) processes. Understanding the complex mechanisms involved in MNT reactions presents significant challenges for theoretical investigations. Credit: Minghao Zhang

Researchers have introduced a model based on the Langevin equation that offers new insights into the formation of exotic nuclei. This development could enhance the ability to produce rare isotopes that are valuable for various applications in science and medicine.

The study is published in the journal *Nuclear Science and Techniques*.

A research team led by Professor Feng-Shou Zhang has developed and applied this model to study multinucleon transfer (MNT) processes in heavy-ion collisions. The model provides a more precise understanding of energy dissipation during heavy-ion collisions, which is important for predicting nuclear reaction outcomes. Simulations of nuclear reactions, such as $^{40}Ar + ^{232}Th$, $^{136}Xe + ^{238}U$, and $^{136}Xe + ^{209}Bi$, have shown that the model's predictions of cross-sections and angular distributions are in good agreement with experimental results.

Modeling nuclear reactions, particularly those involved in producing exotic nuclei, is challenging due to their complexity. Conventional methods like projectile fragmentation and fusion-evaporation have limitations, particularly in synthesizing new transuranium and superheavy elements.

This model addresses these challenges by simplifying the process, reducing the number of adjustable parameters, and focusing on key physical processes. It successfully simulates energy and scattering angle distributions, offering insights into deep inelastic and quasi-fission processes.

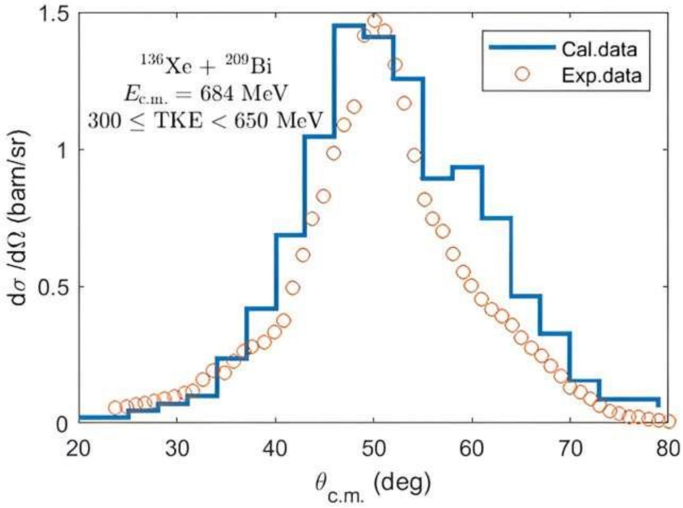

Center-of-mass angular distribution of the damped cross section for events with TKE within the indicated range in the ^{136}Xe + ^{209}Bi reaction at E_{lab} = 1130 MeV. Histogram is the calculation. Credit: Ying Zou

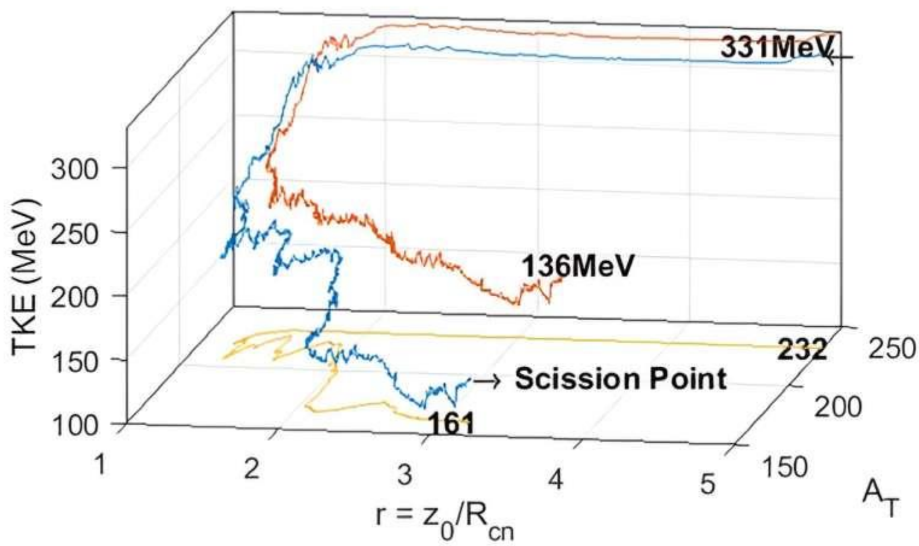

A simulated trajectory for the ^{40}Ar + ^{232}Th collision at E_{lab} = 388 MeV. The trajectory and its projections of the evolution of total kinetic energy (TKE), elongation, and mass of heavier nucleus are illustrated. For each impact parameter, 500 trajectories have been simulated. Credit: Ying Zou

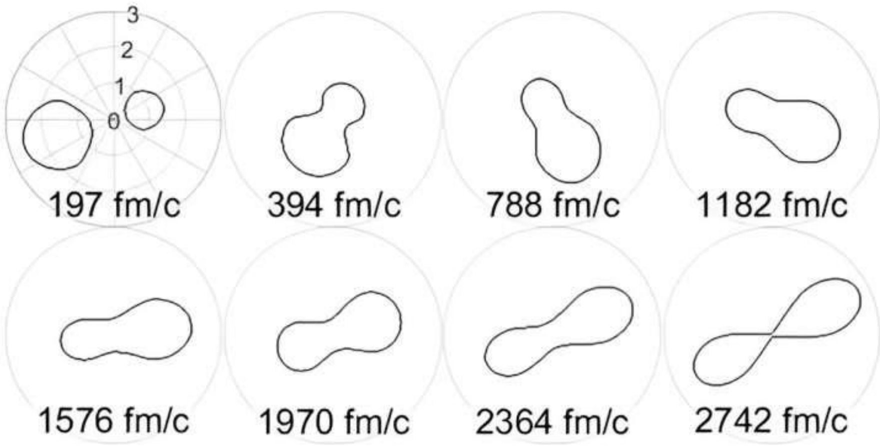

Profile of the trajectory in Fig.2 at the indicated time. The Langevin equation model, as a phenomenological approach, simulates nuclear reactions by solving for the evolution of collective coordinates. The system's shape evolution depicted in the figure illustrates the collective coordinates during the simulation. Credit: Ying Zou

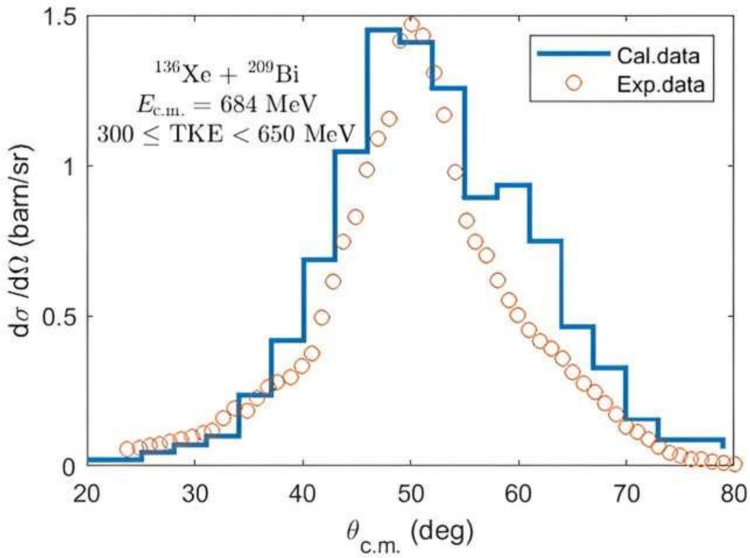

Center-of-mass angular distribution of the damped cross section for events with TKE within the indicated range in the $^{136}Xe + ^{209}Bi$ reaction at E_{lab} = 1130 MeV. Histogram is the calculation. Credit: Ying Zou

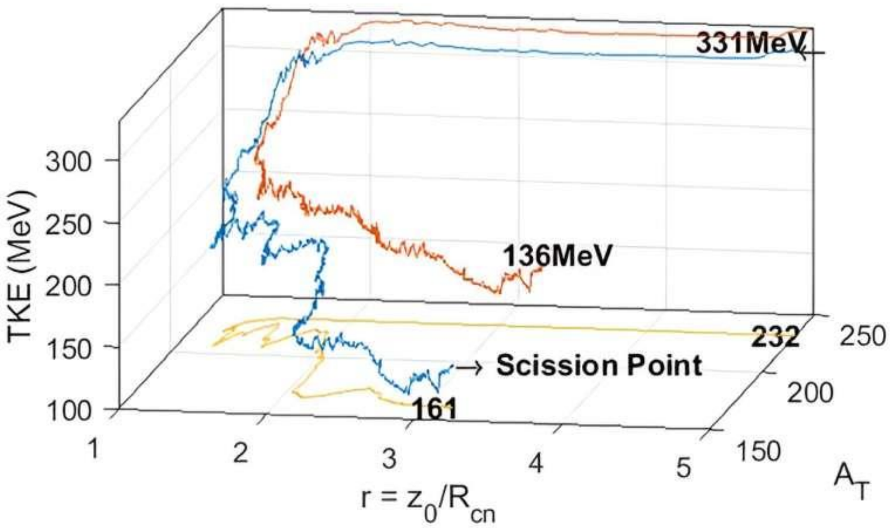

A simulated trajectory for the ^{40}Ar + ^{232}Th collision at E_{lab} = 388 MeV. The trajectory and its projections of the evolution of total kinetic energy (TKE), elongation, and mass of heavier nucleus are illustrated. For each impact parameter, 500 trajectories have been simulated. Credit: Ying Zou

The improved accuracy of MNT reaction predictions provided by this model could facilitate the production of isotopes that are difficult to generate using other methods. These isotopes are valuable for scientific research and medical applications, such as diagnostics and treatments. According to Prof. Zhang, the goal is to keep the model comprehensive yet practical for experimental use.

This development represents a step forward in nuclear physics, contributing to the understanding of exotic nuclei production through MNT reactions. Further refinement of the model may enhance its utility in guiding future research and improving rare isotope production processes.

This research was conducted in collaboration with Beijing Normal University, Beijing Academy of Science and Technology, and the National Laboratory of Heavy Ion Accelerator of Lanzhou.

9 Тексты по электротехнике

TEXT 9.1

Buck Regulators Solve the Power Thirst of the Transmitter Circuit in Current Loops/ Понижающие регуляторы решают проблему энергопотребления схемы передатчика в токовых контурах

October 2022. by Zhongming Ye (17000)

This article explains how to design a compact power supply for a current loop transmitter using the LT8618, a 100 mA high speed synchronous monolithic step-down switching regulator, instead of an LDO regulator. Its performance is evaluated and the components required to satisfy stringent industrial standards are selected. Efficiency, start-up, and ripple test data are provided.(630)

Autonomous control is increasingly prevalent in industrial and consumer applications, but even cutting-edge autonomy solutions rely on an old technique: the current loop. Current loops are a ubiquitous component in control loops that work both directions: they convey measurements from sensors to programmable logic controllers (PLCs) and conversely convey control outputs from the PLC to process modulation devices.

Autonomous Control Solutions

The 4 mA to 20 mA current loop is the dominant industry standard for accurate and reliable data transmission via a twisted pair cable from remote sensors to a PLC. Simplicity, longevity, robustness, proven reliable data transfer over long distances, good noise immunity, and low implementation cost make this interface well-suited to long-term industrial process control and automated monitoring of remote objects in noisy environments. Traditionally, power for the current loops is supplied through linear regulators for many of the previously listed reasons. The downsides to using linear regulators—when compared to switching regulators—are their relative inefficiency and limited current capability. Inefficiencies can lead to heat dissipation problems, and limited current often precludes the addition of desired control system functionality.

New high efficiency, high input voltage buck regulators are robust and small enough to replace linear regulators in many current loop systems. The advantages of a buck over a linear regulator are many—including higher current capability, wider input ranges, and higher system efficiency. Significant performance advantages can be found in buck regulators that feature low minimum tON times at high switching frequencies, yielding compact, robust solutions.

The standard 4 mA to 20 mA current loop shown in Figure 1 can be used for carrying both sensor information from field instrumentation and control signals to the process modulating devices, such as a valve positioner or other output actuator. It consists of four components: (1670)

- The current loop power source: The power supply VDC voltage varies (9 VDC, 12 VDC, 24 VDC, etc.) depending on the application, with at least 10% higher potential than the voltage drop of the combined components in the circuit (for example, transmitter, receiver, and wires). This VDC is tapped by local step-down regulators to supply power to sensors and other components.
- The transmitter: The main component of the transmitter is the sensor or transducer. It converts a physical signal—such as temperature, pressure, current, distance, or a magnetic field—into an electrical signal. If the converted signal is an analog voltage, a voltage-to-current converter that's part of the transmitter is required to convert it to a 4 mA to 20 mA current signal. In the case of a smart-digital output sensor, a DAC converts the digital signal back to an analog signal. A local power supply in the transmitter—LDO or buck regulator—powers all these analog, digital, and reference circuits.
- The receiver or monitor: The receiver converts the 4 mA to 20 mA current signal into a voltage signal, which can be further processed and/or displayed. The conversion of the current signal to use voltage levels is via a high precision shunt resistor RSHUNT, and/or analog-to-digital converter or data acquisition circuit. In the instrument terminal, local buck regulators power the receiver circuits.
- The 2- or 4-wire loop: A complete current loop circuit can stretch over 2000 feet and comprise the series connected transmitter, power supply, and receiver. In 2-wire 4 mA to 20 mA current loops, the power supply shares the same loop with the current loop.

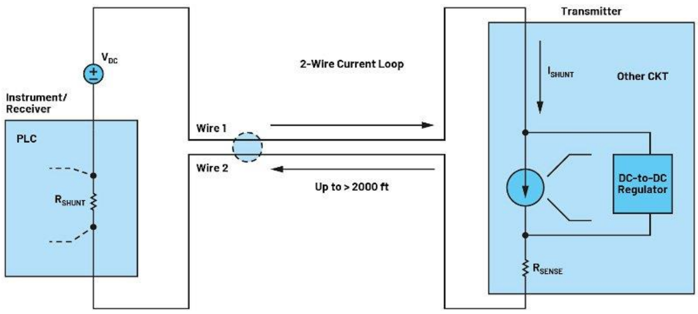

Figure 1. Diagram of a 2-wire current loop.

For example, to measure 0 psi to 50 psi of pressure using a remote pressure transducer, the 4 mA to 20 mA current receiver circuit is in series with the pressure-to-current transducer. On the sensor side, it reads 4 mA when the pressure is 0 psi, and 20 mA when the pressure is 50 psi. On the receiver side, Kirchhoff's first law tells us that an identical current appears at the shunt resistor, where it is converted to a voltage signal.

Autonomous operations in industry, refinery, highway monitoring, and consumer applications require high-performance sensor technologies and reliable, accurate current loops to convey sensor information. The components of the current loop must maintain high accuracy, low power, and reliable operation over an extended –40°C to +105°C industrial range, with required security and system features.

The source voltage at the transmitter (sensor) side can be up to 65 V during transients, which must be converted down to 5 V or 3.3 V. As the sensor circuitry is often designed to draw power directly from the current loop (no additional, local power source), it is typically limited to 3.5 mA. As more functionality and features are added at the transmitter, this limit becomes a problem when traditional linear regulators are used, which cannot provide any additional current. In addition, most of the power in the system using a linear regulator must be burned in the regulator itself, producing significant heat in an encapsulated system.

The LT8618 extends the input range to 65 V and expands the load capability to 15 mA. Its high efficiency takes the thermal constraint out of the current loop system design, where the transmitters are encapsulated and exposed to harsh environmental variations. A low-cost filter is proposed to reduce the voltage ripple and the cable side current ripple. The article analyzes the performance of the power regulator and provides the component selection guideline to meet rigorous industrial requirements. Test data for efficiency, startup, ripple, etc. are provided.

Close the Current Loop Using a Buck Converter With Extended Input and Load Ranges

The LT8618 is a compact buck converter with many features meeting the requirements of industrial, automotive, and other unpredictable power source environments. It readily fits 4 mA to 20 mA current loop applications, with ultralow quiescent current, high efficiency, wide input range, up to 65 V, and compact size. Figure 2 shows a complete transmitter circuit solution using the LT8618 to power the MAX6192C high accuracy reference, voltage-to-current conversion, and other circuits.

The current at the shunt circuit 2SC1623 is proportional to the voltage applied at the positive input of the error amplifier (EA). The 2.5 V reference voltage is produced by the MAX6192C, a precision reference IC with low noise, low dropout, and low-temperature drift of 5 ppm/°C (max). In the case of a smart sensor with a digital output proportional to the environmental variables, a DAC can convert the digital to an analog signal and feed it to the error amplifier.

ISHUNT=(VDC1+VREF)R12R11RSENSE(1)ISHUNT=(VDC1+VREF)R12R1
1RSENSE(1)

Therefore, with the EA, the BJT (2SC1623), and the 100 Ω (±0.1%) sense resistor (RSENSE), the transducer modulates the current in the current loop from 4 mA to 20 mA, where 4 mA represents a live zero and 20 mA represents the maximum signal. The live or elevated zero of 4 mA allows for the device to be powered even with no process signal output from the field transmitter. Hence, the current in the shunt circuit is proportional to the environmental variables, such as pressure, temperature, level, flow, humility, radiation, pH, or other process variables.

The two long wires are part of the information-carrying current loop and are also used to provide power to the transmitter from VDC, the power supply on the receiver side. The minimum voltage of the VDC should be enough to cover the voltage drop across the wires, shunt, and the minimum operating voltage of the transmitter. The source voltage is application dependent, typically 12 V or 24 V, but can be as high as 36 V.

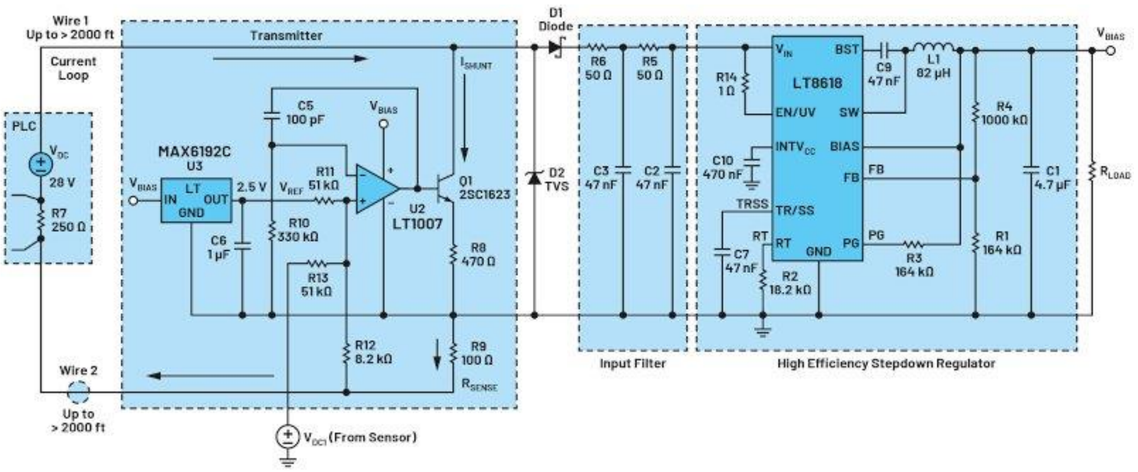

Figure 2. The current loop with LT8618 as a DC power source.

At the remote transmitter terminal, a Schottky diode (D1) protects the transmitter from reverse current flow. Further protection is provided by a Zener or TVS (D2) diode placed across the input to limit transient voltage surges, which are proportional to the inductance of the current loop. The loop voltage is stepped down by the LT8618 high-efficiency monolithic buck regulator to 5.5 V or 3.3 V— to power the reference, DAC, and other function blocks.

In Figure 2, the wires between VDC and the transmitter can range from several feet to 2000 feet. The stray inductance of the current loop forms an LC resonant tank with the input capacitor of the buck regulator. A transient on the power supply side (VDC) also appears at the remote transmitter's input side. For a worst-case undamped oscillation, the peak voltage can double that of the VDC. For instance, if the operating input voltage is 24 V, typical with a maximum specification of 36 V, the maximum voltage on the transmitter side is at risk of going beyond 65 V. Easy protection can be implemented using a TVS diode D2 in front of the transmitter to limit any surge during transient, as shown in Figure 2.

Alternatively, an efficient system could be built by protecting the LT8618 from high voltage excursions with an LDO regulator. In such a topology, the LDO regulator would regulate to the input minus its dropout voltage with the LT8618 converting this ~24 V to 5 V or 3.3 V with high efficiency. The current limit of the LDO regulator should be set below the typical 3.8 mA while also maintaining high efficiency and the input capacitor of the LT8618 basically serves both as a decoupling and reservoir capacitor as well. This would enable short bursts of high loads downstream with minimal to no current draw in the current loop. Since high voltage excursions are short, typically carrying little overall energy, the resulting power loss in the LDO regulator during these transients does not impair overall efficiency; that is, the LDO regulator spends nearly all of its time at a high step-down ratio.

A typical current loop limits the input current of the power circuit that is powering the complete remote transmitter, and available load current from an LDO regulator cannot exceed this input current limit. On the other hand, a buck regulator can multiply the input current supplied to the load. Figure 3 shows output current vs. input current of the LT8618 regulator for a 24 V input to 5.5 V conversion. For an input current limit of 3.8 mA, the output current is almost 15 mA. This extra power simplifies the system designer's job by increasing operational headroom and enabling additional functional blocks.

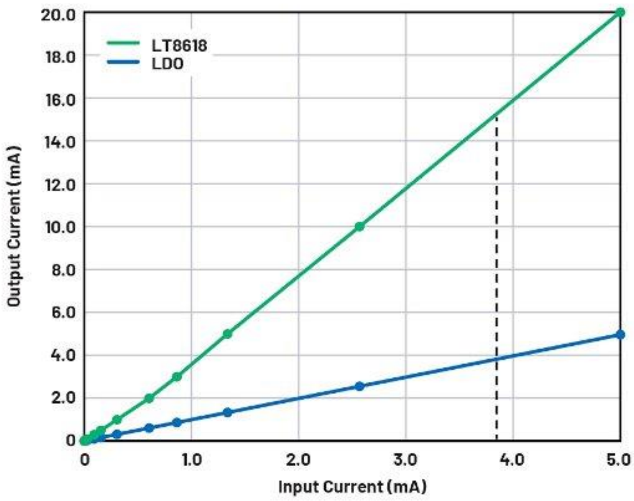

Figure 3. Output current vs. input current, V_{IN} = 24 V, V_{OUT} = 5.5 V.

Burst Mode Operation Improves Efficiency at Tiny Loads

An LDO regulator's efficiency is proportional to the step-down ratio (VOUT/VIN) and can be efficient when the input voltage is slightly higher than the output. The problem arises at high step-down ratios, where efficiency is very low, producing significant thermal stress on the system. For instance, with the input at 55 V and output at 3.3 V, the power loss of the LDO regulator is 0.19 W with 3.8 mA of load current. In contrast, a properly designed buck regulator can be very efficient at high step-down ratios. Furthermore, synchronous buck regulators can increase efficiency over nonsynchronous counterparts by replacing the catch diode with a MOSFET. The challenge with a synchronous buck converter is optimizing the efficiency over the entire load range—specifically, at light loads of 3 mA to 15 mA, when the input can be as high as 65 V.

For a typical synchronous buck converter, three power losses dominate: switching losses, gate drive loss, and losses associated with the converter IC controller logic circuit. Switching and gate drive losses can be significantly reduced if the switching frequency is reduced, so simply running the converter at low frequency reduces the switching and gate losses at light loads.

At light loads, the bias loss of the logic circuits is on par with the relatively low switching-related losses. The bias circuit is normally powered from the output, only taking power from the input via an internal LDO regulator during startup and other transient conditions.

At light loads, the LT8618 addresses logic circuit losses by operating in Burst Mode®, where current is delivered in short pulses to the output capacitor, followed by relatively long sleep periods, where most of the logic control circuits are shut down.

To further improve the efficiency at light loads, a larger value inductor is preferred since more energy can be delivered to the output during the short switching pulses and the buck regulator can remain in sleep mode longer between those pulses. By maximizing the time between pulses and minimizing the switching losses of each short pulse, the LT8618 quiescent current can be less than 2.5 μA while maintaining the output in regulation from inputs up to 60 V. Since many transmitter circuits draw low current most of the time, this low quiescent current is a significant energy saver over typical bucks, which draw tens or hundreds of μA.

Figure 4 shows the efficiency of the current loop solution shown in Figure 2, with the 5.5 VOUT output rail tied to the BIAS pin of the LT8618. The peak efficiency reaches 87% at the full 100 mA load, with 28 V input, and an 82 μH inductor. The 10 mA load efficiency at or above 77% for the same 28 V input is arguably more impressive.

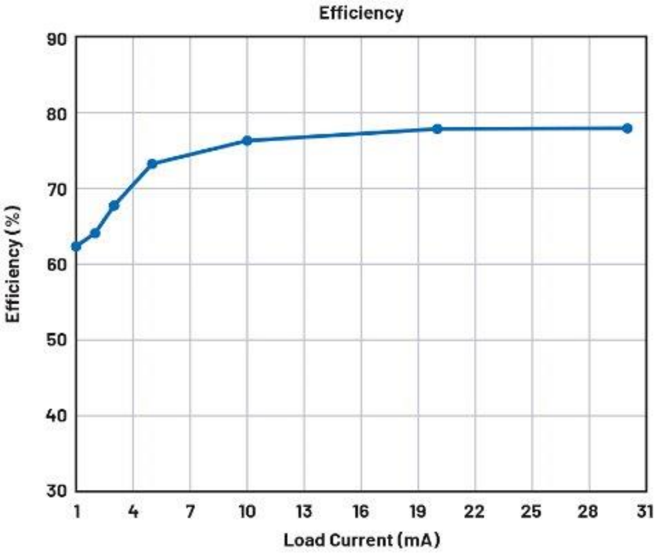

Figure 4. LT8618 high efficiency at light load,

V_{IN} = 28 V, V_{OUT} = 5.5 V, L = 82 µH.

Input Filter to Limit Both Inrush Current and Current Loop Ripple

The input of the power regulator is connected to the current loop, so it is important to limit the ripple current and inrush current during startup or load transients as well, in addition to the steady state current limit. The inrush current during the startup of a power converter depends on the sizes of the input and output capacitors for a given soft start time. This is the trade-off: minimize the input capacitor to prevent large inrush currents while making it big enough to maintain acceptable low ripple.

The input current of a buck converter is pulsed; therefore, the input capacitor plays a key role in providing a filter path for the ripple current. Without this capacitor, a significant amount of ripple current would flow through the long current loop causing the buck to behave unpredictably. Therefore, a minimum input capacitance meets ripple current and ripple voltage requirements. Multilayer ceramic capacitors (MLCC) have the best performance with regard to ripple current, due to their low ESR and ESL.

When the converter operates in Burst Mode, the inductor current follows a triangular waveform. The impedance of the current loop is much higher than the input filter. Therefore, the ripple voltage across the input capacitor can be estimated by the following equation, ignoring the capacitor's ESR and ESL, where IPEAK is the burst current in the buck inductor, and VR is the ripple voltage across the input capacitor (obviously a bigger capacitance is needed for higher burst currents):

C=I2PEAKL2VRVIN(2)C=IPEAK2L2VRVIN(2)

To minimize the input voltage ripple while keeping the input capacitance as small as possible, we prefer a smaller buck inductance. Nevertheless, Burst Mode efficiency is better with a large inductor. For an 82 μH inductance, and 1 V ripple, to avoid triggering UVLO at any minimum input instance, a 100 nF input capacitor is sufficient for this application using the LT8618.

The majority of the ripple current goes through the local decoupling capacitor, and the residual portion shares the same path as the current loop. It is important to keep the current ripple in the cable side small since it will appear across the shunt sense resistor as voltage ripple, and the magnitude of the voltage ripple needs to be smaller than the resolution spec of the ADC reading the voltage across the shunt sense resistor. The current ripple can be further reduced by additional filters. An RC filter is a good design trade-off because the input current is small, and it is low cost compared to an LC filter. Smaller ripple currents can be further achieved with two or three cascaded stages of RC filters.

LTspice® simulations allow us to compare the current ripple at the source cable side for three different input filter structures, with a total resistance of 100 Ω in series in the input path, using the LT8618 with VIN = 28 V and VOUT = 5.5 V, and an 82 μH inductor. A current pulse is equivalent to what the input filter would see as input current to the LT8618 regulator for a 10 mA of output current.

A single-stage RC filter with 100 Ω and 100 nF has a current ripple of more than 60 μA peak-to-peak at the source cable side. The ripple current at the source cable side becomes smaller as more capacitance is added or filtering stages are cascaded. Given the fact that a buck regulator performs better with a bigger direct input capacitor, and that a 2-stage RC filter has a smaller BOM than a 3-stage one while delivering similar current ripple at the source cable side, we recommend the 2-stage filter with 50 Ω and 47 nF per stage. The source cable side ripple current is about 30 μA, and correspondingly it produces about 7.5 mV of ripple voltage across the 250 Ω shunt resistor, which is almost enough for an 8-bit resolution ADC. To further reduce the cable side ripple current, bigger capacitance can be used in the filters. For instance, if the 47 nF caps are replaced by 100 nF caps, the cable side ripple current can be reduced to just 7 μA, corresponding to a ripple voltage of 1.75 mV.

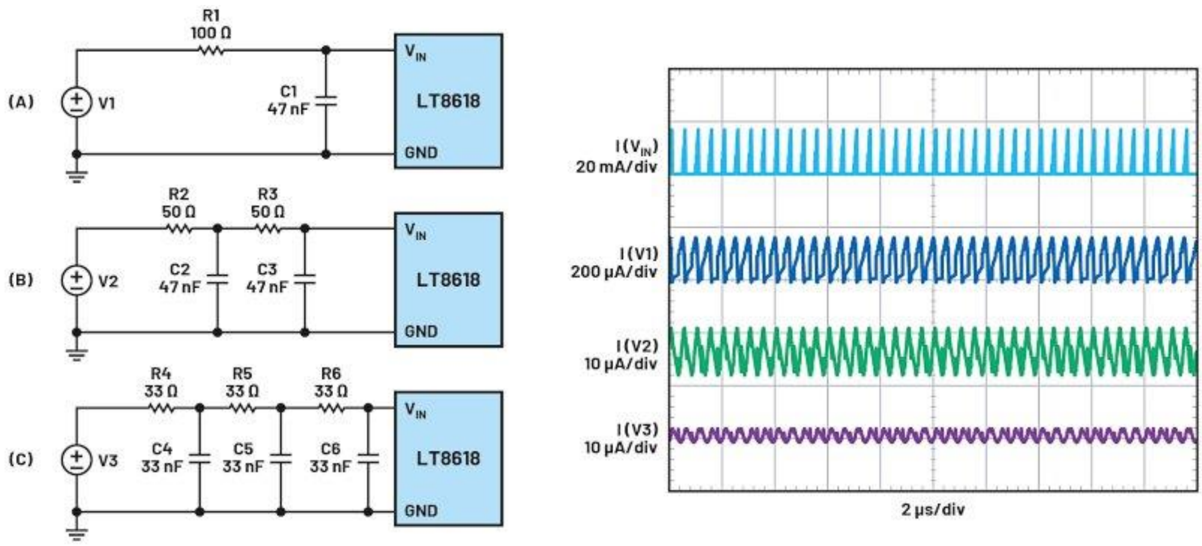

Figure 5. Current ripple at the source side of the current loop.

In typical current loop applications, customers would specify a current limit during startup (3.2 mA, for instance), with the exception of a specified short period of time where this limit could be exceeded. In a buck converter, a high inrush current is common to charge up the input capacitors. The function of the input filter is two-fold: in addition to limit the ripple current at the cable's source side, it also helps limit the start-up inrush current. Figure 6 shows the input current over time during the start-up behavior with the 2-stage input filter, for an input VIN of 24 V, and 4 mA of load current at the output side.

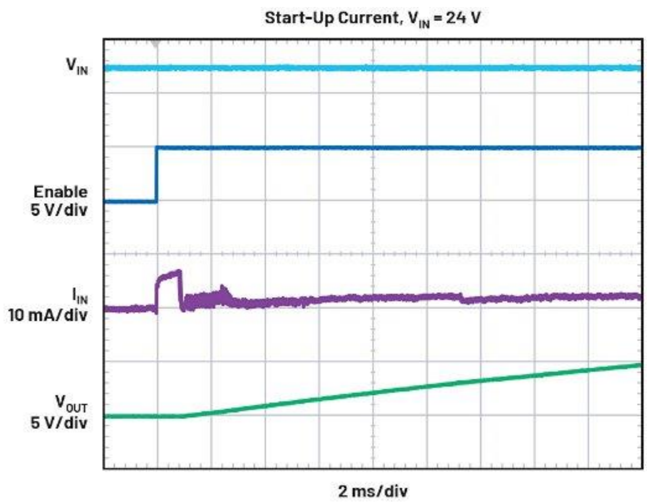

Figure 6. Start-up current with input filter to limit the inrush current (from top: input voltage 20 V/div, output voltage 5 V/div, enable, input current in the cable side, 10 mA/div).

Key Takeaways of Current Loops

Current loops are widely used in industrial and automotive systems to collect and transmit information from sensors to control systems, sometimes over relatively long wires. Conversely, the loop transmits controller outputs and modulation instructions to remote actuators and other devices. Significant efficiency and performance improvements can be realized by improving the power supplies in the current loop, notably by replacing traditionally used linear regulators with high-efficiency buck regulators, which also increases current capability and expands input ranges. High efficiency, high input voltage regulators in tiny packages with low minimum on times make it possible to produce compact overall solutions, comparable in size and robustness to LDO regulator solutions. This article showed how to use the LT8618 in a 4 mA to 20 mA current loop transmitter, meeting rigorous industrial requirements.

This article originally appeared in Bodo's Power Systems [PDF] magazine.

TEXT 9.2

Determining Power Factor Using the Two-Wattmeter Method/ Определение Коэффициента Мощности Методом Двух Ваттметров

September 08, 2024 by Amna Ahmad (7 816)

The ratio of true power to apparent power is called the power factor of the load. When the two-wattmeter method is used to measure the power dissipated in a balanced load, the power factor of the circuit can also be determined from the meter readings.

What is Power Factor?

Power factor is the ratio between the true power in watts and the apparent total power in volt-amps of an electrical load or system. Power factor is a measure of how efficiently the line current of a load or system is being converted into useful work output. The ideal power factor is unity (1 or 100%). Anything less than 1 means additional power is required to accomplish the actual task.

The power triangle below in Figure 1 illustrates the phase angle (θ) between true and apparent power. The cosine of the phase angle is known as the power factor (PF), and its value is inversely proportional to the amount of reactive power. The smaller the angle θ, the less reactive power present and the greater your power factor is.

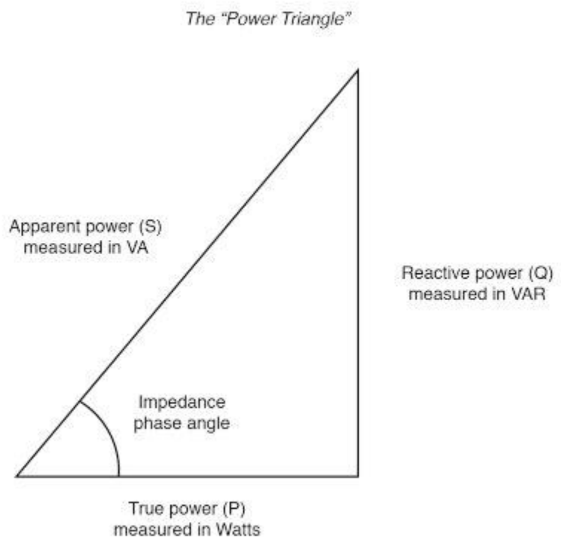

Figure 1. Power factor triangle.

Apparent power (VA) is equal to or greater than the true power (watts), depending on the power factor (PF). Therefore, when sizing circuits or equipment, you must size the circuit equipment according to the apparent power (volt-amperes) and not the true power (watts). Formulas that can be used for determining apparent power are as follows:

$$\text{Apparent Power (VA)} = \text{Volts} \times \text{Ampere (Single Phase)}$$

$$\text{Apparent Power (VA)} = 1.732 \times \text{Volts} \times \text{Ampere (Three Phase)}$$

$$\text{Apparent Power} = \frac{\text{True Power}}{\text{Power Factor}}$$

$$\text{Apparent Power} = \sqrt{(\text{True Power})^2 + (\text{Reactive Power})^2}$$

True power (watts) is the energy consumed by the resistive part of an AC circuit. The true power of a circuit that contains inductive and/or capacitive reactance in addition to resistance is measured with a wattmeter and can be calculated by use of one of the following formulas:

$$\text{True Power (W)} = \text{Volts} \times \text{Ampere} \times \text{Power Factor (Single Phase)}$$

$$\text{True Power (W)} = 1.732 \times \text{Volts} \times \text{Ampere} \times \text{Power Factor (Three Phase)}$$

$$\text{True Power} = \sqrt{(\text{Apparent Power})^2 - (\text{Reactive Power})^2}$$

Reactive power (VARs) is power supplied to a reactive load. Almost all AC circuits include reactive power in the form of inductive reactance and/or capacitive reactance. Inductive reactance is by far the most common since all motors, transformers, solenoids, and coils have inductive reactance. The formulas for determining reactive power are:

$$\text{Reactive Power (VARs)} = \text{Volts} \times \text{Ampere} \times \sin\theta \text{ (Single Phase)}$$

$$\text{Reactive Power (VARs)} = 1.732 \times \text{Volts} \times \text{Ampere} \times \sin\theta \ \text{(Three Phase)}$$

ReactivePower(VARs)=1.732×Volts×Ampere×Sinθ(ThreePhase)

$$\text{Reactive Power} = \sqrt{(\text{Apparent Power})^2 - (\text{True Power})^2}$$

Power factor (PF) is the ratio of true power (watts) to apparent power (VA) and is expressed as a percentage that does not go above 100 %. Power factor measures how far the current and voltage are out of phase with respect to each other. Unity power factor (1 or 100%) can only occur if the AC circuit supplies resistive loads or when capacitive reactance (XC) is equal to inductive reactance (XL). When the power factor is less than 100 percent, the circuit is less efficient and has a higher operating cost because not all current performs useful work.

The formulas for determining the power factor are

$$\text{Power Factor} = \frac{\text{True Power}}{\text{Apparent Power}}$$

PowerFactor=TruePowerApparentPower

$$\text{Power Factor} = \frac{\text{Watts}}{\text{VA}}$$

PowerFactor=WattsVA

Power Factor Determination

Consider the phasor diagram for a balanced Y-connected load, as shown in Figure 2. The phase voltages EAN, EBN, and ECN, have 120° phase differences and line voltages EAB, EBC, and ECA are 30° ahead of EAN, EBN, and ECN, respectively. The line currents IA, IB, and IC (also the phase currents in a Y-connected load) each lag the related phase voltage by phase angle φ.

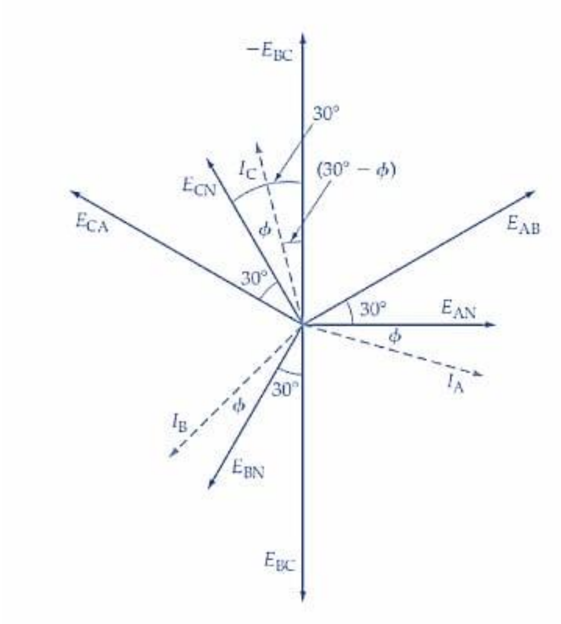

Figure 2. Phasor diagram for a two-wattmeter power measurement method with a balanced Y-connected load. The load power factor can also be determined from the meter readings.

Now, look at the circuit diagram in Figure 3. The current coil of wattmeter W1 carries line current IA, and the potential difference across its voltage coil is line voltage EAB. The phase difference between EAB and IA is (30°+φ) (see Figure1). Consequently, the power indicated by W1 is

$$P1 = E_{AB} I_A \cos(30° + \phi)$$

Because E_{AB} is line voltage V_L, and I_A is line current I_L,

$$P1 = V1IL \cos(30° + \phi) \quad (1)$$

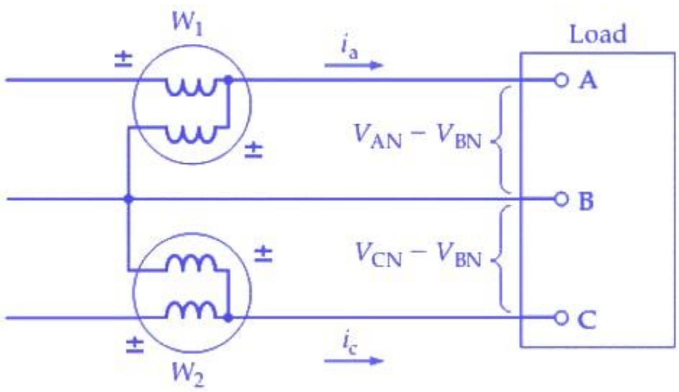

Figure 3. The two-wattmeter method is most often used for measuring three-phase power. It is appropriate for Δ- or Y-connected, balanced or unbalanced loads. The load power is determined by adding the meter readings.

In Figure 3, the current flowing in the current coil of wattmeter W2 is line current IC. The potential difference across its voltage coil is -EBC. If the voltage coil of W2 had been connected with its ± terminal to line B, the voltage would be +EBC. But when connected as illustrated, the voltage coil potential difference is -EBC. As shown in the phasor diagram in Figure 2, there is a 30° difference between -EBC and ECN. Because IC lags ECN by angle ϕ, the phase difference between –EBC and IC is (30°- φ). The power indicated by W2 can now be written as

$$P_2 = E_{BC} I_C \cos(30° + \phi)$$

Or

$$P_2 = V_L I_L \cos(30° - \phi) \qquad (2)$$

$$P_2 + P_1 = V_L I_L[\cos(30° - \phi) + \cos(30° + \phi)]$$

$$= V_L I_L(2 \cos 30° \cos \phi)$$

$$= \sqrt{3} V_L I_L \cos \phi$$

And

$$P_2 - P_1 = V_L I_L[\cos(30° - \phi) - \cos(30° + \phi)]$$

$$= V_L I_L \sin \phi$$

$$\frac{P_2 - P_1}{P_2 + P_1} = \frac{V_L I_L \sin \phi}{\sqrt{3} V_L I_L \cos \phi} = \frac{1}{\sqrt{3}} \tan \phi$$

Giving,

$$\phi = \tan^{-1} \sqrt{3} \left[\frac{P_2 - P_1}{P_2 + P_1} \right] \qquad (3)$$

In deriving Equation 3, it was assumed that ϕ is less than 60°. When ϕ is greater than 60°, (30°+ϕ) exceeds 90°, and cos (30°+ϕ) becomes a negative quantity, making the reading on wattmeter W1 negative. As noted, to get a positive indication, the connections to either the current coil or the voltage coil must be reversed, and the power measured by the wattmeter must be recorded as a negative quantity.

The two-wattmeter method does not indicate whether the calculated power factor is leading or lagging. This must be determined by considering the load. A largely inductive load has a lagging power factor, and a predominantly capacitive load has a leading power factor.

Example

The readings of the two wattmeters connected to measure the total power in a three-phase wye-connected 400-Volts system are 4 kW and 6 kW. Calculate the power factor.

Solution

Wattmeter 1 reading = P_1 = 4000 W

Wattmeter 2 reading = P_2 = 6000 W

Voltage = V_L = 400 V

Using equation 3,

$$\phi = \tan^{-1}\sqrt{3}\left[\frac{P_2 - P_1}{P_2 + P_1}\right]$$

$$\phi = \tan^{-1}\sqrt{3}\left[\frac{6000 - 4000}{6000 + 4000}\right]$$

$$\phi = \tan^{-1}\sqrt{3}\left[\frac{1}{2}\right] = \tan^{-1}(0.3464) = 19.106°$$

Power factor

$$\cos\phi = \cos(19.106°) = 0.945$$

Key Takeaways of the Two-wattmeter Method

The two-wattmeter method is most often used for measuring three-phase power. It is appropriate for Δ- or Y-connected, balanced or unbalanced loads. When this method is employed to measure the three-phase power dissipated in a balanced load, the power factor of the circuit can also be computed from the meter readings. In the two-wattmeter method, there is no indication of whether the power factor calculated is leading or lagging. This must be determined by considering the load.

TEXT 9.3

Battery Sizing Explained/ Объясненения размера батареи

October 11, 2022, by Simon Mugo (7565)

This article will make battery sizing an easy task for engineers.
Electric power has become one of the most significant requirements in the modern world. In the bid for clean and free energy utilization, engineers have come up with battery systems such as solar and electric vehicles, triggering growth in battery utilization. These batteries are designed to meet certain criteria, and engineers need to be able to size such batteries.

What Is Battery Sizing?

A battery is a hardware device employed to supply power to another device giving the device permission to work without being connected to the power cord. Such devices include laptops, cellphones, electric cars, and radios and can be classified as rechargeable or non-rechargeable. The battery can be categorized according to the material used, including lithium-ion, lithium polymer, nickel-cadmium, and nickel-metal hydride.
Battery sizing is balancing the power requirement of a given system and coming up with a battery that meets the client's requirements. Sizing determines the number of kilowatt-hours stored in a particular battery. It is an important action that gives a product lifetime. Undersized batteries reduce the shelf life of an electrical product.
To size a battery, gather the following information:

- load that will be supported by the battery to be designed
- minimal voltage the battery should handle
- backup time

IEEE Sizing Calculations

Our calculations are based on the IEEE-provided standards for the sizing of both nickel-cadmium and lead-acid station application batteries. This is a directive to all users that the calculation here may not be used to design any other battery type unless you refer to the guides provided by the manufacturers of the other types.
The following should guide you during the sizing process:

- Collect the total loads that will be supported by the battery. This step will help the designer determine the total load the battery should supply.
- Develop a load profile. The load profile is determined using the autonomy method, and IEEE standards give the guidelines for the autonomy, discharge, or backup times.
- Select the type of battery to design. Choose the type of battery, for example, lead-acid and follow IEEE-provided guidance on characteristics

of charging and discharging; essentials on cell orientations; the threshold for ambient temperature; cell life; ventilation and maintenance requirements; other physical properties such as battery terminals and weight.

Using the manufacturer's datasheet, determine the battery cell characteristics, including cell temperature; cell floating voltage; end of discharge voltage (EODV, which in most batteries ranges between 1.75 V to 1.8 V per cell if the discharge time is more than one hour and 1.66 V if the discharge time is less than 15 minutes); AH battery cell capacity; electrolyte density in the case of lead-acid batteries.

Choose battery cells that can be linked in series method. For lead acid of a particular size, the list below shows the number of cells that can fit in them.

RATED VOLTAGE (V)	CELLS
6	3
12	6
24	12
48	24
120	60

Table 1. Table Showing Different Battery Voltage Ratings and The Number of Cells Required for The Lead Acid Battery

I would not advise designers to always stick to the list above because they can perform calculations and determine the required number of cells to match a specific load. The formulas here will guide designers in determining the number of cells required, which should not go below or above this limit:

$Nmax=Vdc(1+Vload,max)Vcharging$

$Nmin=Vdc(1-Vload,min)VEODV$

Where

N_{max} = Maximum number of cells needed per battery

N_{min} = Minimum number of cells needed per battery

V_{dc} = Nominal voltage of the battery

$V_{charging}$ = Cell's charging voltage

$V_{load, max}$ = Maximum battery load tolerance computed in %

$V_{load, min}$ = Minimum battery load tolerance computed in %

V_{EODV} = End-of-discharge battery cell voltage

When choosing the number of cells between the two limits, always choose the average number of cells between the two limits for the best outcome.

Calculating Battery Capacity in Ampere-Hour

This can be computed by use of the following equation
Cmin=Ede(kafktcfkcrt)Vdckmdodkse Cmin=Ede(kafktcfkcrt)Vdckmdodkse
Where
C_{min} = Minimum battery desired capacity
E_{de} = Total required energy over the backup time (VAH)
k_{tcf} = Temperature correction factor
k_{af} = The aging factor of the battery
k_{crt} = Battery capacity rating factor
k_{se} = System efficiency in percentage
k_{mdod} = Maximum discharge depth
V_{dc} = Nominal battery voltage
Make sure to choose the battery capacity which is more than the calculated minimum above.
Let's take a quick look at the important elements of the formula above.
Battery Capacity Rating Factor. This factor represents the battery voltage reduction during the discharge process.
The Aging Factor of the Battery. This captures how the battery performance reduces based on how long it will be used.
System Efficiency. This represents the battery and electronic power losses.
Temperature Correction Factor. The battery cell is designed to work at a particular temperature and, if this temperature is violated, a correction factor has to be implemented.

Example of Battery Sizing Calculation

Collect all the connected loads and develop the load profile.

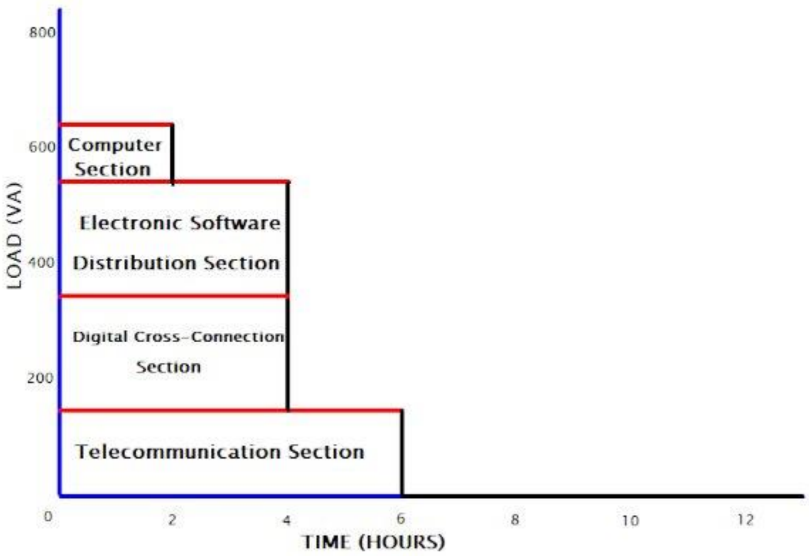

Figure 1. Load powered by the battery to be sized. Image used courtesy of Simon Mugo

From the figure above, we can compute the total design energy demand. It is important to note that the figure represents energy rectangles piled on top of each other.

- Height represents load (VA)
- Width represents the time (autonomy)
- The rectangle area is the total energy of the load

From the graph,
Design Energy Demand, E_{tle} = Total areas of the Rectangles in the graph = 2700 Vah
Design Energy Demand, $E_{de} = E_{tle}(1+k_{cont})\ (1+k_{dm})$
Let k_{cont} = 10% and k_{dm} = 10%
E_{de} = 2700(1+0.1) (1+0.1) = 3267 Vah

Battery Type
For the design calculation example, we are working with the lead-acid battery.
Let’s assume some values as follows to calculate the battery’s number of cells
V_{dc} = 120
$V_{charging}$ = 2.25V/cell
$Vl_{oad, max}$ = 30
$V_{load, min}$ = 15
V_{EODV} = 1.75V/cell
The maximum number of cells that should be required for series connection
Nmax=Vdc(1+Vload,max)VchargingNmax=Vdc(1+Vload,max)Vcharging
Nmax=120(1+0.3)2.25=70cellsNmax=120(1+0.3)2.25=70cells
The minimum number of cells that should be required for series connection
Nmin=Vdc(1−Vload,min)VEODVNmin=Vdc(1−Vload,min)VEODV
Nmin=120(1−0.15)1.75=58cellsNmin=120(1−0.15)1.75=58cells
The total number of cells is the average of the sum of maximum and minimum which is given by (70+58)/2 = 64 cells

Computing Ampere-Hour Battery Capacity

Let’s assume the following values to compute ampere-hour battery capacity.
Cmin = Minimum battery desired capacity
E_{de} = 3267VAh
k_{tcf} = 0.94
k_{af} = 0.2
k_{crt} = 0.15
k_{mdod} = 0.75
V_{dc} = 120V
By use of the parameters listed above, calculate the minimum battery using
Cmin=Ede(kafktcfkcrt)VdckmdodkseCmin=Ede(kafktcfkcrt)Vdckmdodkse

$Cmin=3267(1.2\times0.94\times1.15)120\times0.75=47.09Ah$$Cmin=3267(1.2\times0.94\times1.15)120\times0.75=47.09Ah$

From the above computation, choose a battery size with higher capacity than the calculated battery capacity above.

Key Takeaways of Battery Sizing

- A battery is the hardware used to supply power to electronic and electrical devices that need it.
- Battery sizing is the calculation determining the battery size that will sufficiently support the load.
- The reader has understood the steps that are approached during the sizing of the battery.
- Readers have been fashioned with the formula necessary for battery sizing and provided with a fully solved example.

TEXT 9.4

Overcoming Challenges to Characterize 100V GaN Power FETs/ Преодоление трудностей при характеристике полевых транзисторов мощностью 100 В GaN

October 05, 2022 by Ryo Takeda (14 000)

The applications for 100V (and less) GaN FETs are numerous - from reducing distortion in Class-D audio amplifiers to improving efficiency in synchronous rectifiers and motor drives.

100 V GaN FETs are popular in 48 V automotive and server applications, as well as USB-C, lidar, and LED lighting. However, the small size and minimal packaging parasitics create multiple challenges to dynamically characterize these power devices. This article reviews the challenges GaN semiconductors manufacturers face to characterize these devices, as well as some new technologies that help address these challenges.

In recent years, widebandgap (WBG) devices have significantly progressed in replacing Si-based power MOSFETs and IGBTs in many power-related applications. Their fundamental characteristics enable significant improvements in key areas for power applications. When comparing GaN to Si, it is well known that GaN's higher bandgap, higher electron mobility and larger electric field potential enable important attributes, such as lower losses (i.e., higher efficiency), faster switching (e.g., > MHz) and a significantly reduced size (i.e., higher power density). However, WBG devices have a much shorter history of use in a variety of power applications compared to Si, especially 'high uptime' applications like automotive.

JEDEC® formed the JC-70 Committee in 2017 to develop needed new reliability, characterization, test methods, and datasheet enhancements to appropriately characterize GaN and SiC WBG power devices. The existing Si-based standards were not sufficient to enable designers to determine the most appropriate WBG devices for their application. For example Rds(on), the main parameter characterizing conduction losses, is a dynamic phenomenon in GaN, based on the charge being trapped in the transistor structure (current collapse). JEP-173 was JC-70's first publication (issued in January 2019) to provide a standard for 'Dynamic ON-Resistance Test Method Guidelines for GaN HEMT based Power Conversion Devices'.

Examples of 100V GaN FET Applications

One application of the initial Class D audio amplifiers was automobile sound systems. The amplifier's lower power dissipation and superior efficiency(> 90%) compared to Class A amplifiers enabled 'limited power' automobiles the ability to have multiple speakers and more sound (> 100W). However, the tradeoff for less power consumption was higher total harmonic distortion (THD) created by slower switching power Si MOSFETs. GaN FETs with significantly faster switching speeds (up to 10x) and no reverse recovery charge provide superior linear response and significantly reduced THD. In addition to automotive applications, recently you've probably noticed the boom in portable speakers. In addition to advances in battery technology, this application is enabled by efficient, compact Class D audio amplifiers designed with GaN FETs. Good audio quality is provided because of the lower distortion attributes of GaN, while the ability to run for extended times on batteries is possible because of GaN's high efficiency. There are many other portable consumer devices that can leverage the same attributes as portable speakers.

Automotive systems are moving toward higher voltage operation (e.g., 48V) as more electrical power needs develop for autonomous driving, including radar, cameras, ultrasonic sensors, and lidar. These functions require uninterrupted, highly reliable power. As the 48V bus emerges as one of the new higher voltage power systems, efficiency is again the key with a limited power source (i.e. car battery). GaN technology enables better power density than Si, minimizing additional weight, size, and thermal management. GaN's higher frequency switching, and increased efficiency also reduces necessary passive component size (e.g., inductors) further minimizing the size of the power converter design. DC-DC converters (12V – 48V) made from these GaN FETs, enable the standard 12V power bus to supply power for these emerging automotive system requirements.

Motor drives (e.g. stepper motors, drones, etc.) is yet another large application for 100V and less GaN devices. Low losses often remove the need for heat sinks. GaN enables higher frequency PWM signals and significantly reduces switching losses. Higher frequency switching reduces/eliminates switch node oscillations, often requiring snubber circuits in Si-based designs.

The are many evolving applications primed to take advantage of GaN's superior performance compared to Silicon. But the challenges to characterizing these devices follow the themes described above: small size (power density) and higher efficiency.

Challenges Characterizing 100V GaN Power Devices

The first major challenge is the package size. Many of the 100V (and less) GaN FET packages are ball grid arrays (BGA) ranging from a few mm in the X and Y dimensions to sub mm in the X and Y dimensions. These packages have a 2x2 matrix of solder balls to a 5 x 15 matrix of solder balls. Figure 1 shows an example of an EPC2045, 100 V, 16 A GaN eHEMT device with a specified RDS(on) of 7 mΩ.

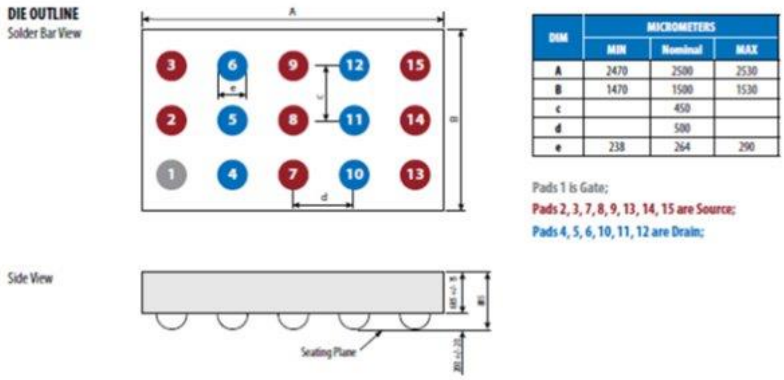

Figure 1. EPC 2045A dimensions (source: EPC2045A Datasheet, 2021.

BGAs like the one used for the EPC 2045A, add little additional parasitic to the die of the GaN devices, making them ideal to take advantage of the superior performance of the high-speed switching applications. Why is minimizing package parasitics important? Primarily for repeatable and reliable dynamic performance of the device. Higher parasitics lead to more ringing and potential instability of the switching power FET. Figure 2 shows a standard DPT test configuration/model with fixture parasitics and the package/ device parasitics. (NOTE: This picture was taken from Keysight's article in the April 2020 edition of Bodo's Power Systems, entitled, "Overcoming Challenges Characterizing High Speed Power Semiconductors". See this article for more details regarding the effects of parasitics in DPT waveforms.).

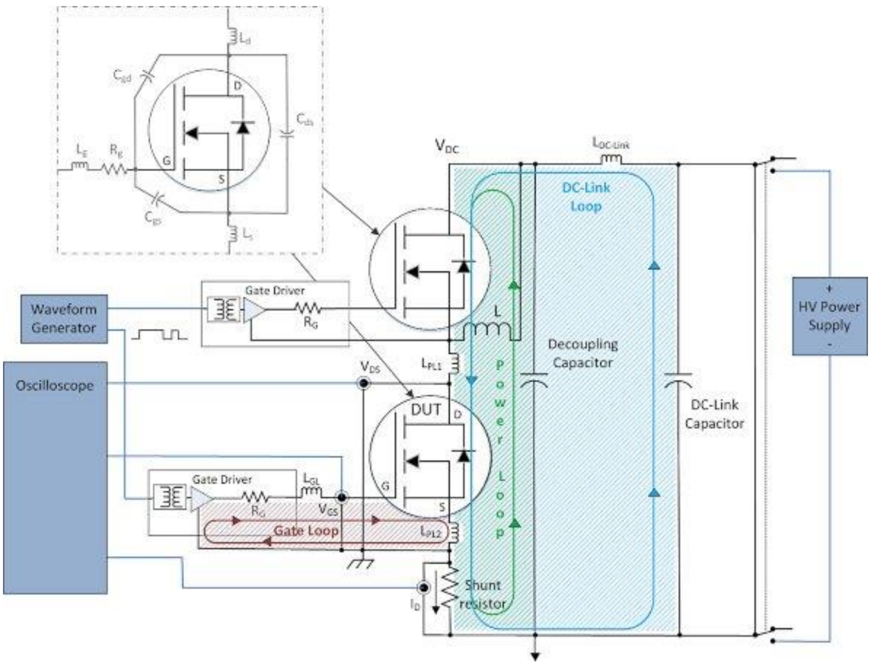

Figure 2. Primary parasitics needing consideration during DPT fixture design.

Because the parasitics of the GaN HEMT and BGA package are so low (e.g. typically < 1 nH, this GaN FET can switch at very high frequencies (e.g. 1MHz). To enable the high frequency switching energy to be accurately characterized, the DPT fixture must also have low parasitics, especially in the power loop and gate loop. These loops should be designed with low single-digit nH inductance (e.g. 3 nH or less) in mind to minimize the effect of the DPT fixture. Ideally, the fixture parasitics are less than the device/package parasitics, which is extremely difficult to accomplish for these small GaN FETS.

Additionally, creating a repeatable and reliable DUT connection method to enable a statistically valid sample size (e.g. >10) of GaN FETs to be tested is very challenging. The ideal situation is to solder each device on the fixture's PCA. However, repeated soldering and unsoldering can easily damage a PCA. The mechanical tolerances needed to repeatably contact a solder ball require sub mm placement accuracy in both X and Y dimensions (see Figure 1: dimensions c, d, and e).

As mentioned above, the other major challenge is repeatably characterizing the GaN FET's efficiency. There are three dynamic parameters that are the main factors that influence efficiency: 1) conduction loss, 2) switching loss, and to a lesser extent 3) drive loss.

1. Conduction Loss ($R_{ds(on)}$) – As mentioned above, $R_{ds(on)}$ is a dynamic measurement for GaN HEMT devices. The JEP-173 provides guidelines for measuring and extracting this parameter. What is needed to determine this parameter repeatably and reliably is a very low parasitic DPT fixture providing clean V_{ds} and I_d switching waveforms. In addition, a fast clamp circuit is needed to settle quickly, enabling a measurement of the clamped V_{ds} and I_d 50-500ns after the switching event. These techniques will provide the best $R_{ds(on)}$ measurement to compare against stress voltages and timeframes to characterize the current collapse in the GaN FET structure.

2. Switching Loss (i.e., $t_{d(on)}$, t_r, $E_{(on)}$, $t_{d(off)}$, t_f, $E_{(off)}$) – These parameters are specified in the IEC 60747-8 standard and are typically specified in Power FET datasheets. The ability to measure and extract these parameters repeatably and reliably is highly dependent on the fixture design and minimization of parasitics. Test conditions typically include V_{ds}, I_d, V_{gs}, sometimes the L_{load}, but almost always the gate resistor R_g. R_g is one of the main controls of the gate drive speed and, ultimately, how hard the device is turned on. Most ideally, R_g is a small value, allowing for a fast-switching transition. However, if the DPT fixture design is not optimized and has unwanted parasitics, then a larger R_g is needed to slow down the switching waveforms to minimize ringing.

3. Drive Loss (i.e., Q_g) – Drive loss is typically the smallest of the losses. Repeatable and reliable measurement and calculation of gate charge (Q_g), requires clean switching waveforms, specifically V_{gs} and I_g. Minimal gate loop parasitics are critical for clean waveforms.

Repeatable and Reliable Dynamic Characterization of 100V Gan FET

The key to obtaining repeatable and reliable dynamic characterization of small GaN FETs is in attention to detail of the DPT fixture design. An EPC 2045A described in Figure 1 was used as the target DUT.

Design Modifications to Keysight's Customized GaN Solution

In the article "GaN Power Semiconductor Device Dynamic Characterization" in Bodo's Power System October 2020 edition, Keysight's solderless DUT connection technology (Figure 3 & Figure 9) for the PD1500A Dynamic Power Analyzer/Double Pulse Tester was presented. However, this connection technology had not been tested with as small a device as the EPC 2045A (1.5 mm x 2.5 mm), requiring repeatable connections to the gate, a single 44.5 µm2 round solder ball target. Fixturing and registration of these small GaN FETs are critical. A customized board for this device was developed to determine if Keysight's solderless contact technology would provide repeatable results for this challenging device (see Figure 3).

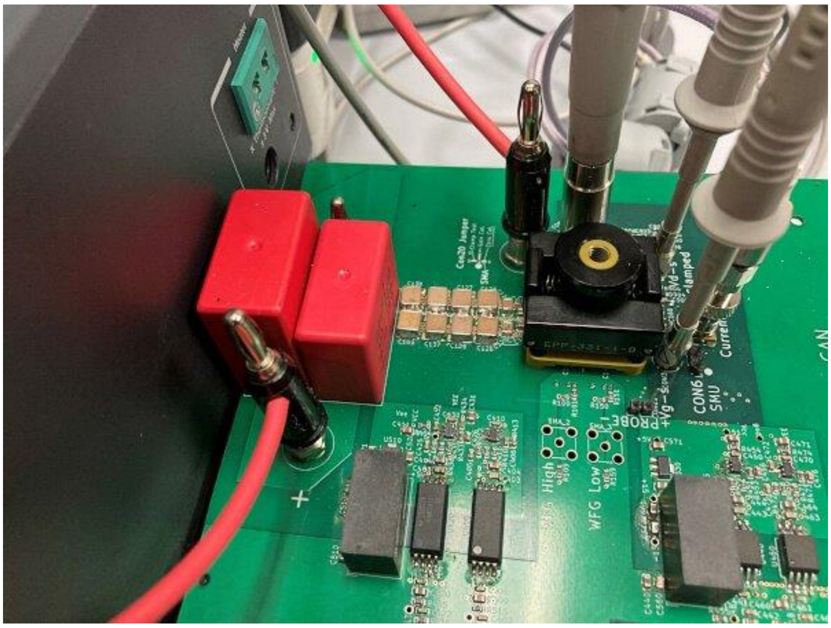

Figure 3. Customized GaN board for EPC 2045A.

After a couple of design iterations to the device holder, including spring tension on the top plate and alignment holes for the base plate part registration, we successfully tested multiple sets of parts with this design.

To further minimize loop areas for the gate loop and power loop, a multi-layer PCB was leveraged, enabling trace routing within different layers to minimize the loop areas. The gate drivers and replaceable Rg daughter boards were placed on the back side of the PCB, further reducing loop areas.

Finally, a simplification of Keysight's patent pending current sensor technology, also mentioned in the October 2020 article, allowed the shunt to be placed closer to the DUT, reducing power loop area, while further minimizing the insertion inductance of the sensor. Together, these modifications to Keysight's existing customized GaN solution enabled industry-leading results for devices like the EPC 2045A.

Conduction Loss (Rds(on))Results

The test system setup to measure dynamic $R_{ds(on)}$ is shown in the table below. To measure the repeatability of the system, 10 tests were performed using the same EPC 2045A GaN FET, reseating the device in between each test. The other table below shows the results. A Max/Min measurement variation of less than 10 mΩ is very good for a solderless DUT connection technology. Keysight has ideas for further improvement of this critical parameter.

Figure 4. Example waveform of Rds(on) measurements.

Switching Loss Results

The test system setup to measure dynamic switching losses, along with some of the standard switching time parameters, is shown in the table below. To thoroughly understand the sources of variation, two groups of 10 measurements were made. The first group looped the DPT 10 times without reseating the part. This enabled an understanding of the variability of the instrumentation measurements and extraction algorithms. In the second group of tests, the GaN FET was reseated in between each test, as was done with the $R_{ds(on)}$ measurements. Statistics were performed for both the Turn-on and Turn-off waveforms (see Figures 5 & 6).

Double Pulse Test Setup	
V_{ds}	60 V
I_d	15 A
V_{gs}	5V / -1V
R_g	4.7 Ω
L_{Load}	207 µH
Extraction Standard	IEC 60747-8
Temperature	~ 25˚C

Figure 5. Example waveform of Switching Loss measurements – Turn on.

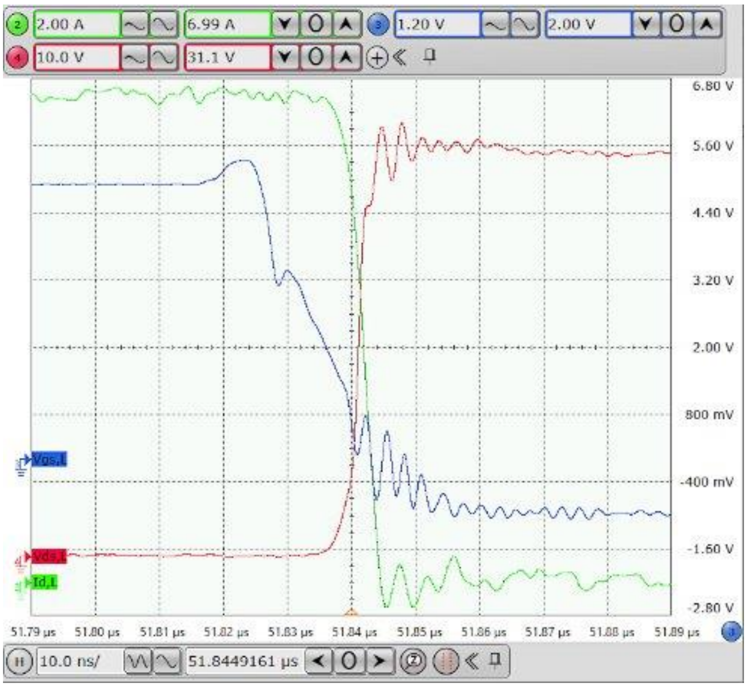

Figure 6. Example waveform of Switching Loss measurements – Turn off.

The results of the statistical analysis are shown in the tables below. It is clear there is not much measurement variation in results when the EPC 2045A was not removed in between tests. Max/Min variations of the switching time ranged from ~ 50 ps to ~ 135 ps. While the switching loss Max/Min variations were only 58 nJ and 79 nJ.

W/O Part Removal	td(off) (s)	tf (s)	E(off) (J)
Avg	9.85114E-09	4.57048E-09	1.0009E-06
Max Value - Min Value	1.3592E-10	6.715E-11	0.000000079
STD/AVG	0.40%	0.40%	2.37%

W/O Part Removal	td(off) (s)	tf (s)	E(off) (J)
Avg	5.49961E-09	2.72765E-09	2.7803E-06
Max Value - Min Value	1.3465E-10	4.875E-11	5.8E-08
STD/AVG	0.75%	0.54%	0.68%

With Part Removal	td(off) (s)	tf (s)	E(off) (J)
Avg	9.969E-09	4.34448E-09	1.0223E-06
Max Value - Min Value	2.44141E-09	1.39377E-09	0.000000127
STD/AVG	6.52%	11.05%	3.19%

With Part Removal	td(off) (s)	tf (s)	E(off) (J)
Avg	5.97761E-09	2.85528E-09	2.9956E-06
Max Value - Min Value	1.74626E-09	5.03222E-10	7.18E-07
STD/AVG	8.07%	5.15%	6.98%

Figure 7. Power Loop Inductance, LPL = Vdroop / dId/dt = 9V / 5.363 GA/s = 1.68 nH.

Even when removing parts, Max/Min variations in the sensitive time measurements were only ~ 500 ps to ~ 2.5 ns and the Max/ Min switching loss variation was less than 1 µJ. These are excellent results, considering the size of the part, a solderless connection, and the difficulty in minimizing parasitics. Not surprisingly, the power loop inductance of the customized GaN board is less than 2 nH (see Figure 7).

Double Pulse Test Setup	
Vds	60 V
Id	15 A
Vgs	5V / -1V
Rg	100 Ω
LLoad	207 µH
Extraction standard	JESD 24-2
Temperature	~ 25˚C

Qg (C)	5.99E-09
Qth(C)	1.19E-09
Vg(pl) (V)	2.19
Qgs(JEP24-2) (C)	1.86E-09
Qgd(JEP24-2) (C)	4.60E-10

Drive Loss Results

The final parameter affecting losses for the power device is Qg. The test system setup to measure and extract Qg is shown in the table above, along with a table reflecting the result of a single measurement of typical Qg parameters. Excellent results were obtained in a large part to the close to ideal raw Qg waveforms and extracted gate charge graph (see Figure 8).

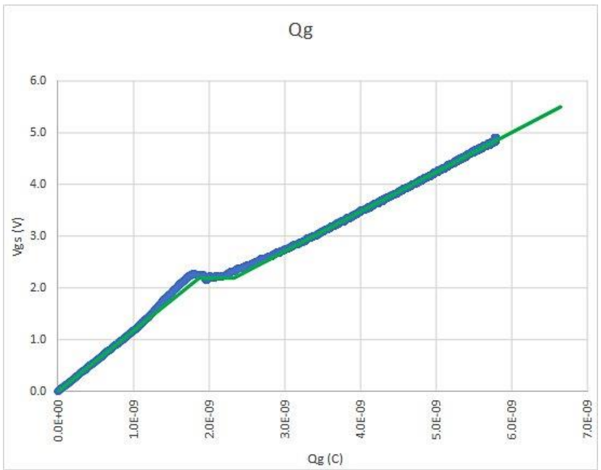

Image used courtesy of Bodo's Power Systems [PDF]

Figure 8. Extracted Qg graph (Vgs vs Qg) and Raw Qg DPT waveform.

Summary

Lower voltage GaN FETs (i.e., 100 V) are reducing size, minimizing cooling requirements, and improving efficiency for many traditional Si-based power MOSFET applications. As discussed, there are many challenges to repeatably and reliably characterize the dynamic performance of these devices. The careful and thoughtful mechanical and electrical design of a customized GaN fixture and test board can overcome many of these challenges, enabling a confident use of these new WBG devices in your power converter designs.

To learn more about Keysight's PD1500A Dynamic Power Device Analyzer and our customized GaN boards, please visit the website (https://www.keysight.com/find/PD1500A). Look for future articles from Keysight with more discussion regarding repeatable and reliable Double-Pulse Test results.

TEXT 9.5

Introduction to Inductor Filter Types and Applications/ Введение в типы и области применения индукторных фильтров

October 10, 2022 by Amna Ahmad (76854)

A frequency filter is a circuit that passes certain frequencies and reduces signal levels at other frequencies. Learn about various types of inductive filters and their power and communication systems applications.

A filter blocks unwanted signals or noise voltages and passes wanted signals with little or no attenuation. Filters are usually classified according to frequency characteristics; a low-pass filter passes low-frequency signals and attenuates all frequencies above a selected cutoff frequency. Similarly, a high-pass filter passes only those inputs with frequencies above the selected cutoff frequency. A bandpass filter passes signals within a selected frequency band, and a notch (or band-stop) filter blocks frequencies within its band.

Frequency filters are used to eliminate harmonics. Power lines also pick up interference (noise) caused by lightning strikes and machine-made radiation from devices like high-power transmitters or radiation devices. This type of interference can cause problems with other types of devices that may be on the line. Frequency filters are used to remove these undesirable signals.

Basic Types of Inductive Filters

The functions of various types of filters are illustrated by the waveforms and typical frequency response graphs below.

Low-Pass Filters

A low-pass frequency filter is a filter that allows all frequencies below a selected frequency to be applied to a load and blocks all frequencies above that point, as shown in Figure 1. The simplest filters consist of an inductor connected in series with a load. Low-pass filters are typically used in DC power and audio applications.

At 0 Hz, an inductor has zero reactance, and the total source voltage is across the load. Under this condition, there is maximum current flow through the load. As frequency increases, reactance increases in direct proportion. Some source voltage is dropped across the inductor, reducing current flow through the load.

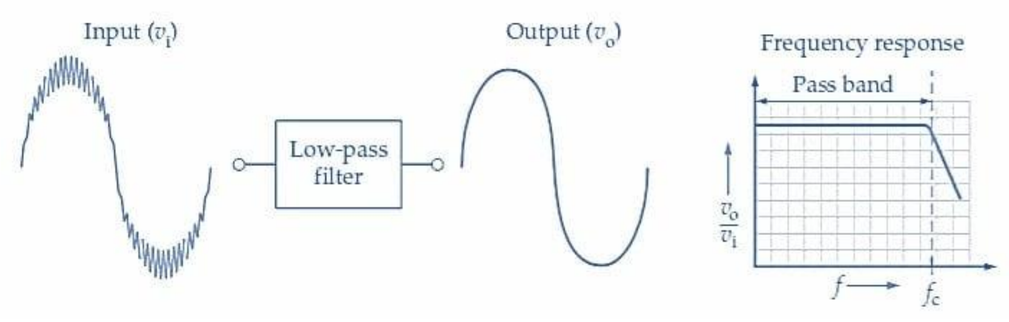

Figure 1. Waveforms and frequency response for a low-pass filter.

The input waveform for the low-pass filter in Figure 1 is composed of a low-frequency signal with an unwanted high-frequency input superimposed. The low-frequency input is reproduced at the output with very little attenuation, while the high-frequency noise voltage is severely attenuated.

The gain/frequency response graph for the filter is a graph of v_o/v_i plotted versus frequency (f). As illustrated in Figure 1, the filter has a low-frequency pass-band where the output voltage approximately equals the input ($v_o/v_i \approx 1$). The pass-band applies to all signal frequencies from zero up to the cutoff frequency. For input frequencies above the cutoff frequency, v_o/v_i is less than one and rapidly falls off to lower values. So, as shown by the graph, signals with frequencies above f_c are attenuated.

High-Pass Filters

The high-pass filter in Figure 2 passes high-frequency input voltages and attenuates low-frequency inputs. In this case, the pass-band is above the cutoff frequency (f_c), and the attenuation band is below f_c. So, low-frequency inputs are attenuated while high-frequency signals are passed to the output terminals. Like low-pass filters, combinations of inductive-resistive-capacitive circuits are designed for this purpose.

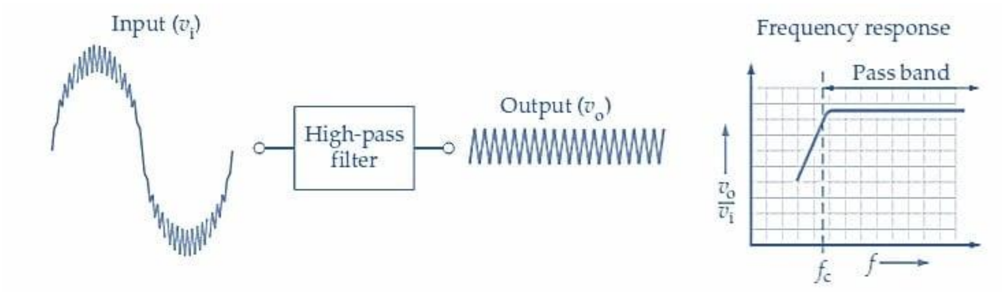

Figure 2. Waveforms and frequency response for a high-pass filter.

The simplest of these filters is an inductor in parallel with a load. High-pass filters are typically used in communications applications, such as radio and television broadcasts, and in residential appliances to eliminate the effects of 60 Hz noise.

Reject frequencies are the ones that are rejected due to amplitude or size. The inductor presents a low reactance at the reject frequencies, which shunts the current around the load resistor. As frequency increases, inductive reactance increases until it is equal to the value of the load. A sharp cutoff curve for a high-pass filter can be obtained using a resonant circuit. At this point, the high-pass band of frequencies flows through the load, delivering half power or more.

Bandpass Filters

A bandpass frequency filter is a filter that passes signals between selected frequencies. A bandpass filter application is illustrated in Figure 3. In this case, a band of frequencies is affected between two cutoff frequencies (f_1 and f_2). As illustrated, the bandpass filter passes a middle range of signal frequencies within its pass band and blocks signals frequencies above and below the pass band.

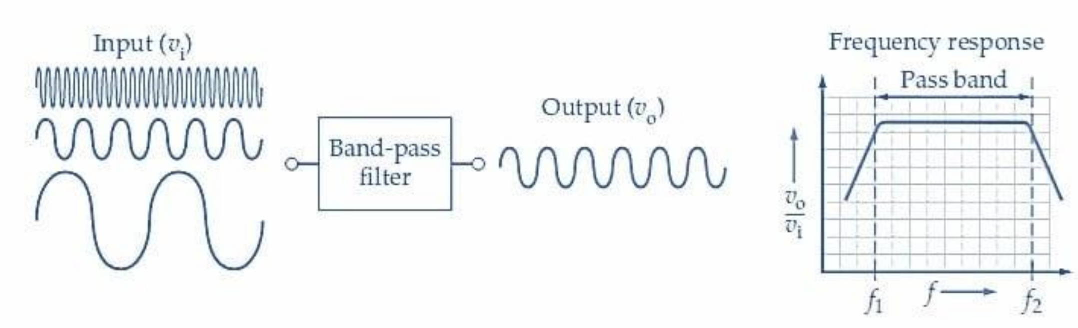

Figure 3. Waveforms and frequency response for a bandpass filter.

Resonance can be used to allow one band of frequencies to be delivered to a load. The simplest circuits are a series resonant circuit and a parallel resonant circuit. Bandpass filters are typically used in communications applications to tune frequency bands.

In a series resonant circuit, capacitance has high reactance below the resonant frequency, and inductance has low reactance below the resonant frequency. Above resonant frequency, the capacitance has a low reactance, while inductance has a high. At the resonant frequency, the inductive reactance equals capacitive reactance, and maximum current passes through the load resistor. Using a bandpass filter, the band of frequencies passed to the load includes those between the half-power points of the curve.

The same bandpass circuit can be obtained using a parallel resonant circuit in parallel with the load. Below resonant frequency, the inductive reactance is low, and the current bypasses the load. Above resonant frequency, the capacitive reactance is low and shunts the current around the load. At the resonant frequency, the impedance of the parallel circuit is at its maximum value, causing the maximum current flow to the load. Resistance limits current flow in the circuit when either the capacitive or the inductive reactance equals zero.

Bandpass filters are used in the reproduction of audio frequencies in stereo speakers. Typical stereo speaker systems have three loudspeakers: small (tweeter), midsize, and large (woofer). A crossover network is an arrangement of bandpass filters to route the appropriate signal to the proper loudspeaker.

Band-Stop (Notch) Filter

A band-stop frequency filter is a filter that reduces signals between selected frequencies. Using a band-stop filter, selected frequency bands can be prevented from reaching the load, as shown in Figure 4.

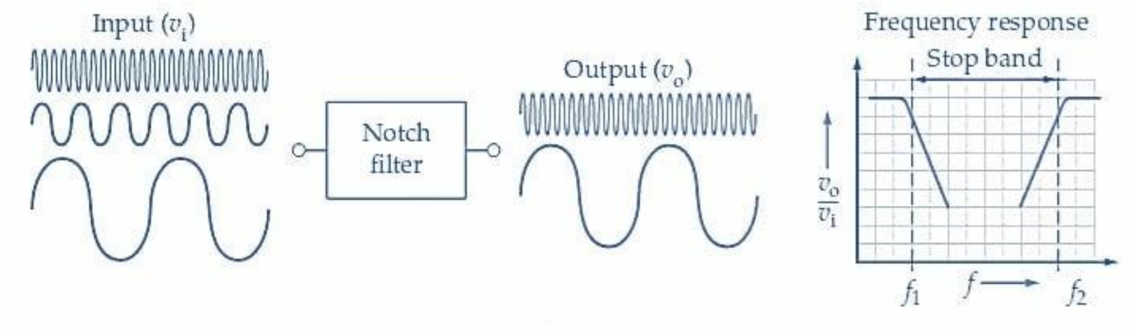

Figure 4. Waveforms and frequency response for a notch filter.

Filtering selected frequency bands is accomplished using a series/parallel resonant circuit designed with a stop band. Band-stop filters are typically used in applications to remove a certain frequency, such as 60 Hz.

When a series resonant circuit is placed in shunt with the load resistor, the series resonant circuit, at its resonant frequency, will short most of the current around the load resistor. Since this arrangement acts as a short circuit, a resistor is used to limit the current flow from the source to a safe level.

Current flow from the source can also be limited by placing a parallel resonant circuit in series with the load. At resonance, placing a parallel resonant circuit in series with the load presents a very high impedance to the source, limiting current flow through the load. The maximum current flow in this circuit is limited by the load's value and the source voltage's value.

Key Takeaways of Frequency Filters

Frequency filters are combinations of inductors, capacitors, and resistors that make it possible to select or reject bands of frequencies. The characteristics of different combinations of these components make it possible to select broadcasts from one radio or television station while excluding others. Frequency filters are generally used for power applications (to eliminate harmonics) and communications applications (to attenuate undesirable frequency signals).

TEXT 9.6

The Evolution of Integrated Current Sensors Takes a Digital Path/
Эволюция Встроенных датчиков тока идет по цифровому пути

October 04, 2022 by LEM (8912)

So far, the evolution of integrated current sensors (ICSs) has been slow and gradual. Current measurement technology has been developed increasingly over the years to focus on the miniaturization of high-density components that can also deliver high levels of performance. Bulky sensors are inevitably losing their market share as more streamlined competitors enter the market.

A recurring question is how to get ahead of the market and determine what users require. Finding out this information and then developing products to meet those needs demands a top-down and bottom-up approach, in which forecasting market trends sits alongside customer-based surveys. Customers usually know what they want from their ICSs, and their feedback has proved essential in driving this evolutionary process.

Input from customers has helped identify the top four key elements to look for in current sensors:

performance over temperature – this relates to drift and sensitivity offset and is the single most important feature

how much current an integrated solution can handle. A small current sensor with an integrated primary limits how much current it can support – 30 amps or 50 amps continuous – and technological breakthroughs come about by pushing these limits

over-current detection – a threshold for protection with overcurrent continually being monitored

insulation (basic or reinforced based on the system voltage) can be a key factor in the choice of sensor

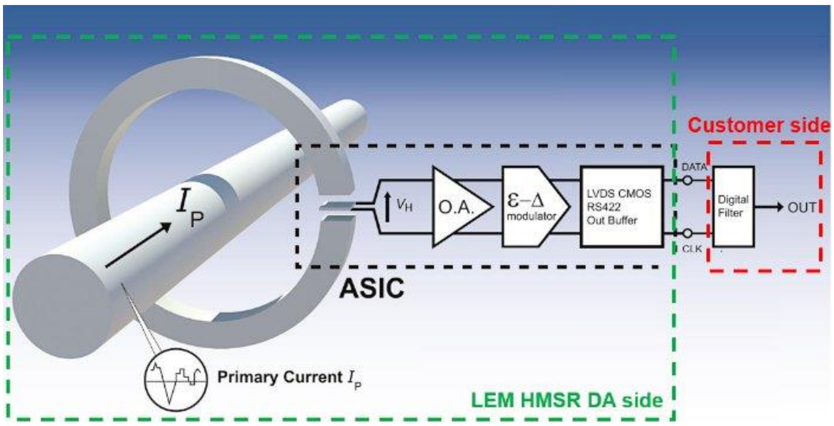

Figure 1. HMSR DA block diagram.

Closed Loop and Open Loop

In recent years, users have benefited from closed loop Hall effect technology – LEM designed a special closed-loop Application Specific Integrated Circuit (ASIC) – and then open loop technology which presented a much lower cost solution. This technology led to the development of the HLSR series of current transducers, a compact, low-cost PCB-mounted solution which took miniaturization to new levels.

Next on the evolutionary path came the HMSR, a high insulated ICS designed to satisfy the continuous market requirements of cost reduction, performance improvements and miniaturization. This new series saw the expansion of miniature current sensors for AC and DC isolated current measurement in highly demanding, switching power applications for commercial and industrial markets. Microcore-based open loop sensors with reinforced insulation and overcurrent detection, the HMSR units featured a low-resistance primary conductor (to minimize power losses), a miniature ferrite and a proprietary ASIC to allow direct current measurement and consistent insulation performance. All of these features made the HMSR ideal for high voltage applications that demand high precision and significant immunity against external fields. The micro magnetic core meant the device was particularly useful in power electronic applications that tend to experience high levels of disturbance.

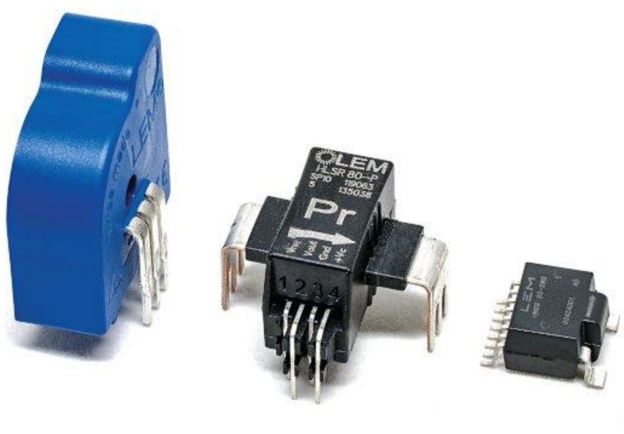

Figure 2. Sensors form factor reduction.

Figure 3. HMSR DA effective resolution vs / PN.

For these reasons, power electronics engineers have been using analog HMSR sensors successfully for many years to measure DC and AC currents. They have particularly enjoyed the benefits of a compact current sensor with strong immunity to stray fields, reinforced isolation and a 300kHz bandwidth.

The latest solution in this continuing evolution of integrated current sensors is the HMSR DA, the first ICS on the market to offer Sigma Delta bitstream output while measuring low current and still delivering high resolution. Using a digital signal means a fixed delay is introduced onto the sensor's output (also known as response time) while quantization noise from the analog-to-digital converter (ADC) is reduced significantly and the digital filter ensures even better resolution of a Sigma Delta modulator (SDM) through noise shaping. Creating an ADC is simple by combining the modulator with a digital filter. Advantages of this include a reduced number of connections, each user being able to define their own system performance levels, and users making two or more converters with different performances. This kind of architecture is particularly well suited to inexpensive CMOS processes.

Another characteristic of a digital current sensor is the settling time, also known as response time or delay. With a 10MHz clock and 128 oversampling ratio (OSR), the settling time of an SDM would be around 38.4us. Yet another benefit of using a Sigma Delta output bitstream is the flexibility offered, meaning that different digital low pass filters can be applied on the customer side, depending on the specific needs of the application. The user has a choice of using a high order slower filter if a high-resolution result is required or a smaller order faster signal for more rapid results but in lower resolution.

Figure 4. HMSR DA effective resolution vs OSR.

Typical ICS Applications

The market is proving to be receptive to an ICS delivering digital output because it offers superior signal shape and lower noise levels simultaneously with a reduced cost and smaller mechanical footprint. Typical applications for this kind of ICS include robotics, servo drives, sewing machines, CNC machine tools, welding equipment and automated guided vehicles (AGVs).

Recently, the automotive sector has begun to show an interest in these sensors. R&D organizations and expert makers who feed into this market are excited by the fact that a digital solution is immune to external noise – including electric and magnetic noise – which is notorious for causing major difficulties when using analog signaling.

On the Digital ICS Roadmap

The HMSR DA sensor – seen as the first step along LEM's digital ICS roadmap – is literally the first of its kind on the market, offering users resolution of between 11 and 13 bits and a 10MHz clock.

The ultimate goal would be to approach the current levels of traditional sensors using an integrated current sensor. At the moment, the HMSR DA can support 30 Arms continuous at 125°C and 75 amps peak but subsequent generations would look to support 100 amps continuous while still being extremely compact and PCB mounted. Future versions will also aim to eliminate the need for a magnetic microcore, which will improve frequency response and do away with potentially problematic magnetic disturbances.

Ideal for applications that are prone to noise, distortion and interference, the HMSR DA achieves genuine cost savings by enabling customers to economize on their bill of materials (BoM). It does this by replacing in a single unit a much more complex and costly alternative system that traditionally includes a shunt resistor, a digital isolator, and low/high power supply circuitry with diodes and capacitors. The shunt is by no means the best solution because of thermal noise when dealing with high currents. Another problem is the space required to contain these separate pieces of equipment, whereas with the HMSR DA there is just one chip that does the same job of those three elements and directly delivers the output to customers. The new sensor also provides customers with features that are not available with those separate units, such as an ASIC and over-current detection that the shunt does not offer.

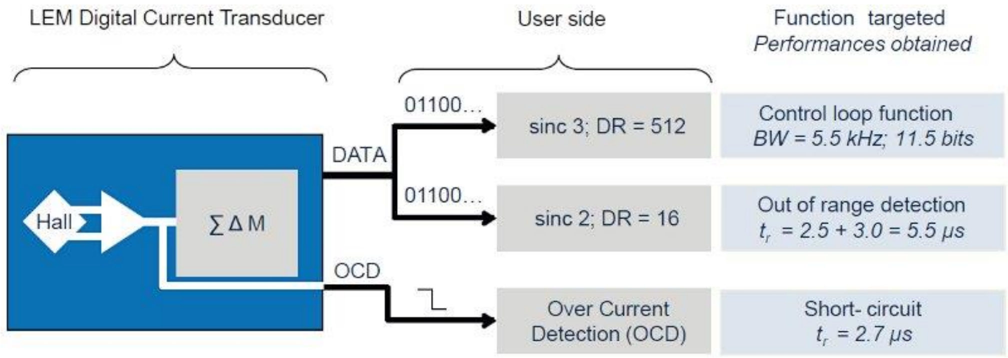

Figure 5. Sigma Delta output is very flexible to use.

Formulating System Design

In addition, different output modes are available – single with the bitstream and the clock but also differential, eliminating the need to purchase output drivers to convert from single mode to differential. A solution based around RS-422 data and an LVDS (low-voltage differential signaling) receiver will deliver output and inverted output as well as clock and inverted clock, which is important when handling differential signals because it becomes possible to remove all noises while operating at low power and high speeds. With the new digital sensor, all these features are incorporated into a single unit.

It is expected that the HMSR DA sensor will enable engineers to look at new ways of formulating their system design. Customers will also be able to use filters to adapt the sensor to meet their specific requirements when working in any industry that needs clean signals but is traditionally subjected to electric noise, vibrations and magneto-electronic noise. Distortion and interference are significant problems in such highly demanding applications and only by pushing the boundaries in terms of digital output can truly ground-breaking developments that address the issues of noisy systems reach the market.

Digital output is still in its infancy and, even today, some customers may still be hesitant to go down this route. However, it is a powerful future trend that will become far more widespread in the coming years. That’s why it is essential to be in on the ground floor with this technology and to encourage credible feedback from users on the viability of applying digital output solutions in their sector.

TEXT 9.7

PCB Power Loop Layout for Chip-scale Package GaN FETs Optimizes Electrical and Thermal Performance/ Схема контура питания печатной платы для микросхемного пакета GaN Fets оптимизирует электрические и тепловые характеристики

October 03, 2022 by John Glaser (10211)

In this article, different power loop layouts are analyzed with simultaneous considerations for thermal management and electric parasitics.

The results show that an improved layout can provide a significant reduction in operating temperature rise while maintaining electrical performance benefits.

Wide bandgap (WBG) power semiconductors like Gallium Nitride (GaN) have demonstrated better switching performance, high reliability and temperature capability with Figures of Merit (FOM) 3 to 10 times larger than comparable silicon devices [1]. GaN devices with small die size and on-resistance ($R_{DS,on}$) reduce parasitic capacitance and inductance, increase switching speeds, and reduce switching losses allowing for much higher power densities and efficiencies. Higher frequencies would require some design attention to layout improvement to minimize added thermal resistance and inductance [2].

Existing PCB Layout Approach

The power loop layout considered in this article is the half-bridge configuration around which most power conversion layouts are built, comprising two power semiconductor switches and a bypass capacitor as shown in Figure 1. The inductor (l) averages the output voltage level of the switch node $v_{SW} = V_{LOW}$, and the capacitor C_{HF}, while in theory not required since it is in parallel with V_{HIGH}, is required in practice to provide a low impedance path for high-frequency currents.

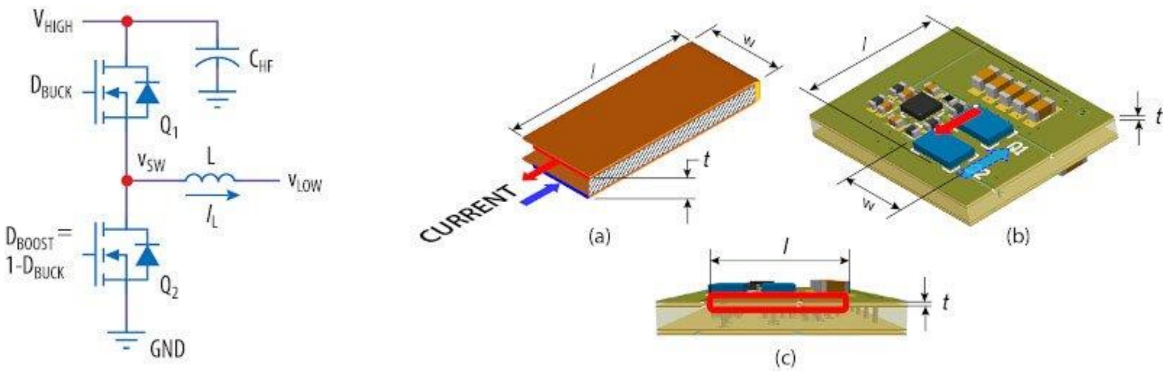

Figure 1. Typical half-bridge building block. Parallel plate shorted transmission line (a). Half-bridge layout employing low-impedance transmission line as power loop structure with corresponding dimensions (b)

and edge view of same (c).

The PCB design that minimizes power loop inductance, estimated by $L_{loop} = \mu 0 \cdot l \cdot t/w$, has been previously discussed [2]. Figure 1(b, c, d) shows a PCB implementation of the power loop. In summary, a PCB layout should minimize length and thickness while increasing the width w. This can be accomplished by the placement used in the layout of Figure 1(c), l and w are determined by the physical dimensions of the components, and t is set by voltage requirements or PCB manufacturability constraints.

The Buck Converter Thermal Challenge with Existing Layout

With the temperature of the switching devices becoming the limiting factor for electrical activation levels in many applications, improving heat dissipation has also become the main design consideration, especially at the PCB level, which plays a major part in removing heat from the FETs [3]. In a buck converter of Figure 1, Q_1 is under a larger thermal load since it exhibits both switching and conduction losses, while Q_2 only exhibits conduction loss. Figure 2 (Layout A) shows an exploded view of the standard layout of Fig. 1 (c). Thermally, the top layer has a higher resistance path for Q_1, because of the interrupted copper plane by CHF. Q_2, on the other hand, has a clear copper plane for heat to effectively spread into the PCB and eventually dissipate to ambient. Moreover, fewer vias are available for Q_1 to avoid heavily perforating the GND return path. Therefore, Layout A is not thermally optimal for buck converter applications and an improved layout is needed to accommodate the higher losses without Q_1 overheating.

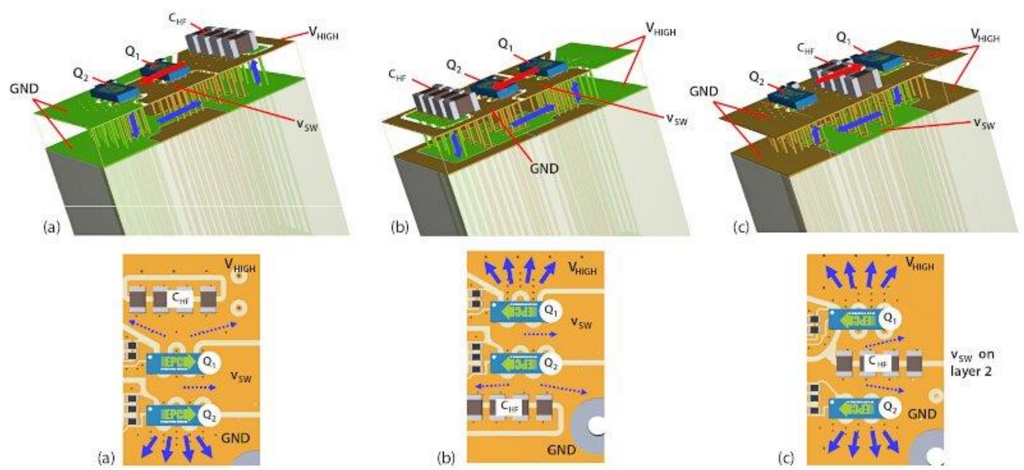

Figure 2. Exploded view of power loop layouts with reference node and return path (GND) highlighted in green (Top). Top view of same with heat flow paths indicated by arrows (Bottom).

Considering a boost converter application on the other hand, the roles of Q_1 and Q_2 are reversed, with Q_2 having the higher loss, in which case, Layout A performs well since Q_2 has a lower thermal resistance.

Optimizing Layout for Buck Converter

As a rearrangement to thermally improve Layout A for buck operation, CHF can move to the side of Q_2 since both are connected to GND (Layout B in Figure 2). This would require the use of layer 2 as a VHIGH plane, which still acts as an AC reference plane, and the dimensions l, w, and t are unchanged. Thermally, Q_1 now has a good path to ambient and thus Layout B should perform better thermally under buck operation, but worse under boost operation since Q_2 is now obstructed by CHF.

Eliminating the Tradeoff with a Capacitor-Centered Layout

For cases where a wide converter operating range, or bidirectional conversion is needed (Buck and Boost), Layout A or B are thermally restricted to one FET or the other. Moreover, in both layouts, Q_1 and Q_2 are closely placed and thus the heat generated is concentrated in a smaller area. These issues can be solved in Layout C by placing CHF in between Q_1 and Q_2. In Layout C, Q_1 and Q_2 are connected through the switch node (SW) in layer 2 shown in Figure 2. Layout C obeys the rules to minimize loop inductance, and while it is conventional to place the switch and signal nodes on the outer layer, it is not required for low impedance. The two nodes V_{HIGH} and V_{LOW} are at the same AC potential due to C_{HF} and thus together form an AC reference plane and do not affect loop inductance.

The thermal benefits are that Layout C increases the spacing between and provides unobstructed copper planes for both Q_1 and Q_2. Also, there is more room for adjacent vias, the return plane is less perforated, and the switch node can be shielded by DC planes with potential EMI benefits.

Some possible drawbacks, not significant in practice, are that the farther spaced FETs may need a longer gate drive path when using a single package gate drive IC, and in some cases the capacitors may be taller than the FETs, which must be accommodated when mounting a heatsink.

Analysis and Verification

To test the above design proposals, hard-switched converters are used for their ease of design and well-understood behavior. The thermal performances of the three layouts design are compared in buck and boost operation. Identical boards with each power loop layout are designed and manufactured. The voltage V_{HIGH} is selected at 150 V which is a typical value for the FETs used for Q_1 and Q_2. The conversion ratio is fixed at VLOW/VHIGH = 0.25, which implies that Q_1 operates at a duty cycle of 0.25 and Q_2 at 0.75. The dc inductor current is fixed at IL = 15 A, since this is near the saturation value of the inductor and a moderate value for the selected FETs. Thus, the converter processes 562W in all test cases. A switching frequency FSW = 100 kHz was chosen to give realistic FET power dissipation values. The above test parameters are the baseline for the conducted tests. Q_1 is thermally overstressed in buck mode and Q_2 in boost mode.

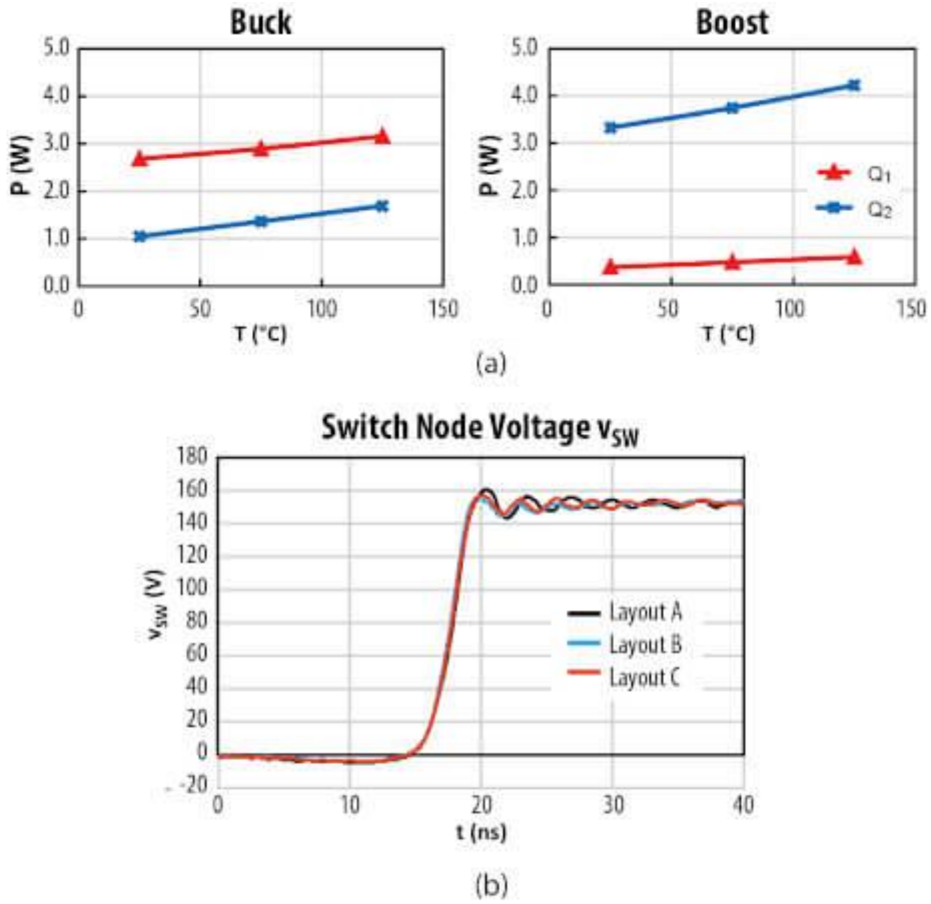

Figure 3. a) Loss simulation results, b) Switch node voltage vSW for buck converter Q1 turn-on transitions.

Electrical Simulation and Measurements

To estimate the heat dissipation in the FETs, electrical simulations were done in LTspice™ which included estimated PCB parasitics. FET losses were simulated as a function of set frequency, duty cycle, and temperature. Results are shown in Figure 3a.

The switching performance is measured to show the inductance difference between the different layouts. The switching waveforms presented in Figure 3b show the switch node voltage for the turn on of Q_1 during buck operation. It can be seen that the three layouts show small differences in the ringing, indicating small effects on the parasitic inductance.

Thermal Testing Setup

Thermal testing is performed in a forced-air cooling test chamber with controlled airflow. Figure 4 shows the test connections and experimental setup. For thermal measurements, a 200 µm-wide hole is drilled through the PCBs in between the pads to provide access for an optical thermal sensor (OPSense®

OTG-F sensor). This sensor is EMI immune and has an extremely small thermal mass.

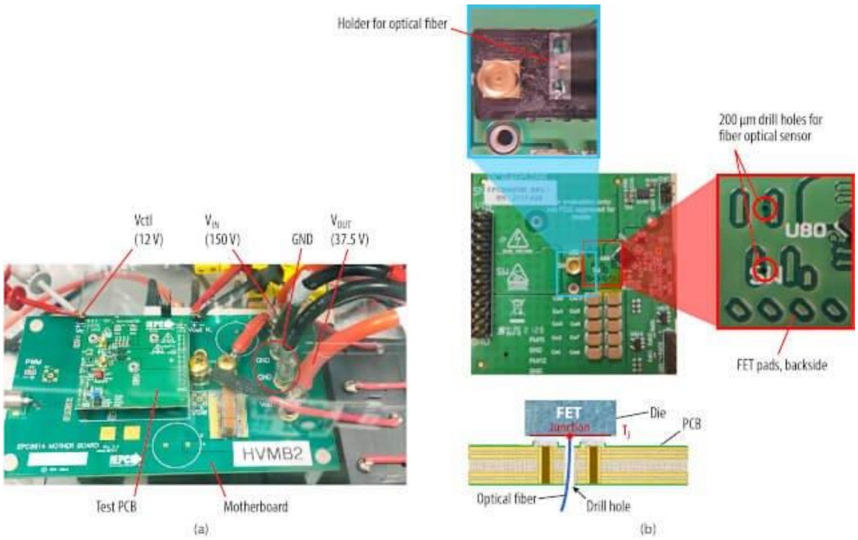

Figure 4. a) Electrical Connections to motherboard and test PCB for thermal testing. b) Optical sensor measurement setup showing PCB drill holes for fiber optic sensor.

Thermal Simulation Model

Thermal simulations are performed using 6SigmaET [4], a commercial thermal and CFD software, to verify the measured observations. The PCB layouts are imported into the software with all the details required (copper conductors, vias, devices). Representative data points are used to validate with measurements.

Forced Air Convection Results

The first set of measurements is performed for the three layouts at 400 LFM air flow. From the thermal simulation results in buck and boost configuration given in Figure 3, the maximum temperature on the high side FETs shows that Layout A has a thermal advantage in boost, while Layout B is more effective in dissipating heat in buck mode.

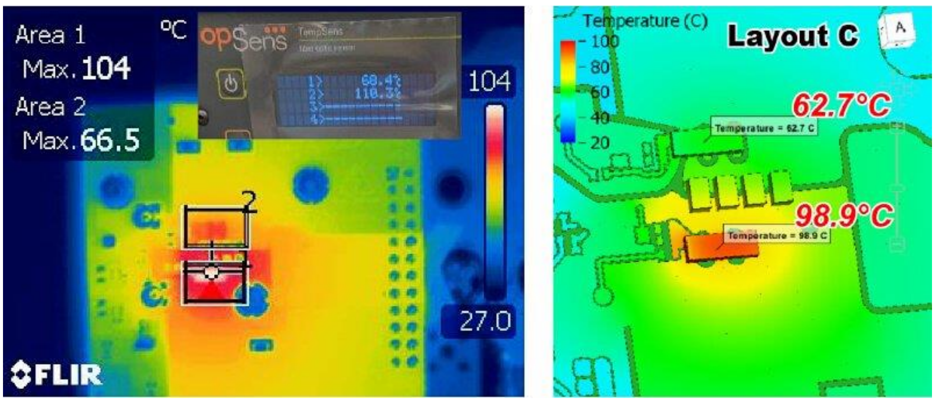

Figure 5. Measurement (IR and fiber optic temperature sensor) and simulation results (surface temperature) for Layout C in boost.

Layout C, when compared to A and B, has similar (within 5%) or better thermal performance than A and B in their optimal operation mode (A in boost and B in buck mode) and a significant improvement over layouts A and B in their sub-optimal operation mode (A in buck mode and B in boost mode). Figure 6 presents the measured Q_1 and Q_2 temperatures in for the three layouts in buck and boost operation. The results show that there is no thermal penalty for layout C in bidirectional operation, whereas thermal performance is significantly lower for layout A in buck (10% higher temperature) and B in boost (25% higher temperature). Additional testing with heatsinks show a similar conclusion, with lower temperatures due to better cooling effectiveness and a larger spacing between Q_1 and Q_2 in Layout C [5].

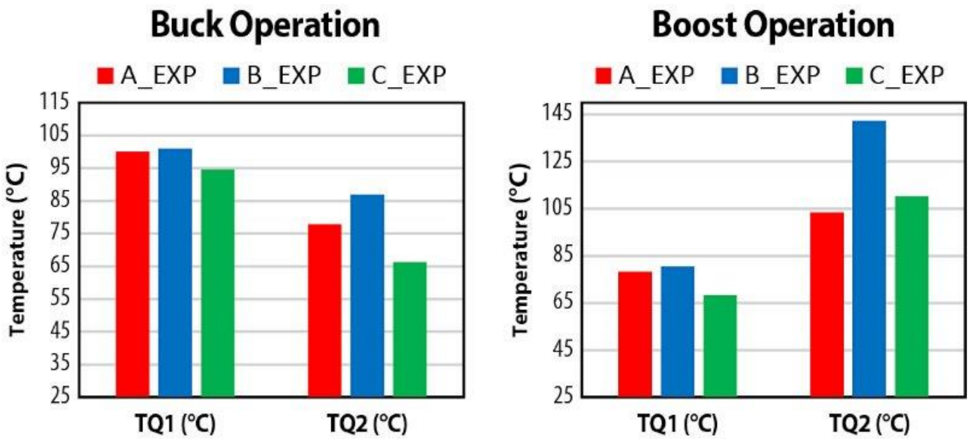

Figure 6. Summary of Measurement Results and Temperature Rise Comparison for the three Layouts.

The three layouts A (C_{HF} adjacent to Q_1), B (C_{HF} adjacent to Q_2), and C (between Q_1 and Q_2) show comparable electrical performance, with minor differences observed in the ringing frequency. Experiments support the supposition that under typical design conditions, Layout A is thermally optimized for boost converter operation and Layout B for buck operation. Layout A is thermally challenged under buck operation and Layout B under boost, showing a large thermal penalty (high peak temperature) if not operated in their optimal mode.

Layout C provides a large unobstructed copper plane and a larger spacing for Q_1 and Q_2 which improves overall thermal performance to what is at least equivalent and often better that Layouts A or B. Layout C is shown to be thermally viable for any operating condition and is particularly suited to wide range applications such as inverters, Class D amplifiers, and solar optimizers, as well as bidirectional applications such as battery interfaces with minimal drawbacks observed in testing.

TEXT 9.8

Resonance Explained/ Резонанс Объяснен

September 29, 2022. by Simon Mugo (8700)

This article introduces resonance and how it is related to impedance and admittance, the parallel and series RLC circuit resonant design, calculations of its parameters and electrical quantities, and the application of the resonance circuits.

In electric circuits, there are energy-storing elements like capacitors and inductors. The energy-storing elements are what cause resonance. Resonance is the driving concept behind the working principle of TV and radio receivers, allowing viewers to select desired frequencies for their TV channels.

Electrical Resonance

For electrical resonance to occur, there must be a cancelation of admittances and impedances of the elements of the circuit at a given resonant frequency. In some special circuits, this can only occur when the impedance between the output and input of the system is about zero and its transfer function is closer to one.

There exist two types of resonance that are series and parallel. These configurations exist based on how elements of the circuits are connected–in either series or parallel. This article presents a wider scope of series and parallel resonance.

Series Resonance

In this type of resonance, all the circuit passive elements are connected in series in what we refer to as a series RLC circuit. Look at the series RLC circuit in Figure 1 below with values represented in the phasor (вектор) domain.

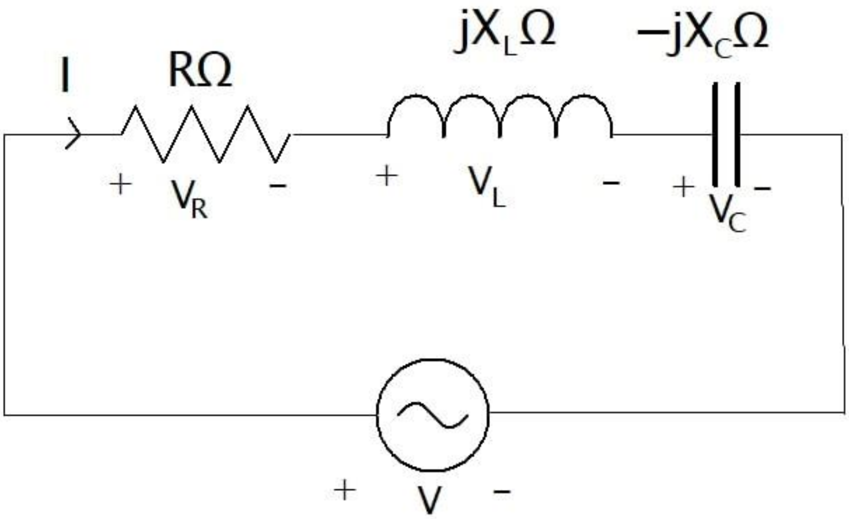

Figure 1. Series Resonance Circuit.

The inductor, resistor, and capacitor which form part of the passive elements are connected in series with the sinusoidal voltage source which serves as the input;

Apply Kirchoff's Voltage Law around the given loop in the circuit:

$$V-V_{R}-V_{L}-V_{C}=0$$

Replacing the values of the inductor, resistor, and capacitor in the above equation gives:

$$V-IR-I(jX_{L})-I(-jX_{C})=0$$

Rearranging the equation:

$$V=IR+I(jX_{L})+I(-jX_{C})$$

Further rearrangement:

$$V=I[R+j(X_{L}-X_{C})]..........(1)$$

Note that equation 1 above is in the form of V = IZ and therefore, the impedance Z is shown by the equation below:

$$Z=R+j(X_{L}-X_{C})]$$

Electrical Quantities and Parameters at Resonance

The series RLC resonance circuit will have several parameters and electrical quantities when at resonance and it shall be very significant if we derive them in this article.

Resonant Frequency

This is the frequency at which resonance occurs and is denoted as fr. When you have a series RLC circuit, resonance when the impedance Z term is equal to zero that is the difference between the value of XL – XC gives us zero.

Equating the above to zero gives us:

$$X_{L}=X_{C}$$

Substituting $X_L = 2\pi fL$ and $X_{C}=\frac{1}{2\pi fC}$ in the equation above gives,

$$2\pi fL=\frac{1}{2\pi fC}$$

Making f the subject of the formula gives:

$$f=\frac{1}{(2\pi)\sqrt{LC}}$$

This translates to the resonance frequency of the series RLC circuit which can be written as:

$$f_{r}=\frac{1}{(2\pi)\sqrt{LC}}$$

Where C is the capacitor's capacitance and L is the inductor's inductance.

While the series RLC resonant frequency is independent of the resistor R, it always depends on the capacitance C and inductance L.

Impedance

From earlier derivations, we found that impedance Z of the series RLC circuit is given by:

$$Z=R+j(X_{L}-X_{C})]$$

But

$$X_{L}=X_{C}$$

And substituting this in the impedance Z equation, we get

$$Z=R+j(0)$$

Hence

$$Z=R$$

This explains that the impedance Z of the series RLC circuit is equal to the resistance R in the circuit.

Current I Flowing Through Series RLC Circuit

Earlier we derived equation (1) as

$$V=I[R+j(X_{L}-X_{C})]$$

Let's substitute XL=XC into the equation.

Therefore,

$$V=I[R+j(0)]$$

$$V=IR$$

Making I the subject of the form gives

$$I=\frac{V}{R}$$

And this is the current flowing through the series RLC circuit at resonance.

In the series RLC circuit, the impedance arrives at the minimum value at resonance. Therefore, the maximum current of the series RLC circuit is attained at resonance.

Voltage Across Resistor

The voltage that goes across the resistor is given by the formula

$$V_{R}=IR$$

Let us substitute the value of I in the equation

$$V_{R}=(\frac{V}{R})R$$

Canceling R out we find that

$$V_{R}=V$$

And that gives as the voltage across the resistor

Voltage Across Capacitor

From the circuit above, the voltage across the capacitor is given by:

$$V_{C}=I(-jX_{C})$$

Substituting the current I value in the equation

$$V_{C}=\frac{V}{R}\Big(-jX_{C}\Big)$$

Opening the bracket

$$V_{C}=-j\Bigg(\frac{X_{C}}{R}\Bigg)V$$

But we know that $\frac{X_{C}}{R} = Q\text{-Factor}$,Hence, the equation becomes

$$V_{C}=-jQV$$

And this is the voltage across the capacitor at resonance.

The magnitude of the voltage across this capacitor at resonance can be found to be

$$|V_{C}|=QV$$

Voltage Across Inductor

This is given by

$$V_{L}=I(jX_{L})$$

By substituting the value of I in the equation;

$$V_{L}=\frac{V}{R}(jX_{L})$$

Rearranging

$$V_{L}=j\Bigg(\frac{X_{L}}{R}\Bigg)V$$

Hence

$$V_{L}=jQV$$

And this gives the voltage across the inductor at resonance.

The magnitude across the inductor at resonance will be

$$|V_{L}|=QV$$

It is significant to take note that series resonance RLC circuits are named voltage magnification circuits because both the magnitude of the voltage across the capacitor and inductor is equal that voltage is equal to Q times the input voltage V.

Parallel Resonance

This is the resonance that occurs on the parallel RLC circuit. Let's look at the parallel RLC circuit below which has a phasor domain representation.

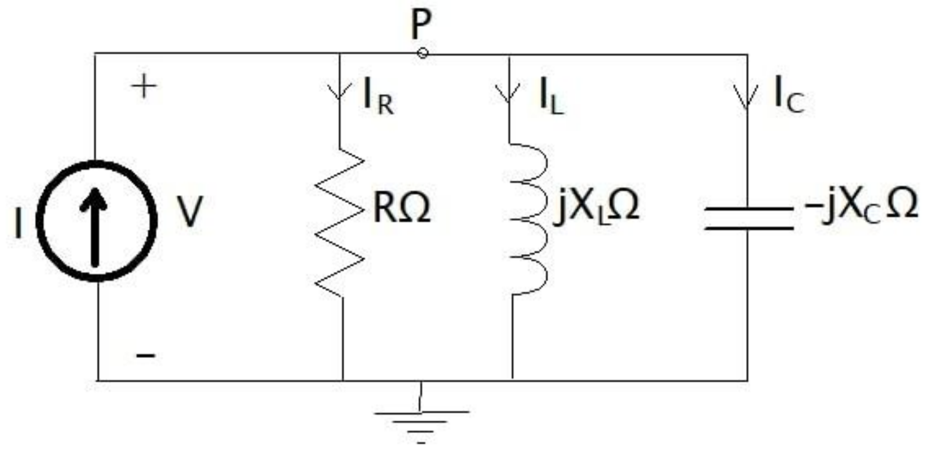

Figure 2. Series Parallel Resonance Circuit.

In this circuit, it is evident all the passive elements' connection is in parallel with the input sinusoidal current source.

We have labeled node P in the same circuit and can write the nodal equation at this point.

$$-I+I_{R}+I_{L}+I_{C}=0$$

By introducing the value of currents across the elements into the equation.

$$-I+\frac{V}{R}+\frac{V}{jX_{L}}+\frac{V}{-jX_{C}}=0$$

Rearranging the above equation, we get:

$$I=V\Bigg[\frac{1}{R}+j\Bigg(\frac{1}{X_{C}}-\frac{1}{X_{L}}\Bigg)\Bigg]..........\text{Equation 1}$$

The equation above is of form I = VY

Where Y is the admittance of the parallel RLC circuit.

Therefore, admittance will be given by:

$$Y=\frac{1}{R}+j\Bigg(\frac{1}{X_{C}}-\frac{1}{X_{L}}\Bigg)$$

Resonance Electrical Quantities and Parameters of the RLC Circuits

Here, we will focus on the derivation of electrical quantities and parameters of the parallel RLC circuits at resonance.

Resonant Frequency

Here, resonance occurs when the term of the imaginary admittance is zero.

$$\frac{1}{X_{C}}-\frac{1}{X_{L}}=0$$

Rearranging you get

$$X_{L}=X_{C}$$

Note that the above resonance condition is similar to the RLC circuit, implying that the resonance frequency fx remains the same.

$$f_{r}=\frac{1}{(2\pi)\sqrt{LC}}$$

Admittance

From the derivation of equation 1, note that admittance is given by:

$$Y=\frac{1}{R}+j\Bigg(\frac{1}{X_{C}}-\frac{1}{X_{L}}\Bigg)$$

But at resonance

$$X_{L}=X_{C}$$

Substituting it in the admittance equation we get

$$Y=\frac{1}{R}$$

Therefore, at resonance, we have the admittance Y being equal to the resistance reciprocal.

Voltage Available Across Each Element

We know that $\frac{1}{X_{C}}-\frac{1}{X_{L}}=0$ and by replacing this into equation 1, find that

$$I=\frac{V}{R}$$

Rearranging

$$V=IR$$

This gives the voltage across the element in the parallel RLC resonance circuit.

Current Through the Resistor

This is given by the formula

$$I_{R}=\frac{V}{R}$$

But we already know the value of voltage as V=IR and can substitute it

Hence,

$$I_{R}=I$$

And this gives us the current flowing through the resistor at resonance.

Current Through Inductor at Resonance

This is given by

$$I_{L}=\frac{V}{jX_{L}}$$

Let’s substitute the value of V in the equation above

$$I_{L}=\frac{VR}{jX_{L}}$$

On rearranging, we get

$$I_{L}=-j\Bigg(\frac{R}{X_{L}}\Bigg)I$$

But $\frac{R}{X_{L}}$ is the Quality factor, Q of the system hence current flowing through the inductor becomes

$$I_{L}=-jQI$$

Therefore, the magnitude of this current flowing through the inductor will be given by:

$$|I_{L}|=QI$$

Current Through the Capacitor

This is given by:

$$I_{C}=\frac{V}{-jX_{L}}$$

Substituting the value of V in the equation gives

$$I_{C}=j\Bigg(\frac{R}{X_{C}}\Bigg)I$$

Hence,

$$I_{C}=jQI$$

Which is the current flowing through the capacitor at resonance.

The magnitude flowing through the capacitor is given by:

$$|I_{C}|=QI$$

The parallel RLC electrical circuits are also known as current magnification circuits because the magnitude of the electrical current that flows through the capacitor and inductor is equal to the quality factor times the current at the input.

Applications of Resonance

- Television broadcasts and radio transmissions
- Voltage magnification especially the series RLC circuit
- Communication systems and signal processing
- Oscillator circuits
- Induction heating
- Key Takeaways of Resonance
- In circuits, there exist energy-storing elements such as capacitors and inductors.
- There exist two types of resonance that are series and parallel RLC circuit resonance.
- Resonance is about the cancellation of admittance and impedances in an electrical circuit.
- The article has introduced us to how to calculate the electrical quantities and parameters of both series and parallel RLC circuits.

TEXT 9.9

Inductors: Energy Storage Applications and Safety Hazards/ Индукторы: применение для накопления энергии и угрозы безопасности

September 28, 2022 by Amna Ahmad (9848)

In this article, learn about how ideal and practical inductors store energy and what applications benefit from these inductor characteristics. Also, learn about the safety hazards associated with inductors and the steps that must be implemented to work safely with inductive circuits.

When an ideal inductor is connected to a voltage source with no internal resistance, Figure 1(a), the inductor voltage remains equal to the source voltage, E. In such cases, the current, I, flowing through the inductor keeps rising linearly, as shown in Figure 1(b). Also, the voltage source supplies the ideal inductor with electrical energy at the rate of p = E *I.

Without the internal resistance, the inductor is lossless because it cannot produce heat or light from the available energy. Therefore, all the energy supplied by the source ends up being stored in the generated magnetic field – exactly how energy is stored in rubber bands when stretched. The rising current causes more and more energy to be stored in the magnetic field due to the expansion of the magnetic lines of forces. The lack of a resistive element in the circuit means the current will continue to rise. In such an ideal scenario, the inductor has an infinite capacity and will continue to charge forever until the circuit is broken. The stored energy can be recalled at any time by breaking the circuit of Figure 1(a), causing a breakdown of the magnetic field and releasing its energy.

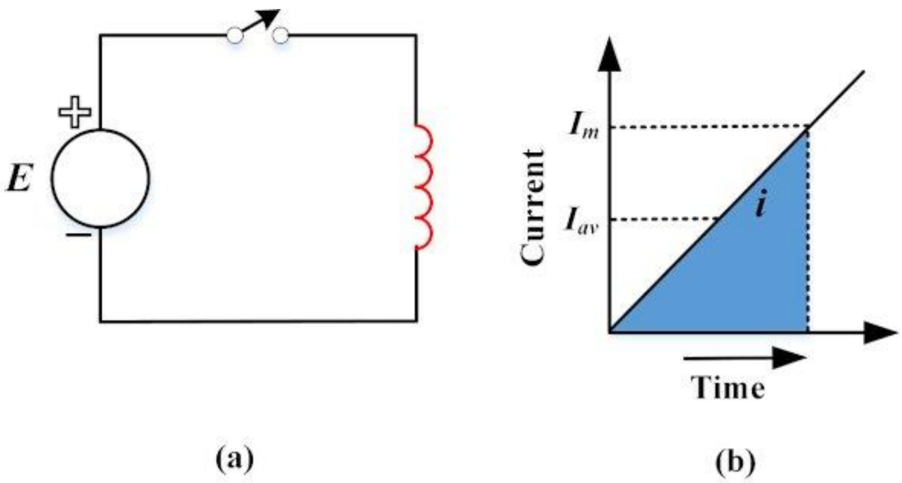

Figure 1. (a) Simple Inductor circuit. (b) Rising current profile.

In a purely resistive circuit, the voltage and current are not a function of time. Therefore, they do not change with time. In such circuits, the source transfers energy to the resistance equal to W = P *t = V *I *t.

However, in a purely inductive circuit, the current increases linearly with time, as the voltage remains constant for the circuit in Figure 1(a). This means there is a constant rate of change in the system's current. Therefore, the average current value, I_{av}, will be equal to I_m / 2 as the current goes from zero to I_m. And the resultant stored energy W will be equal to:

$$W=V\times 12Im\times tW=V\times 12Im\times t$$

And due to the constant rate of change of current, the inductor voltage will be equal to:

$$V=L\times didt=LImtV=L\times didt=LImt$$

By substituting the value of V in the equation for W, we get the total energy stored by the magnetic field of the inductor:

$$W=LImt\times 12Im\times tW=LImt\times 12Im\times t$$

$$W=12LI2mW=12LIm2 \quad (1)$$

For a practical or a non-ideal inductor circuit, the internal resistance cannot be ignored because it plays an essential role in limiting the system current to an upper value of I_m = E/R. In this circuit, the instantaneous current and voltage profiles are not linear or constant. They both vary with time and are continuously changing at a non-constant rate. Therefore, it is important to find the instantaneous values of the inductor voltage and current, v and i, respectively, to find the momentary rate of energy storage. Much like before, this can be found using the relationship p = V * i. Figure 2 shows the voltage and current profiles of the non-ideal inductor circuit and the subsequent energy profile.

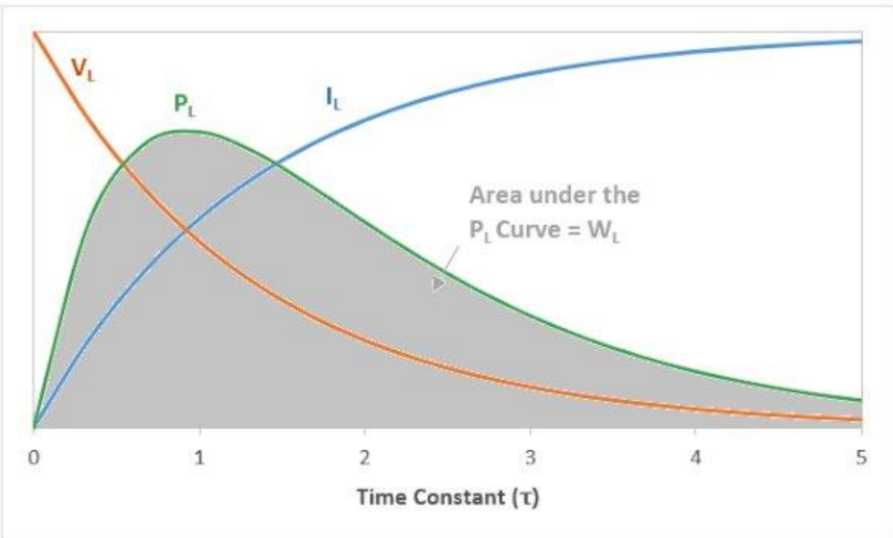

Figure 2. Voltage, current, and energy stored profiles for a practical inductor.

The inductor starts resisting the current flow and the magnetic field's formation, but as it increases, the magnetic field continues to expand. When the current gradually approaches its steady-state value Im and becomes constant, the magnetic field ceases to expand further. In this instance, the inductor voltage also falls to zero, indicating that the inductor now behaves like a short circuit that allows maximum current flow. Thus, the power delivered to the inductor p = v *i is also zero, which means that the rate of energy storage is zero as well. Therefore, the energy is only stored inside the inductor before its current reaches its maximum steady-state value, Im. After the current becomes constant, the energy within the magnetic becomes constant as well. Thus, the inductor takes no more energy, albeit its internal resistance does cause some losses as the current flows through it, such that Plosses= Im2R. These losses are unavoidable because the constant current flow is necessary to maintain the magnetic fields.

The energy within the magnetic field can be taken as a product of the average power and the elapsed time since switch closure. This is highlighted as the area under the power curve in Figure 2. The energy in the inductor can be found using the following equation:

$$w=12Li2w=12Li2 \quad (2)$$

Where i is the current (amperes), L is inductance (Henry), and w is the stored energy (joules).

Applications of the Stored Energy in Inductors

Switched-mode power supplies (SMPS)

Switched-mode power supplies (SMPS) convert AC and DC supplies into the required regulated DC power to efficiently power devices like personal computers. An Inductor is used in SMPS because of its ability to oppose any change in its current flow with the help of the energy stored inside it. Thus, the energy-storage capabilities of an inductor are used in SMPS circuits to ensure no ripples in the SMPS output current.

The inductor subdues any output current fluctuations by changing its behavior between a load and a supply based on the SMPS current ripple. The inductor behaves like a load and stores energy to prevent ripples from producing excess current. It acts like a current supply when the ripple reduces the current value. In each case, the inductor prevents the ripples from influencing the regulated DC.

Buck Regulator

An inductor can be used in a buck regulator to function as an output current ripple filter and an energy conversion element. The dual functionality of the inductor can save the cost of using separate elements. But the inductor's inductance value must be selected to perform both functions optimally. Large inductor values give low ripples and maximum power output. However, the value should not be too high because the inductors can get very bulky and provide a poor transient response.

Limiting Inrush Currents

Some AC/DC and DC/DC applications (motors, transformers, heaters, etc.) can cause high Inrush currents to flow in an electrical system. These currents are needed to produce charging effects and magnetic fields when these devices are initially energized. These high-value currents are a part of the system and must be tolerated for the first few cycles. However, the high current can cause overcurrent protection devices like fuses and relays to trip the circuit to protect converters and other equipment from failure. In such cases, an inductor can be added to limit the inrush current. Here, the inductors slow down current surges or spikes caused by the inrush current while still allowing the delivery of the inrush current to required applications.

Safety and Hazards

An inductor in an electrical circuit can have undesirable consequences if no safety considerations are implemented. Some common hazards related to the energy stored in inductors are as follows:

When an inductive circuit is completed, the inductor begins storing energy in its magnetic fields. When the same circuit is broken, the energy in the magnetic field is quickly reconverted into electrical energy. This electrical energy appears as a high voltage around the circuit breakpoint, causing shock and arcs. An accidental shorting of the inductor element can also cause it to release its stored energy as a heavy current. Both of these conditions can damage the circuit or cause injuries to nearby people.

The inductor is surrounded by its magnetic field. Therefore, it can attract other magnetic materials in its area of influence. If the magnetic material is part of nearby devices, these devices can suffer mechanical stress.

Before the current through an inductor reaches a steady state, the magnetic field continues to be built up as the current keeps increasing. This magnetic field can be considered a time-varying field that can induce emf and eddy currents in nearby conductive materials. These currents can produce heat and form their own magnetic field that interacts with the source field and causes mechanical stress in the conductive element.

Considerations for Safe Operation of Inductive Circuits

Automatic Discharge

Automatic shorting devices like varistors and freewheeling diodes can be used to provide additional current paths when the excitation is interrupted. This way, a path is provided to the inductor to release its energy without forming arcs at the circuit break point.

Connections

When an excited inductor loses connection to the supply, it quickly breaks its magnetic fields and tries to continue the connection to the supply with the converted energy. This energy can cause destructive arcing around the point where the connection is lost. Thus, the connectivity of the circuit must be continuously observed.

Eddy Currents

Self-induction and mutual induction due to the inductor's magnetic field can cause eddy currents to flow in the body of the inductor and any nearby conductors. These are undesirable because they produce mechanical stress, heat, and energy losses. Therefore, considerable mechanical and electrical support should be provided to dissipate any stress or heat produced safely.

Verify De-energization

Another safety consideration is to verify the de-energized state of inductors. Any residual energy in inductors can cause sparks if the leads are abruptly disconnected.

The exponential characteristics of a practical inductor differ from the linear behavior of ideal inductors; both store energy similarly–by building up their magnetic fields. These magnetic fields have undesirable effects on the inductors and nearby conductors, causing several safety hazards. It is essential to mitigate these safety concerns by making appropriate considerations and implementing proper failsafe technologies.

TEXT 9.10

How to Design a Transformer: Size and Selection/ Как спроектировать трансформер: размер и выбор

September 27, 2022 by Simon Mugo (9315)

Transformers are key electrical components useful in determining the power reaching the load from the supply. In this article, you will learn how to design a transformer through a well-documented guide that will enable you to select and size transformers.

A transformer is one of the major components when focusing on electricity distribution. It significantly impacts the electrical system's performance, either during normal operations or disturbances. Therefore, smart engineers ensure transformers are correctly selected and perfectly sized for a particular purpose and can deliver sufficient power to the electric loads under certain conditions and regulations.

A transformer helps power systems become scalable, flexible, and cost-efficient by ensuring minimal power loss. This article teaches you how to select and size a transformer.

Transformer Nameplate

Transformer selection and sizing involve determining the transformer's basic parameters such as primary and secondary voltages, KVA, winding connection, power factor, cooling methods, winding conductor material, types, mounting arrangement, efficiency, and frequency of operation. All these parameters are written on a plate known as the nameplate, which is fitted on the transformer. When you check on any transformer well, you will see a well-fitted detailed sticker with all the transformer's necessary parameters.

Parameters to Consider When Sizing a Transformer

Voltages Both Primary and Secondary

Primary voltages are all the voltages supplied on the input side of any given transformer, while the secondary voltage is the voltage output by the transformer.

If the supply voltage available is 414 V three-phase and the output required is 240 V single-phase, you must go for a transformer rated 415 V at the input and 240 V at the output.

KVA Rating

Calculating the KVA during the selection and sizing of transformers is crucial. This represents the maximum apparent power that a transformer can handle. KVA depends on power factor, voltage, and current. Below are the formulas for KVA calculations:

- Single-phase transformers

kVA = (load voltage x load current)/(1000 x load power factor)

- Three-phase transformers

kVA = (1.723 x load voltage x load current)/(1000 x load power factor)

Operational Frequency

A transformer operates at a specific frequency. The magnetic current, rated current, and kVA are directly proportional to the transformer frequency. Therefore, the transformer should operate at a rated frequency. The rated frequency of the transformer should always be equal to the input power supply and the load's operating frequency.

Winding Connections

For single-phase transformers, the winding connection is not something to worry about, but the winding connection is a significant parameter for three-phase transformers. Below are several examples of windings configured in a three-phase transformer connection.

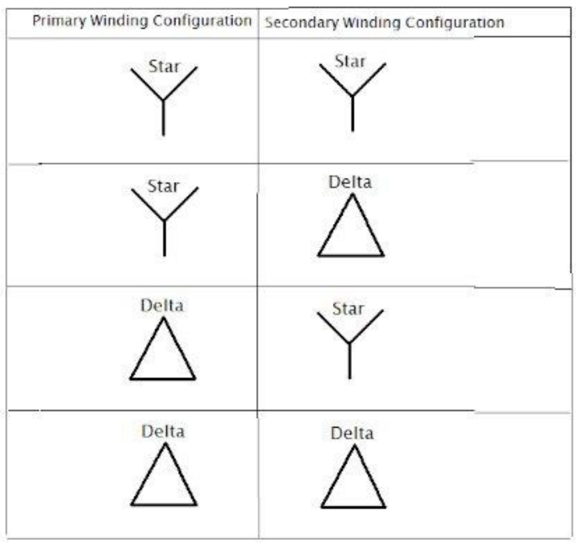

Figure 1. Winding Connection Configurations for Three-phase Transformers.

Apart from the above-listed parameters, other parameters such as the power factor, transformer type, cooling arrangements, operating temperatures, impulse withstanding capacity, voltage regulation, and mounting arrangements are also considered when selecting a transformer.

Calculating Transformer Design Parameters

For educational purposes, we are going to design a small transformer. We will be designing a 60 VA step-down transformer of 230 V to 12 V. The reader needs to have basic knowledge about transformers. Detailed calculations are included in this article.

Note that we are designing a small transformer, hence we are going to ignore copper and core losses as they do not affect small transformers.

Core Calculations

To design a transformer, we need to have a specific number of turns on both the secondary and primary sides of the transformer to achieve a specific rating. Therefore, finding voltage per turn and turns per voltage design is the first priority. This can be obtained from the existing transformer's voltage equation below:

$$E=4.44fB_{in}A_{i}$$

The equation above is a derivation from the basic equations, and we will derive it step by step.

From basic knowledge, we understand that induced EMF is the rate of change in flux:

$$e=N\frac{d\varphi}{dt}$$

The Root Mini Square value (RMS) is given as:

$$\sqrt{}2$$

With peak value

$$e=\sqrt{}2E$$

Putting all this together, we get:

$$E=\frac{N}{\sqrt{}2}\frac{d\varphi}{dt}$$

$$\varphi(t)=ABsin(\omega t)$$

Let's take the derivative with respect to t:

$$\frac{d\varphi(t)}{dt}=\omega ABcos(\omega t)$$

To have maximum flux linkage:

$$\frac{d\varphi(t)}{dt}=2\pi fAB_{in}$$

From electronics, we know that:

$$\omega=2\pi f$$

And

$$E=N\frac{2\pi FAB_{in}}{\sqrt{}2}$$

The formula above gives the total induced EMF.

The main focus is the voltage per turn and hence dividing both sides with total number of turns (N) we get:

$$E_{T}=4.44fAB_{in}$$

Turns per volt will be given by:

$$T_{E}=\frac{1}{4.44fB_{in}A}$$

Rearranging the above formula, we get the formula below, which is used to calculate the area of the core:

$$A_{i}\frac{1}{4.44fB_{in}T_{e}}$$

Where

Ai = Area of Core, f = Operating frequency, Bin = Magnetic Flux Density and Te = Turns per Volts

- Assumptions

We know the power system frequency. The focus is to have the turns per volt and the magnetic flux. For a smaller transformer design, the magnetic flux density ranges between 1 and 1.2.

Inputting the values in the formula, should result in the area of the core.

Let's take the copper wire density to be 2.2 to 2.4A/mm^2

f = 50Hz

Bin =1.2 Wb/m^2

Te = 4 (Turns Per volts)

Ai =1.45 $inch^2$

$$T_{E}=\frac{1}{4.44fB_{in}A}$$

Inputting the values in the formula, we get that:

Te = 2.6 turns per volts.

For the design, make sure to choose the core that is readily available in the market. From the check, the readily available core is 1.5"x1.5" which gives 2.25 inch2

That is the core area used to calculate turns per volt of 2.6.

Calculations of the Primary Winding

For the transformer, calculate the primary side parameters then end with the secondary side.

Primary Side Current Calculations

Primary voltage = Vp=230 V

Primary Current (I1):

$$I_{1}=\frac{VA}{V_{p}}=\frac{50}{230}=0.218A$$

But a transformer cannot perform at 100% and hence the efficiency is at 95%, so the primary current becomes

$$I_{1}=\frac{VA}{\eta V_{p}}=\frac{50}{0.95\times230}=0.23\,A$$

Hence, 0.23 A is the primary current.

Number of turns

The total number of turns in the primary side can be calculated as

Total Number of Turns (N1)= Turns per Volts×Primary Side Voltage

$$N_{1}=2.6\times230=598\,Turns$$

This is approximately 600 turns.

Primary Conductor Size

Current density is Current divided by the unit area.

$$\delta=\frac{I}{A}$$

For copper material, current density is given as 2.3 A/mm2

The copper area on the primary side a1 is given by

$$a_{1}=\frac{0.23}{2.3}=0.1mm^{2}$$

Use the standard AWG table to determine the size of the 0.1 mm2 where it is 27 AGW.

Calculations of the Secondary Windings

The secondary Voltage = VS =12 V

Calculating the Secondary Current

$$I_{S}=\frac{VA}{V_{s}}=\frac{50}{12}=4.2\,A$$

Calculating Secondary Wire Size for Design of Transformer

$$a_{2}=\frac{4.2}{2.3}=1.83mm^{2}$$

Checking at the AWG standard table for transformer wire thickness, the thickness will be 15 AWG.

Therefore, secondary wire size = 15 AWG.

Number of Turns on The Secondary Side

Calculate this by

Total Number of Turns(N2) = Turns per Volts×Secondary Side Voltages

$$N_{2}=2.6\times12=32\,turns$$

Estimating the Weight of the Transformer Winding

This happens when we know:

The density of copper is 8960kg/m^3

Approximate length of copper wire = number of turns x perimeter of bobbins.

Cross-sectional area of copper

Volume = approximate length x cross-sectional area

Mass = copper density x copper volume

Primary Side calculation of Copper Weight

Perimeter of the bobbin = 1.75 x 4 = 7 inch = 0.1778 m

Therefore, the length of the turn is 0.1778

The primary side total length of the turn = L_1

Total length = length of a single turn x total number of turns in the primary side = 0.1778 x 600 = 106 m

The volume of copper wire = area x length = 0.1 x 10^{-6} = 1.06 x $10^{-5}$$m^3$

But we know the density of copper as 8960 m^3; hence we can now calculate the weight of copper:

Weight = density x volume = 8960 x 1.06 x 10^{-5} = 0.095 kg =95 grams.

Therefore, we need 95 grams of 27 gauge wire at the primary side of the transformer.

Calculating Winding Weight on the Secondary Side

As calculated, the length of the turn = 0.1778 m

For 32 windings on the secondary side L2 = 0.1778 X 32 = 6 m

The area of the secondary winding wire is 1.83 mm2

Therefore, the volume of the secondary winding = 1.83 x 10-6 x 6 = 1.098 x 10-5 = 0.098 kg

So, we can approximate the weight at 100g of wire size 15 gauge at the secondary side winding.

At this level, all the calculations for the transformer design are done, along with all the transformer-relevant characteristics. Implement the transformer project by building the hardware according to the calculations.

Key Takeaways of Transformer Sizing and Selection

A transformer is a common electrical component used in stepping up or stepping down power.

Every transformer has a transformer nameplate with all the parameters of the transformer.

We have listed almost all the parameters that every transformer must have.

We have learned how to calculate transformer parameters which are key to designing, selecting, and sizing transformers.

TEXT 9.11

Power Factor: Determining how Much Electricity Your Power System Consumes/ Коэффициент Мощности: Определяет, сколько Электроэнергии Потребляет Ваша Энергосистема.

September 22, 2022 by Simon Mugo (9635)

Here, we will define power factor; differentiate between good, poor, and bad power factor; jump deeper into what causes and how to correct poor power factor; and introduce how to calculate power factor, reactive power, apparent power, and capacitance when faced with a power factor correction problem.

Power factor has been used to measure how efficiently electrical equipment utilizes the amount of power supplied to it. The higher the power factor, the better the equipment's performance. Equipment with low power factor means that power has not been efficiently used and hence power losses occur. Direct current has no power factor because it is accompanied by zero frequency. For alternating current voltages, power factor is a norm and ranges between zero and one, where one is the perfect system, and zero is the bad system.

Defining Power Factor

First, note that power factor is a ratio meaning it is unitless. It is a ratio between the energy a device can transmit to the output and the energy it consumes from the input electrical source. It is one of the key figures used by designers of electrical and electronic devices to meet the power requirements and regulations within several countries and other organizations.

In other words, power factor is the ratio between the system's true power (kW) and its apparent power (kVA):

Power_Factor=True_Factor(kW)Apparent_Power(kVA)Power_Factor=True_Factor(kW)Apparent_Power(kVA)

PF=kWkVAPF=kWkVA

Everything about power factor can be simplified using the power triangle. For learning purposes, we will use the leading PF, which is the easiest to understand.

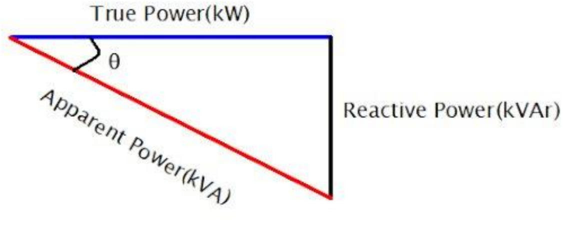

Figure 1. Power Triangle.

From the triangle, the adjacent line represents the true power, the opposite is reactive power, and apparent power is represented by the hypotenuse at an angle theta from true power.

From observation of the power triangle, note the increase in reactive power subsequently increases the apparent power of the system.

From the power triangle above, and by use of trigonometry and the Pythagorean theorem, come the following formulas:

True_Power(kW)=Apparent_Power(kVA)×coscosθTrue_Power(kW)=Apparent_Power(kVA)×coscosθ

Reactive_Power_(kVAr)=Apparent_Power(kVA)×sinsinθReactive_Power_(kVAr)=Apparent_Power(kVA)×sinsinθ

Apparent_Power(kVA)=√True_Power(kW)2+Reactive_Power(kVAr)2Apparent_Power(kVA)=True_Power(kW)2+Reactive_Power(kVAr)2

Power_Factor=coscosθ=True_Power(kW)Apparent_Power(kVA)Power_Factor=coscosθ=True_Power(kW)Apparent_Power(kVA)

Good, Poor, and Bad Power Factor

The system’s power factor shouldn't fall below a certain level because if it does so reactive power charges will occur. In most cases, most power suppliers will define a charge anytime the power factor falls below 0.95.

A perfect power factor is at 1.0 and this can, in most cases, be achieved by an ideal system. For the commercial building, the below table explains their power factor definition;

Power Factor	Explanation
Good	- 0.95
Poor	0.95 - 0.85
Bad	0.85 and below

Table 1. Good, Poor, and Bad Power Factor

In most cases, commercial buildings have a power factor rated between 0.98 and 0.92, while most industries fall below 0.7.

Let’s look at the practical example of what happens when comparing two different motors with different power factors.

Where Do Poor Power Factors Originate?

Power factor is mostly affected by inductive loads, and to have a good understanding of this, we will look at three scenarios:

- Purely resistive load

- Purely Inductive load
- Purely capacitive load

Let’s get started with the first one.

Purely Resistive load

An example of such a system is an electrical resistive heater.

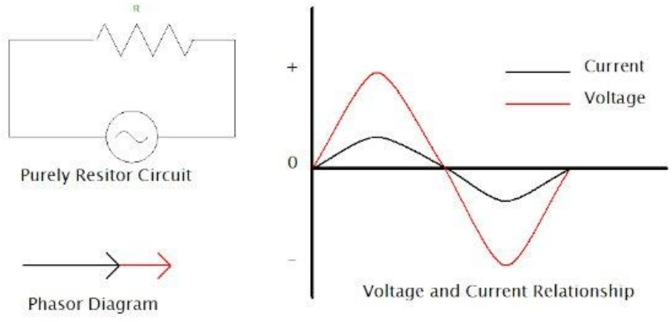

Figure 2. Purely Resistive Load Circuit, Phasor Diagram, and Voltage and Current Waveform Relationship.

The current and voltage waveform are almost identical. They both pass their minimum and maximum point and finally pass the zero axis at the same point in time. This is an indication that the system has a power factor of 1.

The phasor diagram shows that both the current and the voltage are in parallel, and this tells us all the energy taken by the system is utilized (and in the case of the electric resistor) to create heat. The purely resistive system is said to have a unity power factor.

Purely Inductive Load

A good example of such a system is an <u>induction motor</u>. The circuit, the curves, and the phasor diagram for the system are shown in Figure 3 below.

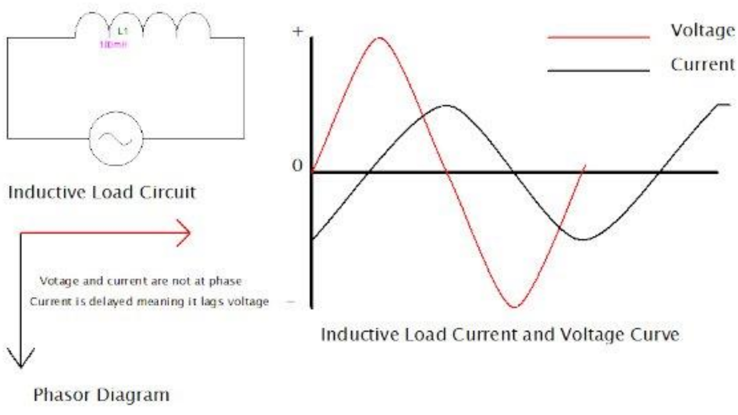

Figure 3. Purely Inductive Load Circuit, Phasor Diagram, and Voltage and Current Waveform Relationship.

An inductive load such as a motor has a coil that contains a magnetic field that holds back current resulting in a phase shift where voltages and currents waveforms end up being out of sync, making a current pass through the zero point after the voltage has already passed. The outcome of the waveforms is called the lagging factor.

Reactive power is not that important, but a little of it is needed to maintain the electromagnetic effect of the motor so that it can enable the motor to rotate. The reactive power becomes a waste when we cannot utilize it but still pay for it.

On the phasor diagram, the current line is at an angle but below the voltage line. This implies that not all the consumed electricity is utilized by the inductive system.

Pure Capacitive Load

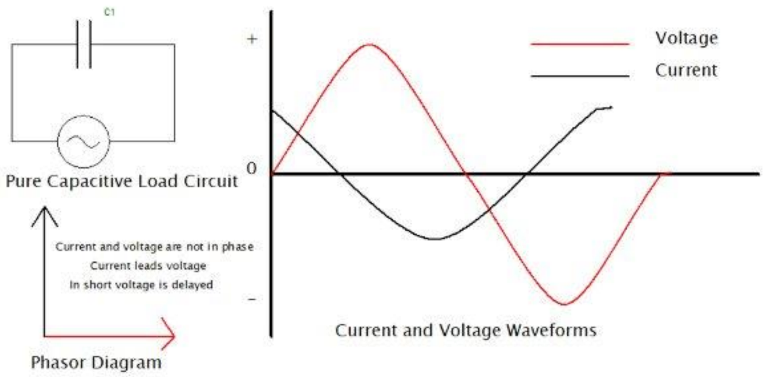

Figure 4. Purely Capacitive Load Circuit, Phasor Diagram, and Voltage and Current Waveform Relationship.

For the capacitive load, the opposite of the inductive load discussed above will happen. The current and voltages will be out of phase, but this time, voltage instead of current is held back. The resultant effect is a leading power factor. Again, this implies we are not using all the electricity to perform work, but we will end up dishing out cash to clear its bill.

On the phasor diagram, the current line is at an angle and above the voltage line since it is leading.

How to Correct Power Factor

The most common problem encountered is the lagging power factor. For poor power factor correction, capacitors and sometimes inductors must be added to the circuit system. The capacitors and the inductors will help realign the voltage and the current into the required phase and convert the power factor to one or closer.

When the problem is due to a lagging power factor, which is brought about by high inductive loads, then capacitors can solve the problem. When the problem is a leading power factor caused by high capacitive loads, inductors must be added to the circuit system to solve it.

Don't add capacitors and inductors blindly into the system. You need to calculate them, and we will do that at the end of the article.

Reason for Fixing Poor Power Factor

Poor power factor means the system is drawing more power from the source for it to do the same quantity of work, and therefore, a larger cable is needed. This will increase the cost of electrical installation more than usual.

When a power factor is too low, expect a penalty charge or a reactive power charge from the electric company.

Sometimes poor power factor causes losses in equipment, for example, transformers, due to high heat gains associated with it. It also leads to voltage drop, which interferes with the life expectancy of some equipment.

Calculating Capacitance for Power Factor Correction

As indicated earlier, we shall end the article by looking at how to calculate the capacitance needed to correct the poor power factor in a building setup. Let's look at the practical example below.

Problem

A building in Nairobi City has a power supply of 415 V with a total electrical load of 70 kW. The building's electrical system has a power factor of 0.76, but according to power supply authorities, the building should have a power factor of 0.97 for the owner to avoid penalty charges if found in violation. Calculate the capacitance needed to correct the power factor from 0.76 to 0.97.

Solution

Total_Apparent_Power(kVA)=True_Power(kW)PFPF=0.76,TruePower70kWTotal_Apparent_Power(kVA)=True_Power(kW)PFPF=0.76,TruePower70kW

Therefore,Apparent_Power=70kW0.76=92.11kVATherefore,Apparent_Power=70kW0.76=92.11kVA

TheTotal_Reactive_Power(kVAr)=√Total_Apparent_power(kVA)2−True_Power(kW)2TheTotal_Reactive_Power(kVAr)=Total_Apparent_power(kVA)2−True_Power(kW)2

TheTotal_Reactive_Power(kVAr)=√92.112−702TheTotal_Reactive_Power(kVAr)=92.112−702

=59.87kVAr=59.87kVAr

Targeted_Total_Apparent_Power=700.97=72.16kVATargeted_Total_Apparent_Power=700.97=72.16kVA

TheTargeted_Total_Reactive_Power=√72.162−702=17.52kVArTheTargeted_Total_Reactive_Power=72.162−702=17.52kVAr

Capacitor_Size=Total_Reactive_Power−Targeted_Total_Reactive_PowerCapacitor_Size=Total_Reactive_Power−Targeted_Total_Reactive_Power

Capacitor_Size=59.87−17.52=42.35kVArCapacitor_Size=59.87−17.52=42.35kVAr

Key Takeaways of Power Factor

- Power factor is a ratio of true power to apparent power.
- There exist good, bad, and poor power factors with specific ranges where 1.0 to 0.95 is said to be good, 0.95 to 0.85 poor, and 0.85 and below is said to be bad.
- When the system achieves a power factor of 1.0, the system is approved to be perfect.
- Poor power factor originates from a system's resistive, inductive, and capacitive loads.
- Lagging power factor is the most likely problem an engineer will encounter regularly.
- A balance of capacitors and inductors in the systems solves the problem of poor power factor.
- It is important to fix poor power factors to avoid high power bills, increase the life of equipment, and reduce the cost of electricity installation associated with it.
- Formulas exist to determine the power factor, apparent power, reactive power, true power, and capacitance needed to solve problems around the power factor.

TEXT 9.12

Understanding Impedance Matching/ Понимание Соответствия Импедансу

September 21, 2022 by Simon Mugo (10175)

Impedance matching is a significant process in electrical and electronic project design. Here, you will learn all about impedance matching from maximum power transfer theorem through circuits, formulas, and applications.

In electrical and electronic engineering, there is a need to match the input resistance characteristic with that of the output. Achieving equilibrium of input and output resistance from the source to the load gives a stable system. The process of balancing the input and output resistances of a given electrical system is what we refer to as impedance matching.

Defining Impedance Matching

Impedance is defined as the total resistance of a given electric component or circuit to an alternating current originating from the reactance and resistance of the given system. Unlike resistance, which has magnitude only, impedance has both phase and magnitude in alternating current circuits. For direct current, there is no difference between resistance and impedance as the impedance has zero phase angle, just like resistance has no phase angle.

We can define impedance matching as the process where the input impedance and the output impedance of a given electrical load are designed to reduce signal reflection and maximize the power transferred to the electric load. For a better understanding of impedance matching, let's look at the maximum power transfer theorem.

Maximum Power Transfer Theorem

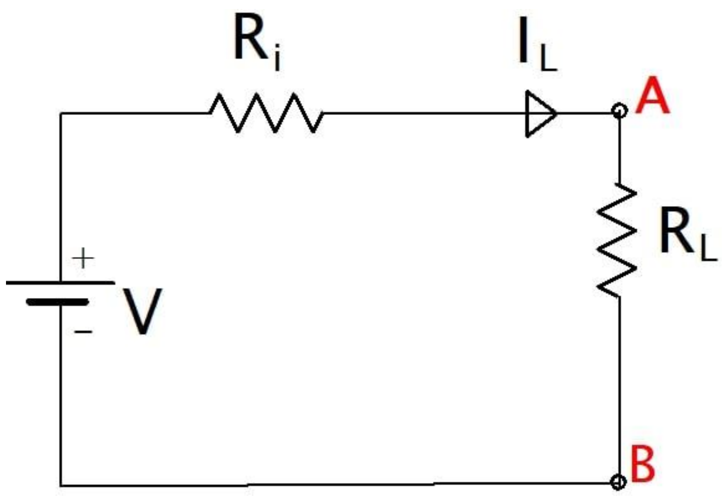

Figure 1. Maximum Power Transfer Theorem Circuit.

Suppose we have a system with a voltage source V of internal resistance Ri and powering an electric load of resistance RL. The maximum power theorem will be used to determine the value of the load resistance RL, allowing maximum power to be transferred from the source to the load. The maximum power transferred to the load depends on the size of the load resistance.

From the circuit above, power transferred to the load resistance is

P=I2LRL=V2RL(Ri+RL)2P=IL2RL=V2RL(Ri+RL)2

Figure 2. Equation of Power Transferred to the Load.

For maximum power, we differentiate the above equation to the load resistance RL and equate the outcome to zero. We shall have

dPdRL=V2(Ri+RL)2−2RL(Ri+RL)V2(Ri+RL)4=0⇒RL=RidPdRL=V2(Ri+RL)2−2RL(Ri+RL)V2(Ri+RL)4=0⇒RL=Ri

Figure 3. Differentiated Equation and Equated to Zero.

Note that maximum power can only be transferred from the source to the load when the internal resistance of the voltage source is equal to the resistance of the load. Impedance matching ensures that the source resistance is equal to the load resistance. Another thing to note is that the load reactance should also be equal to the negative of the source reactance for maximum power to be reflected at the electric load side. This means the load power can only be at maximum when the load impedance is equal to the source impedance complex conjugate.

Impedance Matching Formulas and Circuits

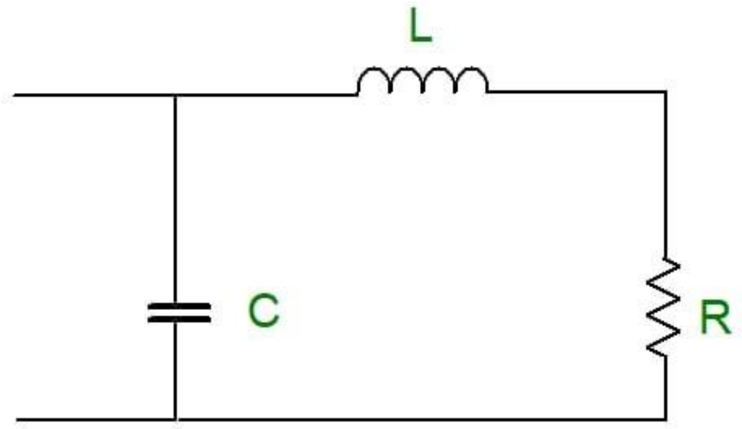

Figure 4. Impedance Matching Circuit.

For an available resistance R, we shall find the circuit that will match the resistance R' at a certain frequency w0 and develop a design of the L matching circuit displayed in Figure 4 above.

Let us start by finding the admittance Yin of our circuit above.

From the figure, we can note that the resistance R and the inductor L are in series, and the combination of the two is in parallel with capacitor C.

The impedance will be given by

Z=(R+jωL)//1jωCZ=(R+jωL)//1jωC

Z=[(R+jωL)×1jωC](R+jωL)+1jωCZ=[(R+jωL)×1jωC](R+jωL)+1jωC

Z=R+jωL(R+jωL)(jωC)+1Z=R+jωL(R+jωL)(jωC)+1

Yin=1Z=[(R+jωL)(jωC)+1](R+jωL)Yin=1Z=[(R+jωL)(jωC)+1](R+jωL)

Yin=jωC+1(R+jωL)Yin=jωC+1(R+jωL)

Let us use complex conjugates to separate the real and imaginary parts of the above equation.

Yin=jωC+1(R+jωL)×(R−jωL)(R−jωL)Yin=jωC+1(R+jωL)×(R−jωL)(R−jωL)

Yin=jωC+R(R2+(ωL)2)−jωL(R2(ωL)2)Yin=jωC+R(R2+(ωL)2)−jωL(R2(ωL)2)

Reorganizing the above equation, we get

Yin=R(R2+(ωL)2)+j[ωC−ωL(R2+(ωL)2)]Yin=R(R2+(ωL)2)+j[ωC−ωL(R2+(ωL)2)]

Finally, we have

Y=RR2+(ωL)2Y=RR2+(ωL)2 (1)

And

ω0=√1LC−(RL)2ω0=1LC−(RL)2 (2)

At the frequency of ω= 0, the resistance of Yin should be set to R’.

R′=1Y=R2+(ω0L)2RR′=1Y=R2+(ω0L)2R

R′=R+ω02L2RR′=R+ω02L2R

Separate R from the equation to get

R′=R[1+(ω0LR)2]R′=R[1+(ω0LR)2]

Let ω0LRω0LR be the Q-factor for L and R networks and our equation becomes

R′=R[1+Q2]R′=R[1+Q2] (3)

From the above equations, it is easy to solve the impedance matching problems in any electrical circuit.

Why Impedance Matching Is Needed

Impedance matching has great use in high-frequency and high-speed devices. When designing printed circuit boards that require such characteristics, ensure that the impedance at the source matches the impedance at the load.

When designing applications of ultra-high frequencies, impedance matching becomes a difficult operation for designers. The challenge is also reflected while designing microwaves and radio frequency circuits. When you get a wrong impedance matching, expect distorted pulses and high signal reflections.

An increase in frequency decreases the window of errors. The electrical circuit works the best when we have a perfectly matched impedance. If the impedance matching is not done, expect the system to work abnormally because of the effects such as the signal reflections. The reflected waves cause data delays and distortion of the phase and minimize the ratio of signal to noise.

Application of Impedance Matching

The goal of any electrical and electronic design engineer is to ensure that there is maximum power delivery from the system source to the electric load. In almost all electrical and electronic applications, impedance matching is a necessity.

Let us have a look at a few applications of impedance matching below.

Transformer Impedance Matching

Transformers are one of the components used to match the impedance of the source to load. The power input of the transformer is similar to the power output by it. The transformer changes the electrical energy c\voltage level and does not affect the power level of the system.

To match the impedance of both sides, you have to set the turn ratio accordingly. Low voltage has fewer turns, and this tells us that the impedance of the low voltage winding is lower when compared to that of the high voltage winding.

Therefore, to ensure that we have matched our impedance, a transformer with proper winding turns is connected between the source and the load. The transformer is known as a matching transformer.

We can define the matching transformer turn ratio as the square root of the ratio of the resistance of the source to the resistance of the load.

TurnsRatio=√SourceResistanceLoadResistanceTurnsRatio=SourceResistanceLoadResistance

Figure 5. Transformer Turn Ratio Calculation Formula.

Impedance Matching Transmission Line

Transmission of electrical energy from the source to the load is done using a transmission line. While transferring this energy, it is important to zero or minimize energy losses that occur. For this to be possible, we should match the source and load impedances to the transmission line being used.

The characteristic impedance is defined as the voltage and current wave ratio at any given point along the transmission line. If the transmission line in discussion is long, then we expect to have a different characteristic impedance at different distances along this transmission line. If we fail to do the impedance matching, the signs reaching the load will be reflected in the source of the origin, giving rise to a standing wave. The amount of power reflected is measured using the coefficient of reflection, which is calculated using the equation below:

$$\Gamma=ZL-Z0ZL+Z0\Gamma=ZL-Z0ZL+Z0$$

Figure 6. Transmission Line Reflection Coefficient Calculating Formula

With ZL being Line Impedance and Z0 Characteristic Impedance.

An ideal system has a load impedance similar to the characteristic impedance. The system is said to be ideal when the reflection coefficient is zero. In practice, it is difficult to achieve a zero-reflection coefficient; hence, in the transmission line, the reflective coefficient is kept close to zero.

Antenna Impedance Matching

The antenna needs to be coupled with a television. For this to be achieved, impedance matching is employed. Here, the antenna becomes our source as it has to give signals to the television, whereas the TV becomes the load because it gets signals from the antenna.

Let us take an example where the antenna and its cable have a resistance of 150 ohms, and the resistance of the TV is 600 ohms. These conditions indicate a different impedance between the source and the load, and hence it becomes impossible to have maximum power transmitted; therefore, poor signals are received by the TV.

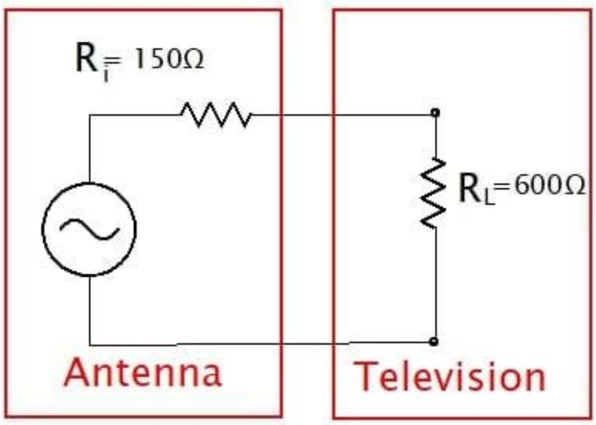

Figure 7. Antenna Impedance Matching.

To avoid the above condition, we have to use a transformer to achieve the antenna and television impedance matching. We had already introduced the formula for the turn ratio of the transformer calculation in this article, and will input the values accordingly, as shown below:

$$n=\sqrt{}RLRinn=RLRin$$

$$n=\sqrt{}600\Omega 150\Omega n=600\Omega 150\Omega$$

$$n=2n=2$$

From the calculations above, our turn ratio is 1:2, and we have to connect our transformer as in the circuit below:

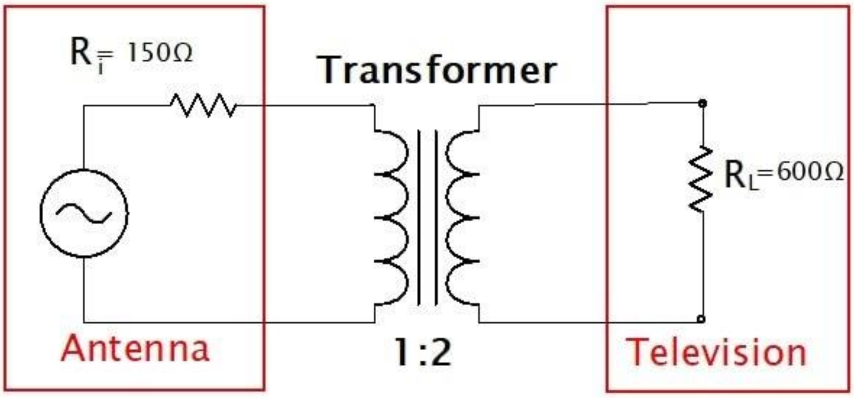

Figure 8. Impedance Matching of Antenna with Transformer.

Headphone Impedance Matching

In the case of the headphone, the signal source is the device where the headphone is plugged. The headphone is the load. For the system to attain quality audio output, the source, and the load impedances must be matched. By matching the impedances, we make sure that there is maximum power transfer from the source of the audio to the headphone.

When building portable devices, ensure that low-impedance headphones are built. This makes the system work well with proper sound quality.

Key Takeaways of Impedance Matching

- Impedance matching is the balance between the source and load impedance to ensure the load receives maximized power.
- Maximum power theorem is important in transferring energy from the source to the load.
- Impedance matching is needed to allow maximum power transfer from the source to the load by reducing reflections.
- Impedance matching has several applications, such as matching the impedance of transformers, headphones, transmission lines, and antennas.

TEXT 9.13

Understanding Frequency, Phase Angle and Wavelength in AC Systems/ Понимание частоты, фазового угла и длины волны в системах переменного тока

September 20, 2022 by Amna Ahmad (7048)

In this article, learn what is meant by frequency, phase angle, and wavelength and how to find a phase relationship between two sine waves.

Frequency is the number of cycles per second in an AC sine wave. The Hertz is the international unit of frequency equal to 1 cycle per second. Frequency is also used to describe the power used in residential, commercial, and industrial facilities. For example, most power in North America operates at 60 Hz.

A wavelength (λ) is the distance covered by one complete cycle of a given signal frequency as it passes through the air. There is an inverse proportion between the wavelength of a signal and its frequency. Signals of different wavelengths fall into different frequency categories, including radio waves, infrared light waves, visible light waves, X-ray light waves, and cosmic waves.

Phase (φ) is the time relationship of a sine wave to a known time period. Sine waves often depict the relationships between two or more signals. In-phase sine waves have peak values and baseline crossings that occur simultaneously, while out-of-phase sine waves have peak values and baseline crossings at different times.

Frequency

Consider Figure 1, which illustrates the sine wave output from an AC generator. It has been shown that when the conductors in the simple generator are rotated through one complete revolution, the output voltage goes through one complete cycle of sinusoidal change. The time taken for one cycle of change (from zero volts through +Em, zero, and -Em back to zero again) is referred to as the time period of the waveform and is designated as T (see Figure 1). If T=1 s, the waveform has a frequency (f) of 1 cycle per second or 1 hertz (Hz).

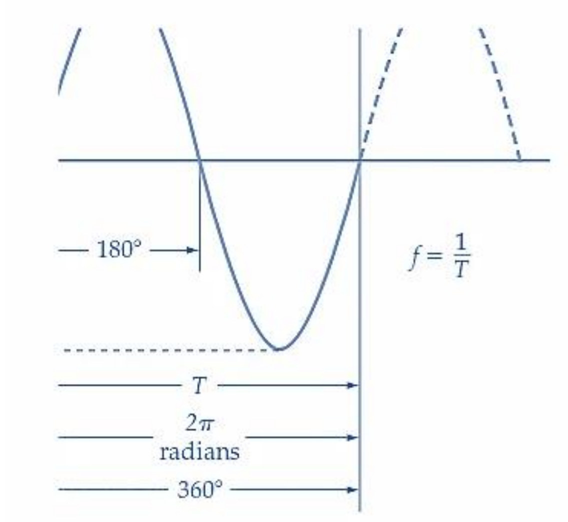

Figure 1. One cycle of a sinusoidal voltage waveform. The instantaneous voltage (e) increases from zero to Em, then decreases through zero to Em, and returns again to zero. Image used courtesy of Amna Ahmad

A waveform's frequency is always calculated by inverting the time period.

f=1T (1)

where T is in seconds and f is in Hertz.

The frequency for domestic and industrial AC supplies across North America is 60 Hz [see Figure 2]. In electronics, the AC waveforms' frequencies range from zero (in the case of DC) through kilohertz (kHz) and megahertz (MHz).

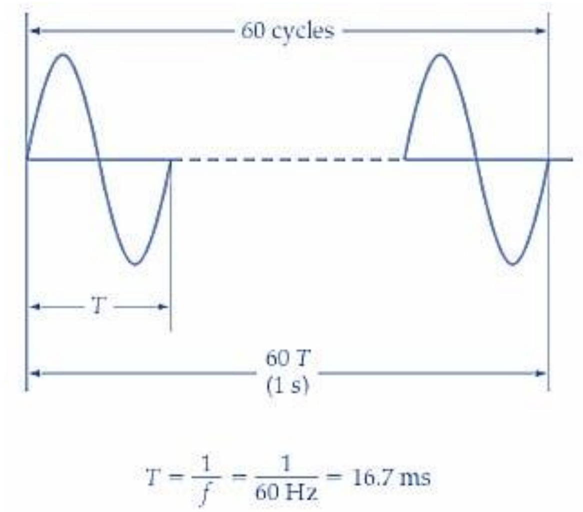

Figure 2. The waveform's frequency is measured in cycles per second or Hertz (Hz).

Phase Angle

For one complete revolution, the conductors in the simple generator rotate through 360°. If the angle of rotation of the conductors is measured in radians instead of degrees, one complete revolution represents 2π radians. As T is the time period in seconds (or time for one complete revolution), the angle through which the conductors move in 1 s is given by,

$$AngularVelocity=1Trevolutionssecond$$

$$=360Tdegreessecond$$

Or,

$$AngularVelocity=2\pi Tradianssecond$$

And the phase angle (θ) of the generated voltage at any instant t1, t2, t3, … measured from t =0 is,

$$\theta=2\pi T\times tradians$$

Also,

$$\theta=360T\times tdegrees$$

Because f=1/T, the phase angle equations can be rewritten,

$$\theta=360ftdegrees$$

And,

$$\theta=2\pi ftradians$$

Or,

$$\theta=\omega tradians$$

Where ω is the angular velocity in radians/s (i.e., ω=2πf).

Now, the AC waveform can be represented by the following equation:

$$e=Emsin\omega t \quad (2)$$

Also,

$$e=Emsin(360ft)^{\circ}$$

Figure 3 illustrates the use of Equation 2.

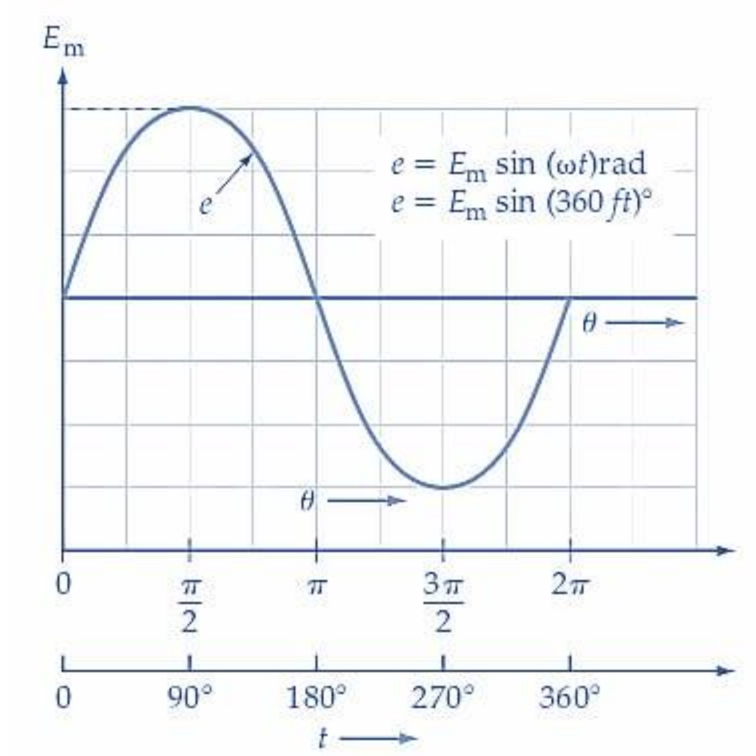

(a) e can be determined from ωt or 360 ft

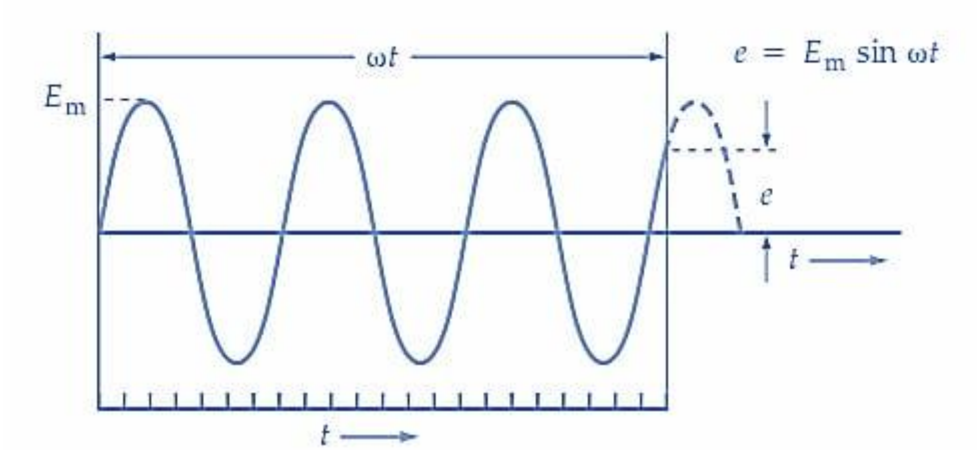

(b) e can be determined at any point in a waveform containing many cycles

Figure 3. The phase angle of a waveform can be expressed in degrees or radians, and either can be used in calculating instantaneous level

Example 1

An AC waveform with a frequency of 1.5 kHz has a peak value of 3.3 V. Calculate the instantaneous voltage levels at t_1=0.65 μs and at t_2=1.2 ms.

Solution

Equation 2,

$$e=E_m \sin 2\pi ft$$

At t1,

$$e=3.3V\times sin(2\pi\times 1.5kHz\times 0.65\mu s)rad\approx 20.2mV$$

At t2,

$$e=3.3V\times sin(2\pi\times 1.5kHz\times 1.2ms)rad\approx -3.1V$$

Phase Difference

Four different waveforms are illustrated in Figure 4. Waveforms B, C, and D have smaller amplitudes than waveform A. Waveform B goes through its cycle of change exactly at the same time as waveform A, so the two are said to be in phase with each other.

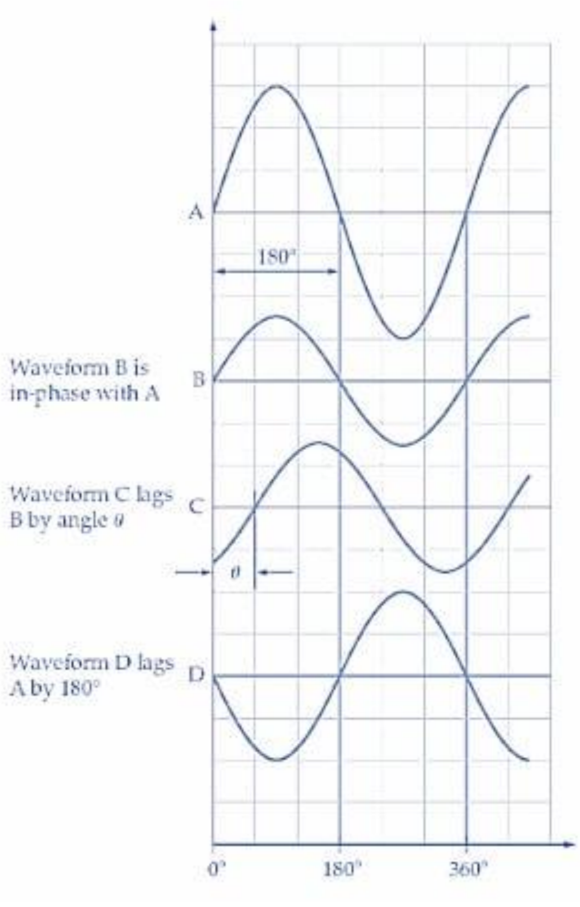

Figure 4. In-phase and out-of-phase sine waves. Waveform B is in phase with waveform A. Waveform C lags waveforms A and B

Waveforms C and D are out of phase with waveforms A and B. Because waveforms A and B commence their cycles ahead of C by an angle (degrees or radians), A and B are said to lead C by D . Alternatively, waveform C may be said to lag waveforms A and B by . The angle may also be referred to as the phase difference between the waveforms. Waveform D lags A and B by 180°

and is said to be in antiphase to A and B because it is at its negative peak when A and B are at their positive peak levels, and vice versa.

Wavelength

The wavelength of an AC waveform depends on its velocity. In the case of radio waves, the velocity is the speed of light, which is,

$$c=3\times108ms$$

For voltage waves moving along widely spaced conductors, the transmission speed is also 3 *108m/s. When the conductors are close together, the velocity depends on the insulation employed. Figure 5 (a) shows a pair of long conductors connected to a generator, and parts (b), (c), (d), and (e) show the instantaneous voltage levels at points on the conductor as the terminal voltage changes.

In Figure 5(b), e1 represents the initial or zero level of a voltage waveform at the beginning of a long conductor. A fraction of a second later, in Figure 5 (c), e1 has traveled some distance along the conductor, and the instantaneous level of the voltage at the generator terminals has changed to e2. Both e1 and e2 are traveling along the conductor at a velocity of 3 *108m/s. In Figure 5(d), the voltage at the generator terminals has changed to e3. By the time the generator terminal voltage has gone through one complete cycle [Figure 5(e)], e1 has been moving along the conductor for the time period T. So, during one complete cycle, the distance traveled by e is,

$$distance=c\times Tmeters$$

$$=(3\times108ms\times T)m$$

This distance represents the wavelength (λ) of the alternating voltage. The equation for wavelength is,

$$\lambda=c\times T$$

Or,

$$\lambda=cf\ (3)$$

Where λ is wavelength in meters, c is the velocity of light in m/s, and f is the frequency of the waveform in Hertz.

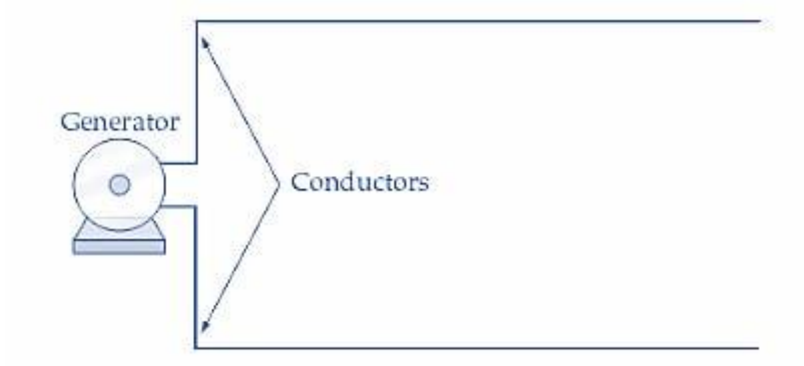

(a) Generator with two long conductors

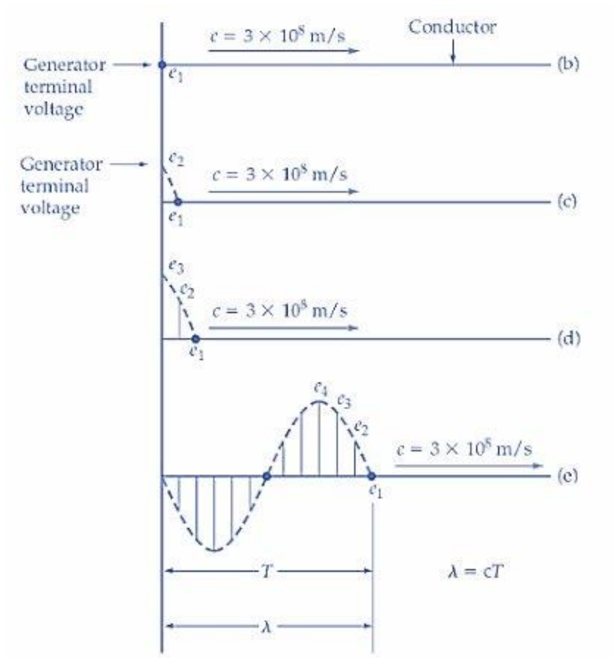

Figure 5. An alternating voltage wave moves along widely spaced conductors at the speed of light (c = 3 108 m/s). The time period of one cycle is T = 1/f, and the wavelength is = cf.

Example 2

Determine the wavelengths of 60 Hz and 1 MHz alternating waves. Calculate the frequency of a voltage that has a wavelength of 33 m.

Solution

For 60-Hz,

Equation 3,

$$\lambda=cf=3\times108ms60Hz=5\times106m$$

For 1 MHz,

$$\lambda=cf=3\times108ms1MHz=300m$$

From Equation 3,

$$f=c\lambda=3\times108ms33m=9.09MHz$$

Key Takeaways of Alternating Current

Alternating current (AC) is the voltage found in residential, commercial, and industrial locations. The direction of current flow in an AC system reverses periodically. Terminology commonly used with AC circuits includes phase angle, frequency, wavelength, and phase difference. These terms are particular to AC systems and are used when designing and troubleshooting AC electrical systems.

TEXT 9.14

What Are Magnetically Coupled Inductors?/ Что Такое Индукторы С Магнитной Связью?

September 19, 2022 by Blaine Geddes (9618)

This article discusses magnetically coupled inductors, more commonly known as transformers.

This is just one of a number of articles in the EE Power inductor series. Please see the rest of the articles here:

- What is an Inductor?
- Inductors in Series
- Inductors in Parallel

A transformer is a passive AC circuit device that performs a voltage transformation to either step up or step down the input voltage.

The Basic Transformer Equation

Faraday's law for a single conductive loop is:

$$\varepsilon=-d\phi dt,\varepsilon=-d\phi dt, \quad [1]$$

where ε is the electromotive force, or voltage, and dΦ/dt is the rate of change of magnetic flux with time.

A multi-turn coil is the equivalent of individual loops connected in series, therefore the voltages add and Faraday's law becomes:

$$\varepsilon=-Nd\phi dt,\varepsilon=-Nd\phi dt, \quad [2]$$

For two separate coils wound around the same magnetic core with perfect flux coupling, the dΦ/dt is common, so

$$\varepsilon 1=-N1d\phi dt,\text{and}\varepsilon 1=-N1d\phi dt,\text{and}$$

$$\varepsilon 2=-N2d\phi dt,\text{therefore}\varepsilon 2=-N2d\phi dt,\text{therefore}$$

$$\varepsilon 1\varepsilon 2=N1N2,\varepsilon 1\varepsilon 2=N1N2,$$

which says the voltage ratio equals the turns ratio and this is the fundamental defining equation of transformer operation.

Field Strength and Frequency

Rewriting Equation [1] in integral form gives:

$$\Phi=-\int\varepsilon dt\Phi=-\int\varepsilon dt \quad [3]$$

If the applied voltage is sinusoidally time varying, then Equation [3] can be written as

$$\Phi=-\int\varepsilon 0\sin(\omega t)dt\Phi=-\int\varepsilon 0\sin(\omega t)dt$$

$$=\varepsilon 0\omega\cos(\omega t)=\varepsilon 0\omega\cos(\omega t)$$

This says that the flux is inversely proportional to the frequency of the applied voltage. Flux is the integral of the normal component of the magnetic field B over the cross-section of interest.

$$\Phi=\int BdA\Phi=\int BdA$$

If Φ is sinusoidally time varying with an amplitude that is inversely proportional to frequency, then B must also be sinusoidally time varying with an amplitude inversely proportional to frequency and can be written as:

$$B=B0\omega\cos(\omega t)B=B0\omega\cos(\omega t) \quad [4]$$

The significance is that as the frequency of operation is decreased, the magnetic field strength increases.

The B-H Loop

In a ferromagnetic material, the total magnetic field in the material is the sum of the applied field and the internal field generated by the alignment of magnetic domains. The total field in the material is represented as B and over some linear region can be approximated as

$$B=\mu o\mu rH,B=\mu o\mu rH,$$

Where μo is the magnetic permeability of free space and μr is the relative permeability of the material, assuming a linear magnetic behavior. A representative B-H loop, which plots the field B as the applied field is cycled, is shown in Figure 1. At high magnetic field strengths the curve becomes very non-linear and the material is said to have reached magnetic saturation. As magnetic saturation is approached, an increase in H results in a much lower increase in the value of B.

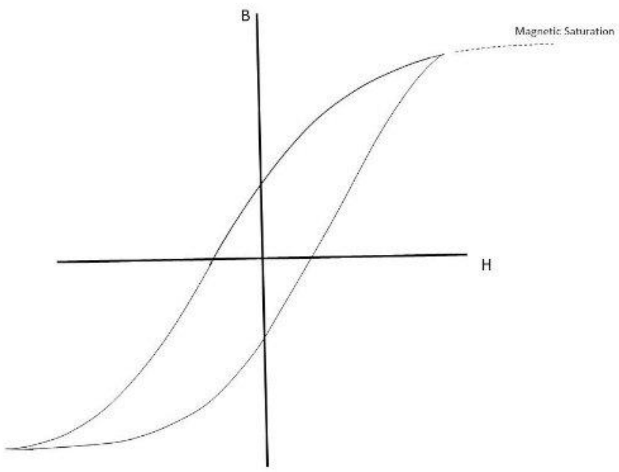

Figure 1. Representative B-H loop for a ferromagnetic material.

The energy dissipated in cyclically magnetizing the material is the hysteresis loss and is given as the integral of the B-H loop. The area of the B-H loop depends on the magnetic remanence of the material which is a function of the energy required to realign the domains. Ferromagnetic materials with low remanence are known as soft. Hard ferromagnetic materials have a much more open B-H loop because they tend to retain their magnetic state once magnetized. For use in AC circuits, clearly soft ferromagnetic materials are much preferred.

As magnetic saturation is reached, not only is the hysteresis loss at a maximum, but any increase in current flow produces a negligible increase in the magnetic field strength, so it is just wasted as I2R losses in the windings.

From Equation [4], the magnetic field rises as the applied frequency is reduced, so to avoid magnetic saturation, the physical size of AC magnetic devices such as transformers, motors, etc., must be made larger as the line frequency is lowered.

Sizing the Core

The maximum working field strength for silicon electrical steel is typically in the 1.3 – 1.7 T range, although some grain-oriented alloy steels can support higher field strengths. The saturation field strength of M-6 electrical steel (grain oriented 3% Si) is specified as 1.9 T. The closer to magnetic saturation that the core is required to operate, the greater the losses, so some margin is required. The first step in sizing the core will be to choose the allowable maximum operating magnetic field strength in the core, and this will be dependent on the grade of electrical steel chosen for the core.

Faraday's law for a multiturn coil gives dΦ/dt for a given applied voltage and number of turns. Integrating dΦ/dt will give the total flux Φ. For a sinusoidal circuit, Φ will be sinusoidal with a 1/ω factor on its amplitude.

Applying = BdA, allows the field B to be determined for a given core area, or the area to be determined given a specified maximum allowable field B. Increasing the cross-sectional area or increasing the number of turns will reduce the maximum field strength, so these are the main variables of adjustment to provide an acceptable design respecting size, cost, and performance trade-offs. Transformer size scales inversely with frequency, so the line frequency is a vital parameter. A transformer designed for 60 Hz, will work acceptably at 120 Hz, although it will be oversized, but it may become very inefficient and overheat if operated at 30 Hz.

Once the number of turns is chosen for the primary winding based on the above considerations of trading off the number of turns and core cross-sectional area to achieve an acceptable maximum field strength B, the number of turns in the secondary winding is simply set by the desired voltage ratio. The core also needs enough space to accommodate the winding coils. The wire gauge of the coils will be set by the required current flow to keep the current density in the windings at an acceptable level to minimize I2R losses in the windings. The core window area must be large enough to accommodate the windings which scales with the number of turns and the required wire gauge based on maximum current flow.

Applying all of the equations and the tradeoffs makes transformer design an iterative procedure where some assumptions would need to be made and calculations repeated. Various formulas have been developed for estimating a core size given the inputs of Volt-Ampere rating for the transformer, maximum allowable B field, lowest operating frequency, core geometry parameters, and possibly other parameters such as wire resistivity, allowable conductor losses, etc. All such formulas are based on the fundamental principle of Faraday's law and basic geometry.

A transformer is a deceptively simple passive device, but designing one involves manipulating many variables to produce a properly optimized design.

Transformer Construction

Transformers for power line frequencies and frequencies up to a few kilohertz are constructed of interleaved sheets of electrical steel stamped to shape to provide the core for the coil and a window area for the windings. The laminated structure reduces eddy current losses. The surfaces of the sheets are coated with a thin layer of a high resistivity finish. Figure 2 shows a typical transformer indicating its laminated core structure. Various core geometries are common. This one has its windings wound together in the same form.

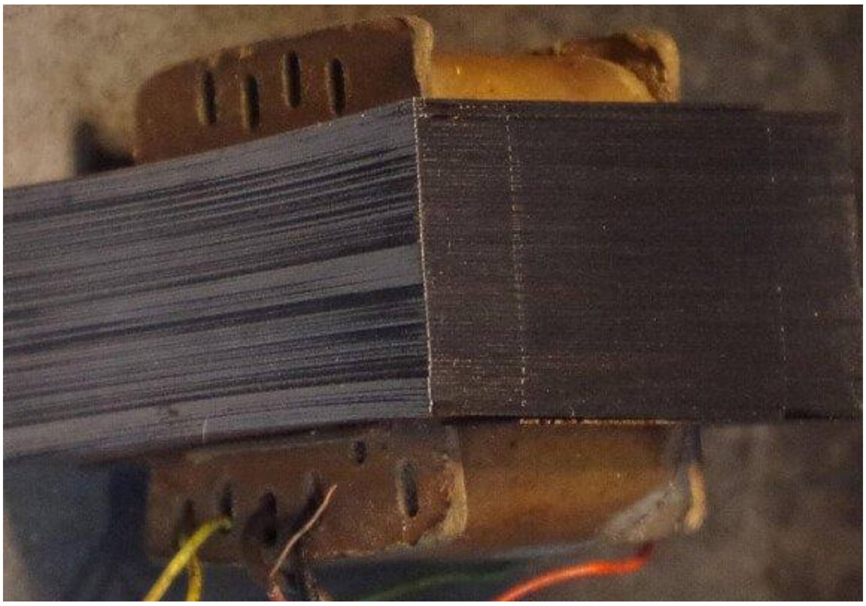

Figure 2. Photograph of a transformer showing the laminated core structure. The dotted seam indicates how the sheets are interleaved.

Transformer Equivalent Circuit

An equivalent circuit of a transformer with all quantities referred to the primary side is shown in Figure 3. The quantities from the secondary side reflect to the primary with a 1/N2 factor, where N is the secondary to primary turns ratio.

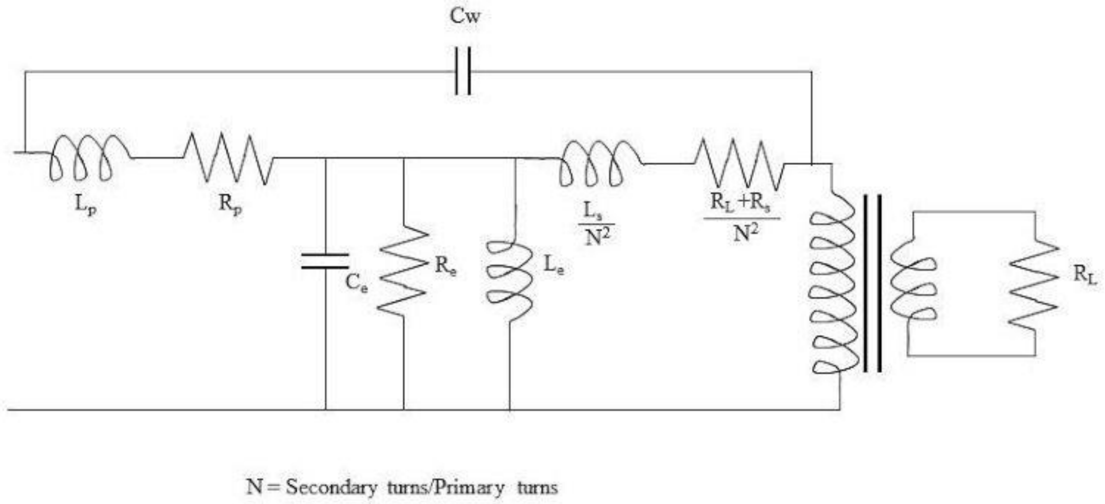

Figure 3. Equivalent circuit of a transformer with all quantities referred to the primary side.

In the equivalent circuit model, RL is the load resistance. Rs is the secondary winding resistance. Ls is the secondary winding inductance. Rp and Lp are the primary winding resistance and inductance, respectively. Re represents the core losses and it is composed of eddy current losses and hysteresis losses. Le represents the effect of cyclical magnetization of the core, which involves the shifting of domains of the ferromagnetic material, so it is modeled as an inductor.

The parasitic capacitances created by the close interwinding spacings and the windings to case capacitance are lumped together as a single pair of capacitors, Cw and Ce, but they are complicated because of the many windings creating a myriad of parasitic capacitance effects. Fortunately, these capacitive effects are small and can be neglected at low frequencies.

Transformers at High Frequencies

The physical size of inductors and transformers shrinks as the frequency of operation increases because of the 1/ω effect on the flux density in the core.

Hysteresis losses increase with frequency because of the increased rate of cycling around the B-H loop, therefore, very soft ferromagnetic materials are required for high frequencies. Eddy current losses are proportional to the square of the frequency, because, by Faraday's law, the induced voltage driving the eddy currents is proportional to dΦ/dt. Laminated electrical steel core transformers are used to frequencies up to a few kiloHertz. For frequencies beyond about 10 kHz, ferrites are commonly used.

Ferrites are ceramics. They are blends of metal oxides composed mainly of oxides of iron, manganese, zinc, and nickel. Ferrites have much lower permeabilities but vastly higher resistivities. The magnitude of the induced eddy current varies inversely with the material's resistance, so the eddy current I2R loss will drop proportionally with an increase in resistivity.

TEXT 9.15

Measuring Power Using AC Wattmeters/ Измерение Мощности С Помощью Ваттметров Переменного Тока - RYABININ

September 15, 2022 by Amna Ahmad (6525)

The wattmeter is a combination of an ammeter and a voltmeter. It measures both voltage and current and determines the resultant power.

Electric power is measured using an instrument called a wattmeter. The wattmeter comprises two coils–one for current and the other for voltage.

Power Dissipation

Heat is dissipated when an electric current flows in a conductor due to work done in moving electrons past atoms. Work is also performed in a lamp filament when the electric current is converted into light. Similarly, work is done when a speaker converts electric current into sound and when an electric motor produces motion.

The time rate of doing work is Power (P).

If a certain amount of work (W) is done in a time (t), then P=W/t. It can be demonstrated that the power supplied to any electrical component is:

$$Power=Current\times Voltage$$

Or

$$P=EI \quad (1)$$

The watt (W) is the unit of electric power.

When an applied potential difference of 1 V causes a current of 1 A to flow in a circuit or device, the power supplied is

$$P=EI=1V\times1A=1W$$

From Ohm's Law,

$$E=IR\,and\,R=\frac{E}{I}$$

Substituting for I in Equation (1) gives

$$P=\frac{E}{R}\times E$$

Or

$$P=\frac{E^{2}}{R} \quad (2)$$

And substituting for E in Equation (1) gives

$$P=I\times IR$$

Or

$$P=I^{2}R \quad (3)$$

From Equations 1, 2, and 3, it is seen that power can be calculated from a knowledge of any two of E, I, and R.

Electric heating elements convert electricity into heat for boiling water, space heating, etc. As illustrated in Figures 1 (a) and (b), power supplied to an electric lamp is converted into light, and a speaker converts input power into sound. The instrument employed for measuring power is called a wattmeter.

a. The power dissipated in a lamp is converted into light.

b. Power supplied to a speaker is converted into sound.

Figures 1 a and b. Power is dissipated when an electric current flows. Power can be converted into light, heat, sound, and mechanical motion.

AC Power Measurement

The dynamometer instrument can be employed as a voltmeter or ammeter or, in its major application, as a wattmeter. Consider the illustrations in Figure 2 that show the field coil and moving coil of a dynamometer instrument connected in series. With current flowing in the direction shown in Figure 2(a), the field coils set up fluxes with N poles on the right-hand side and S poles on the left-hand side. Also, the moving-coil flux has the polarity illustrated, S at the bottom and N at the top. The N pole of the moving-coil flux is repelled from the adjacent N pole of the field coil flux, and the two adjacent S poles also repel each other.

The moving coil is deflected clockwise, causing the pointer to move over the scale from left to right.

Now consider the effect of reversing the direction of the current through the coils. As illustrated in Figure 2(b), the field coil fluxes are now S on the right-hand side and N on the left-hand side. The moving-coil flux is also reversed, having S at the top and N at the bottom. Once again, like poles are adjacent to each other, and the pointer moves from left to right over the scale.

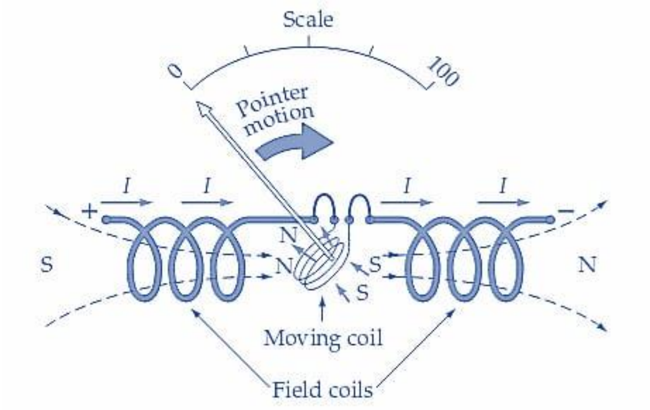

a. Current flowing from left to right produces a positive deflection

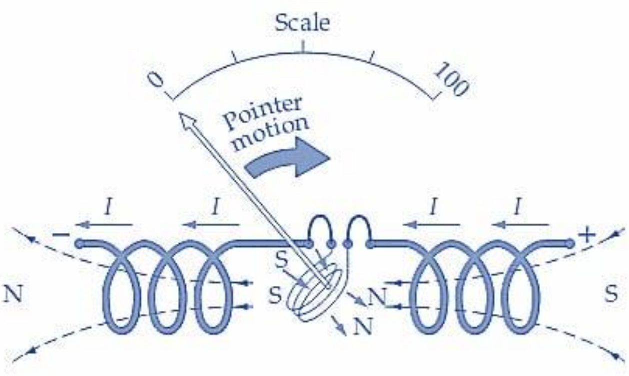

b. Current flowing from right to left produces a positive deflection

Figures 2 a and b. When the current flow through a dynamometer instrument reverses, both the field flux and the moving-coil flux reverse directions. The pointer deflection is unaffected. This makes the instrument suitable for application to AC measurements, as well as DC measurements.

It is seen that the dynamometer instrument has a positive deflection, regardless of the direction of the current through the meter. The meter terminals are not marked positive (+) or negative (-); the dynamometer instrument is un-polarized. So, the instrument gives a positive deflection when either direct or alternating current flows through the coils. As an ammeter, the instrument's scale can be read as direct current when measuring DC and as the rms value of alternating current when measuring ac. Similarly, as a voltmeter, the dynamometer instrument indicates DC volts or rms AC volts. The instrument's scale can be calibrated on DC and then used to measure AC.

For AC and DC, the major application of the dynamometer instrument is as a wattmeter.

As illustrated in Figure 3(a), the connection for measuring AC power is similar to that for measuring power in a DC circuit. The input terminals of the voltage and current coils are identified with a ±, ↓, or * sign. The marked terminal of the current coil should be connected to the supply, and the voltage coil marked terminal connected to the load side of the current coil. In alternating-current applications, the load current could lead or lag the load voltage by a phase angle (ϕ). The instrument deflection is proportional to the in-phase components of current and voltage. Thus, as shown in Figure 3(b), the instrument indication is proportional to EI cosϕ. The true power dissipated in a load with an AC supply is P =EI cosϕ. So, when used as an AC wattmeter, the dynamometer instrument measures the true power supplied to the load.

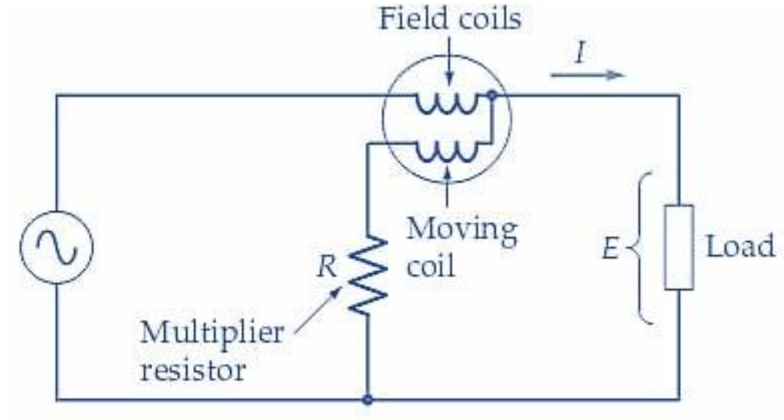

a. Dynamometer instrument as an AC wattmeter

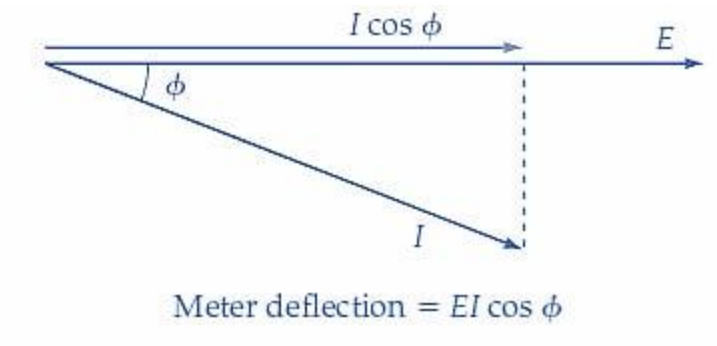

b. Phasor diagram of load current and voltage

Figure 3. The deflection of the pointer on a dynamometer wattmeter is proportional to EI cosϕ, so the instrument measures true AC power.

Example 1

A wattmeter measures the AC power delivered to a load as 100 W, and an ammeter and voltmeter indicate that the load current and voltage are 1.5 A and 100 V, respectively. Calculate the phase angle between the current and voltage.

Solution

$$True\,Power=P=EI\cos\varphi$$

So,

$$\cos\varphi=\frac{P}{EI}=\frac{100W}{100V\times1.5A}=0.667$$

And,

$$\varphi=\cos^{-1}(0.667)=48.2°$$

Example 2

A 115 V source supplies 700 mA to a load. If the power supplied to the load is measured as 75 W, determine the phase angle between the load current and the supply voltage.

Solution

$$\cos\varphi=\frac{P}{EI}=\frac{75W}{115V\times100mA}=0.932$$

And,

$$\varphi=\cos^{-1}(0.932)=21.3°$$

Key Takeaways–AC Wattmeters

Electric power can be measured with test instruments such as wattmeters, power quality meters, and clamp-on ammeters. A wattmeter is a test instrument to measure true power in a circuit. A wattmeter is provided with a scale that is usually graduated in watts (W), kilowatts (kW), or megawatts (MW). A wattmeter is used to analyze circuits by measuring the true power. Depending on the system connections (whether a Wye-connected or Delta-connected), several wattmeters can be used to measure true power in a three-phase system.

Рекомендуемые источники

1. Савинова Е.С.Как читать по-английски математические, химические и другие символы, формулы и сокращения. Справочник. – URL: https://chembaby.ru/materialy/savinova-e-s-kak-chitat-po-angliiski-matematicheskie-khimicheskie-i-drugie-simvoly-formuly-i-sokrashcheniia-spravochnik (дата обращения 21.11.2024)
2. Проблемы перевода научно-технических текстов//Научные переводы. – 2021. – URL: https://xn--80aegcaa6cbngm5a6c1ci.xn--p1ai/perevod-nauchno-tehnicheskogo-teksta/ (дата обращения 21.11.2024)
3. Научно-популярный журнал Magnetic Metals. – URL: https://www.magneticmetals.com/ (дата обращения 21.11.2024)
4. Научный журнал Electricity-Energy Systen-Iiea – URL: https://www.iea.org/energy-system/electricity (дата обращения 21.11.2024)

Приложение А

Определения электрических единиц измерения/ Electrical Units Definitions

Volt (V) Volt is the electrical unit of voltage.	One volt is the energy of 1 joule that is consumed when electric charge of 1 coulomb flows in the circuit. 1V = 1J / 1C
Ampere (A) [ˈæmpeə] Ampere is the electrical unit of electrical current.	It measures the amount of electrical charge that flows in an electrical circuit per 1 second. 1A = 1C / 1s
Ohm (Ω) Ohm is the electrical unit of resistance.	1Ω = 1V / 1A It measures the rate of consumed energy.
Watt (W) [wɒt] Watt is the electrical unit of electric power.	1W = 1J / 1s 1W = 1V · 1A
Hertz (Hz) [hɜːts] Hertz is the unit of frequency.	It measures the number of cycles per second. 1 Hz = 1 cycles / s
Decibel-Watt (dBW)	Decibel-watt or dBW is a unit of electric power, measured with logarithmic scale referenced to 1W. $10dBW = 10 \cdot \log_{10}(10W / 1W)$
Farad (F) Farad is the unit of capacitance.	It represents the amount of electric charge in coulombs that is stored per 1 volt. 1F = 1C / 1V
Henry (H) Henry is the unit of inductance.	1H = 1Wb / 1A
Siemens (S) [ˈsiːmənz] siemens is the unit of conductance, which is the opposite of resistance.	1S = 1 / 1Ω

Coulomb (C) [ˈkuːlɒm] Coulomb is the unit of electric charge.	1C = 6.238792×10^{18} electron charges
Ampere-hour (Ah) Ampere-hour is a unit of electric charge.	One ampere-hour is the electric charge that flow in electrical circuit, when a current of 1 ampere is applied for 1 hour. 1Ah = 1A · 1hour One ampere-hour is equal to 3600 coulombs. 1Ah = 3600C
Tesla (T) Tesla is the unit of magnetic field.	1T = 1Wb / 1m^2
Weber (Wb) Weber is the unit of magnetic flux.	1Wb = 1V · 1s
Joule (J) Joule is the unit of energy.	1J = 1 kg · m^2 / s^2
Kilowatt-hour (kWh) Kilowatt-hour is a unit of energy.	1kWh = 1kW · 1h = 1000W · 1h
Kilovolt-amps (kVA) Kilovolt-amps is a unit of power.	1kVA = 1kV · 1A = 1000 · 1V · 1A

Приложение Б

Чтение химических формул/ Reading Chemical Fomulars

Буквы латинского алфавита, обозначающие названия элементов, читаются так же, как буквы английского алфавита, например: H_2O— [‘eitʃ 'tu: 'ou];

Знак + читается *plus, and* или *together with.*

Знак – обозначает одну связь и не читается.

Знак = читается *give(s)* или *form(s).*

Знак → читается *give(s), pass(es) over to* или *lead(s) to.*

Знак ↔ читается *forms and is formed from.*

Примеры:

$AgNO_3$ ['ei'dʒi: 'en 'ou 'θri:];

$C + O_2 \rightarrow CO_2$: C plus O two give CO two or: one atom of carbon reacted with one two-atom molecule of oxygen and produces one molecule of carbon dioxide;

$N_2 + 3H_2 \rightarrow 2NH_3$: N two plus three molecules of H two from and are formed from two molecules of NH three ['en 'tu: plʌs 'θri: 'mɔlikju:lz əv 'eitʃ 'tu: 'fɔ:m ənd a: 'fɔ:md frəm 'tu: 'mɔlikju:lz əv 'en 'eitʃ 'θri:]

Чтение уравнений/Reading equationы:

$Zn + H_2SO_4 \rightarrow ZnSO_4 + H_2$

"One atom of zinc reacts with one molecule of sulphuric acid producing one molecule of zinc sulphate and one molecule of hydrogen".

$H^+ + NaHCO_3 \rightarrow Na^+ + H_2CO_4 \rightarrow Na^+ + H_2O + CO_2$ ['haidrədʒən 'aiən 'plʌs 'en 'ei 'eitʃ 'si: 'ou'θri: 'givz 'neitriəm 'aiən 'plʌs 'eitʃ 'tu: 'si: 'ou 'θri: 'givz 'neitriəm 'aiən 'plʌs 'eitʃ 'tu: 'ou 'plʌs 'tu:'si: 'tu:].

Приложение В

Список химических элементов/List of Chemical Elements

Ac — actinium [æk'tiniəm] актиний
Al — **aluminium** [,ælju'minjəm] алюминий
Ag — argentum [a:'dʒentəm] серебро
Am — **americium** [,æmə'risiəm] америций
Ar — argon ['a:gɔn] аргон
As — **arsenic** ['a:snik] мышьяк
At — **astatine** ['æstə'ti:n] астат
Au — **aurum=gold** ['ɔ:rəm], [gould] золото
B — boron ['bɔ:rɔn] бор
Ba — **barium [**'bɛəariəm] барий
Be — **beryllium** [be'riljəm] бериллий
Bi — **bismuth** ['bizməɵ] висмут
Bk — **berkelium** [,bə:ki'liəm] беркелий
Br — **bromine** ['broumi:n] бром
C — **carbon** ['ka:bən] углерод
Ca—**calcium** ['kælsiəm] кальций
Ce — **cerium** ['s:riəm] церий
Cd — **cadmium** ['kædmiəm] кадмий
Cf—**californium** [,kæli'fɔ:niəm] калифорний
Cl — chlorine ['klɔ:ri:n] хлор
Cm — **curium** [‘kju:riəm] кюрий
Co — **cobalt** [kə'bɔ:lt] кобальт
Cr — **chromium** ['kroumjəm] хром
Cs — caesium ['si:zjəm] цезий
Cu — **copper** ['kɔpə] медь
Dy — dysprosium [dis'prousiəm] диспрозий
Er — erbium ['ə:biəm] эрбий
Es — **einsteinium** [ain’stainiəm] эйнштейний
Eu — europium [ju:'roupiəm] европий
F — **fluorine** ['fluəri:n] фтор
Fe — **ferrum** ['ferəm] железо
Fm — **fermium** ['fə:miəm] фермий
Fr — **francium** ['frænsiəm] франций
Ga —**gallium** ['gæliəm] галлий
Ge — **germanium** [ʤə:'meiniəm] германий

Gd — gadolinium [gædə'liniəm] гадолиний
H — hydrogen [‘haidriʤən] водород
He — **helium** ['hi:ljəm] гелий
Hf — **hafnium** ['hæfniəm] гафний
Hg — hydrargyrum=mercury [hai'dra:ʤirəm], ['mə;kjuri] ртуть
Ho — **holmium** ['houlmiəm] гольмий
I — **iodine** [‘aiədi:n] йод
In — **indium** ['indiəm] индий
Ir — **iridium** [ai'ridiəm] иридий
К — **kalium** ['keiliəm] калий
Kr — krypton ['kriptɔn] криптон
Ku — **kurchatovium** [,kurʧə'tɔviəm] курчатовий
La — **lanthanum** ['lænθənəm] лантан
Li — lithium ['Iiθiəm] литий
Lr — lawrencium [,lɔ:'rensiəm] лоуренсии
Lu — lutecium [lju:'ti:ʃiəm] лютеций
Md —**mendelevium** [,mendə'leviəm] менделевий
Mg — magnesium [mæg'ni:zjəm] магний
Mn — **manganese [,**mæŋgə'ni:z] марганец
Mo — **molybdenum** [mɔ‘libdinəm] молибден
N — nitrogen ['naitriʤən] азот
Na — **natrium** ['neitriəm] натрий
Nb — **niobium** [nai'oubiəm] ниобий
Nd — **neodymium** [,ni:ə'dimiəm] неодим
Ne — **neon** ['ni:ən] неон
Ni — **nickel** ['nikl] никель
No — **nobelium** [nou'beliəm] нобелий
Np — **neptunium** [nep'tju:njəm] нептуний
O — **oxygen** ['ɔksiʤən] кислород
Os — **osmium [‘ɔ**zmiəm] осмий
P — **phosphorus** ['fɔsfərəs] фосфор
Pa — **protactinium** [,proutæk'tiniəm] протактиний
Pb — plumbum ['plʌmbəm] свинец
Pd — **palladium** [pə'lerdiəm] палладий
Pm — **promethium** [prə'mi:θjəm] прометий
Po — polonium [pə'louniəm] полоний
Pr — **praseodymium** [,preiziə'dimiəm] празеодим
Pt — **platinum** ['plætinəm] платина

Pu — plutonium [plu:'tounjəm] плутоний
Ra — radium ['reidjəm] радий
Rb — rubidium [ru:'bidiəm] рубидий
Re — rhenium ['ri:niəm] рений
Rh — rhodium ['roudjəm] родий
Rn — radon ['reidɔn] радон
Ru — ruthenium [ru:'θi:niəm] рутений
S — sulphur ['sʌlfə] сера
Sb — antimony ['æntiməni] сурьма
Sc — scandium ['skændiəm] скандий
Se — selenium [si'li:njəm] селен
Si — silicon ['silikən] кремний
Sm — samarium [sə'mɛəriəm] самарий
Sn — stannum ['stænəm] олово
Sr — strontium ['strɔnʃjəm] стронций
Ta — tantalum ['tæntələm] тантал
Tb — terbium ['tə:biəm] тербий
Tc — technetium [tek'ni:ʃiəm] технеций
Te — tellurium [te'ljuəriəm] теллур
Th — thorium ['θɔ:riəm] торий
Ti — titanium [ti'teinjəm] титан
Tl **— thallium** ['θæliəm] таллий
Tm — tullium ['tʌliəm] тулий
U — uranium [juə'reinjəm] уран
V — vanadium [və'neidjəm] ванадий
W — wolfram [‘wulfrəm] вольфрам
Xe — xenon [‘zenɔn] ксенон
Y — yttrium ['itriəm] иттрий
Yb — ytterbium [i'tə:bjəm] иттербий
Zn — zinc [ziŋk] цинк
Zr — zirconium [zə:'kounjəm] цирконий

Приложение Г

Список сокращений используемых в схемах/
List of Abbreviations Used in Schemes

A/C Hed	Синхрозвуковая головка
ABC(automatik brighess limiter)	автоматическое ограничение яркости
AC (alternating curent)	переменный ток
ACC(automatic color control)	автоматическая стабилизация уровня цветности (вспышек поднесущей)
ACK(automatic color killer)	автоматическое подавление сигналов цветности
ADC(analog to digital converter)	Аналого-цифровой преобразователь
ADD (adder)	дополняемое
A.DUB(audio dubbing)	перезапись звука
ADJ(adjust)	регулировка
AE(audio erase)	стирание фонограммы
Aerial	антенна
Af (audio frequency)	звуковая частота
AFC(automatic frequency control)	автоматическая подстройка частоты(АПЧ)
AFT(automatic fine tuning)	точная автоматическая настройка
AGC(automatic gain control)	автоматическая регулировка усиления (АРУ)
ALC(autamatic level control)	автоматическая регулировка уровня (сигнала)
AM(amplitude modulation)	амплитудная модуляция
AMP(amplfier)	усилитель
APC(automatic phase control)	автоматическая подстройка фазы(АПЧ)
APC(automatic phase control)	автоматическая подстройка фазы(АПФ)
APS(automatic program search)	автоматический поиск программы

ASO(active sidband optimum)	узел восстановления верхней боковой полосы видеосигнала
AUX(auxiliary)	вспомогательный
AWB(automatic white balance)	автоматический баланс белого
B (BLU)(color signal BLUE)	сигнал синего цвета
BF(burst flag)	частотная вспышка(сигнал цветовой вспышки)
BGP(burst gate pulse)	строб-импульс вспышки
Bias	напряжение смещения, подмагничивания
BPF(bandpass filter)	полосовой фильтр
Brake	прервать, остановить, тормоз
BSP(bandstop foiter)	заграждающий фильтр
BLK(blankin)	гашение, бланкирование, выключение
C(CHROMA)	составляющая цветности
C_ERR	погрешность вращения ведущего вала
CAM SW	программный переключатель
CAPST (capstan)	двигатель ведущего вала
CARR(carrier)	несущая частота
CATV(cabl TV)	кабельное телевидение
C.FG/CFG(capstan frequency generator)	сигнал датчика частоты вращения ведущего вала
C.F.R./C.FREE RUN(cfpstan free run)	свободное вращение видео головок(при отключенной системе автоматического регулирования ведущего вала)
CH(chennel)	канал
Circuit	схема
Clip(Clipper)	ограничитель, клипер
CLK(clock)	тактовый сигнал

COL(color)	цвет
Comb	гребенчатый фильтр
Comp(a)(comparator)	Компаратор
COMPE(compensator)	компенсатор
COMP(o)(composite)	полный, смешанный
Connector	Разъем, соединение
Control Unit	управляющее устройство, регулировочный узел
CONV(converter)	преобразователь
CORR(correlation)	корреляция, сравнение
COUNT(counter)	счетчик
CPU(central processing unit)	центральный процессор
Cros modulation	перекрестная модуляция
CS(converter subcarrier)	преобразованная поднесущая сигналов цветности
CST(cassette)	кассета
C.SYNC(composite synchronizing signal)	полный (общий) сигнал синхронизации
CTL(control track pulse (control))	регулировка, управление
CTL-HEAD	синхроголовка
CUE	ускоренное воспроизведение в прямом направлении
CVS(composite videj signal)	полный видеосигнал
Cyrrent	ток
CYL(cylinder)	блок видео головок
D(drum)	барабан, двигатель "блока вращающихся головок"
D/A (digital to analog converter)	цифро-аналоговый преобразователь
D.AFC	система автоматического регулирования

	частоты вращения "блока вращающихся головок"
D.APC	система автоматического регулирования "блока вращающихся головок"
D-D(direct drive)	прямой провод
D.LIM(dark limiter)	ограничитель(пиков) темного
D.FG(drum frequency generator)	датчик(сигнал датчика) частоты вращения "блока вращающихся головок"
D.PG(drum frequency generator)	сигнал датчика положения видео головок
D/C (dark clip)	ограничитель
DATA	Данные
DDC(direct drive cylinder)	Прямой электропривод "блока вращающихся головок"
DE-MPH(A) (deemhasis)	Коррекция поднесущей
DEV(deviation)	Девиация
DIFF.AMP (defferiminator amplifier)	Дифференциальный усилитель
DISCR(discriminator)	дискриминатор
DISP(display)	Экран, дисплей
DL(delay line)	Линия задержки
DM (drum motor)	Двигатель "блока вращающихся головок"
DO(dropout)	выпадения
DOC(dropout compensator)	Компенсатор выпадения
DRV(drive)	Схема управления
D/W(dark/white)	Черно/белое
E-E(electronic to electronic)	Режим контроля входного видео сигнала на мониторе с использованием компонентов канала воспроизведения
E.Q.AMP	Усилитель корректор
E.S.(end sensor)	Датчик конца ленты

E.SW(electronic switch)	Электронный ключ
EMPHA(emphasis)	Предискажения
ENV	Огибающая
EQ(equalizer)	Корректор, эквалайзер
Erase current	Ток стирания
ETC(electronic tape counter)	Электронный счетчик длины ленты
ETX(external)	Внешний, наружный
F(fuse)	Предохранитель
F.ADV(frame advance)	Покадровый просмотр
F/V(frequency to voltage convertor)	Преобразователь частота-напряжение
F.FWD(fast forward)	Перемотка вперед
FG(frequency generator)	Генератор частоты
FH	Высокая частота
Fl	Низкая частота
FM(frequency generator)	Частотная модуляция
FREQ.COMP.(frequency compensator)	Частотный корректор
FS(frequency shift)	Сдвиг (уход) частоты
FSC(sub carrier frequency)	Частота поднесущей
FV(false vertikal)	Импульсы замещения кадрового сигнала вперед
Gain	Усиление
Gate	Строб
Gen(generator)	Генератор
GND(g) (ground)	Земля, корпус, общий
H(horizontal)	Горизонтальный, строчный, строка
H(high)	Высокий логический уровень

H(head)	Головка
HD(horizontal drive)	Сигнал строчной синхронизации
H.SYNC(horizontal sync)	Строчный синхроимпульс
HG(Hall generator)	Генератор(датчик) Холла
H.P.AMP	Усилитель верхних частот
HPF(high pass fillter)	Фильтр верхних частот
HSP(H.SW.P)(head switching pulse)	Импульсы переключения предварительных усилителей воспроизведения
HSS(helical scan system)	Система наклонно-строчной записи-воспроизведения
HSS(horizontal sync.separator)	Селектор строчных синхроимпульсов
IC(integrated circuit)	Интегральная схема
IF(intermediate frequency)	Промежуточная частота
IND(I)(indicator)	Индикатор
INT(internal)	Внутренний
INV(inverter)	Инвертор
I/O(input/output)	Вход/выход
IR(infrared rays)	Инфракрасный луч
KILL(killer)	подавитесь
L(laoding)	Загрузка(кассеты)
L(LUM)	Яркость, яркостная и синхронизирующая составляющие полного телесигнала
L(LOW)	Низкий логический уровень
LCD(liquid crystal display)	Жидкокристаллический дисплей
LED(liquid emitting diode)	Светодиод
LF(lof frequency)	Низкие (звуковые) частоты
Lin(linear,line)	Линейный, линия

LIM(limiter)	Ограничитель
LM(loading motor)	Двигатель загрузки (кассеты)
LNC(line noise canceller)	Схема подавления шума
LP(long play)	Замедленное воспроизведение
LPF(lov pass filter)	Фильтр низких частот (ФНЧ)
L/R(left/right)	Левый/правый
M.C.A.(motor control amlifier)	Усилитель сигнала управления двигателем
MAN(manual)	Руководство, панель управления
MEM(memory)	Память
MIC(microphone)	Микрофон
MIX(mixer)	Микшер
MMV(monostable multivbrator	Ждущий мультивибратор
MOD(modulator)	Модулятор
MODE SW	Переключатель режима
MPX(multiplex)	Мультиплексор
MPU(microprocessor)	Микропроцессор
MUTE	Блокировка звука
MX(matrix)	матрица
NC(not connected)	Свободный, не подсоединенный (вывод)
N.CAN(noise cancel)	Устройство шумопонижения
NFB(negative feed back)	Отрицательная обратная связь
NL(noise reduction)	Ограничитель
NOC(normally open contact)	Замыкающий контакт
NR(noise reduction)	Шумоподавление
NTSC(National Television System Committe)	Система цветного телевидения США
OSR(oscillator)	Генератор, осциллятор

OSC-CTR	Управление частотой генератора
OSD(on screen display)	На экране дисплея
OTR	Оперативная запись
Output	Выход
PS(Phase shift)	Фазовращатель
PA(pulse amplifier)	Импульсный усилитель
PB(playback)	Воспроизведение
P.cont(power control)	Управление блоком питания
PB FM.Level	Уровень воспроизведения ЧМ сигнала
Peaking AMP	Усилитель со схемой ВЧ-корекции
PEL(picture element)	Элемент изображения
PIF(picnure intermediate frequency)	Промежуточная частота изображения
PG(pulse generator)	Генератор импульсов, используется также для обозначения сигнала ОС по положению видеоголовок
PIP(picture in picture)	Картинка в картинке
PLL(phase locked loop)	Фазовая подстройка частоты
Pre.Amp	Предварительный усилитель
PWB(printer wiring board)	Печатная плата
PWM(pulse width modulation)	Широтно-импульсная модуляция(ШИМ)
R(red)(color signal red)	Сигнал красного цвета
RAM(random access memory)	Запоминающее устройство с произвольной выборкой (ОЗУ)
RC(reading clock)	Отсчет кадров
RCP(remote control panel)	Пульт дистанционного управления
REC(record)	Запись
RECT(rectifier)	Выпрямитель, детектор

REF(reference)	Опорный сигнал
REG(regulator)	Стабилизатор, регулятор
REEP (reel pulse)	Импульсы с датчика вращения(подкатушечника)
REW(rewind)	Перемотка
REV(reverse)	Реверс, назад
RF(radio frequency)	Радио частота
ROM(read only memory)	Постоянное запоминающее устройство (ПЗУ)
RT(rotary transformer)	Вращающийся трансформатор
RUN IND (runing indicator)	Датчик вращения
SC(sand castle)	Стробирующий импульс
SCR	Тактовые импульсы центрального процессора
SCL	Тактовая шина
SDA	Шина данных
SEL(select)	Выбор
SENS(sensor)	Датчик
SERVO	Система автоматического регулирования(САР)
SEP(separator)	Селектор
SI(serial-data in)	Последовательный вход шины данных
SLD(side lock detector)	Детектор внешней синхронизации
SIF(sound intermediate frequency)	Промежуточная частота звука
Sol(solenoid)	Катушка электромагнита
SO(serial-data out)	Выход последовательных данных
S/N(signal to noise)	Отношение сигнал/шум
SP(standart play)	Стандартное воспроизведение

S.REEL(supply reel sensor)	Датчик подающего подкатушечника
SRCH(search)	Поиск
SRV(servo)	Серво
S.TRACK(slow tracking)	Замедленный трекинг
STBY(standby mode)	Режим ожидания(готовности)
S-VHS(syper VHS)	Система видеозаписи
SW 25/30HZ(25/30 Hz head switching pulse)	Сигнал переключения видеоголовок
SYNC(sinchronizing sighal)	Сигнал синхронизации
Sys.con(system control)	Управление системой
PHOTO(take up photo)	Фотодатчик(сигнал фотодатчика) ракорда начала ленты
T/L(tuner/line)	Сигнал переключения входов
TP(test point)	Тестовая точка
T.REEL(take up reel sensor)	Приемная катушка (датчик)
TRAP	Режекторный фильтр
UL(unloading)	Выброс, разгрузка(кассеты)
V(vert)(vertical)	Вертикальный, кадровый
V.D.(vertical defrlection)	Вертикальное отклонение
V.LOCK(vertical lock)	Частота следования кадровых синхроимпульсов
V.DRV(vertical drive pulse)	Кадровый импульс
VDUB(video dubbing)	Перезапись видео сигнала
V/F(voltage to frequency cjverter)	Преобразователь напряжение-частота
VHS(video home sistem)	Система видео записи
Vol(volume)	Громкость
V-REF(voltage reference)	Опорное напряжение
VP(vertical pulse)	Кадровый импульс

VSS(vertical sync separator)	Селектор кадровых синхроимпульсов
Vss(voltage super source)	Напряжение питания
VTR(video tape recorder)	видеомагнитофон
WC(write clock)	Ввод тактовый
WTH(color signal WHITE)	Сигнал белого(цвета)
WTH BAL CONT(wite balanse control)	Контроль баланса белого
Y(liminance signal)	Сигнал яркости
Y/C (luminance/cromiminance)	Сигнал яркости/цветности
YE(YEL)(color signal YELLOW)	Сигнал желтого (цвета)
YL(luminance signal (low companent))	Сигнал яркости(низкая компонента)

Приложение Д

Чтение математических формул/ReadingofMathematical Formulas

1. **Arithmetic, college algebra and geometry.**

Common fractures

Числитель выражается количественным числительным (например, one, four, twenty- five и т.д.), а знаменатель — порядковым числительным (например, first, fourth, twenty- fifth и т.д.). Если числитель больше единицы, то знаменатель принимает окончание множественного числа s. Если дробь является буквенным выражением, то обычно используется конструкция “числитель” over “знаменатель”.

$\frac{1}{2}$	one half
$\frac{1}{3}$	one third
$\frac{2}{3}$	two thirds
$\frac{26}{38}$	twenty six thirty eights
$2\frac{1}{2}$	two and a half
$3\frac{4}{5}$	three and four fifth
$\frac{m}{n}$	m over n

Decimal fractions

В десятичных дробях целое число отделяется от дроби точкой, называемой “point”. Каждая цифра читается отдельно. Ноль читается либо как “o [ou]”, либо как “zero”. Ноль целых может совсем не читаться.

0.2	1. o point two 2. zero point two 3. point two
0.06	1. o point o six 2. zero point zero six 3. point o six 4. point zero six
1.25	1. one point twenty five 2. one point two five

Indexes, powers and roots

Верхние и нижние индексы в английском называются соответственно “subscript” и “superscript”. Например, произносится как “x sub n”, произносится как “z super k”. Часто, когда не возникает путаницы с верхними и нижними индексами, (например, если верхние индексы не используются) слова “sub” и “super” опускаются, и тогде произносится как “a two”.

a_m	a sub m (a m)
a_0	1. a zero 2. a naught
b^n	b super n (b n)
c_{mn}^{jk}	c sub m n super j k

Возведение в степень по-английски — “raise to the power”. Например x^2, произносится как “x raised to the fifth power”. Укороченными вариантами являются “x to the fifth power” или просто “x to the fifth”. Для второй и третьей степени обычно используются выражения “x squared” и “x cubed”. Корень n-ой степени читается как ‘the n-th root”. Корни 2-й и 3-й степени читаются как “square root” и “cube root” соответственно.

x^2	1. x squared 2. x raised to the second power 3. x to the second power 4. x to the second 5. the square of x 6. the second power of x
y^3	y cubed
z^{-10}	1. z to the negative tenth 2. z to the minus tenth
$t^{\frac{3}{2}}$	t to the three halves
$\sqrt{a}$	the square root of a
$\sqrt[3]{7}$	the cube root of seven
$\sqrt[n+k]{7}$	the root of the power n plus k of three
$\sqrt[5]{b^4}$	the fifth root of b to the fourth

Certain mathematical signs and expressions.

+	plus (the addition sign)
$a + b$	1. a plus b; 2. sum of a and b;
–	minus (the subtraction sign)
$a - b$	1. a minus b; 2. difference of a and b
$-x$	1. minus x; 2. negative x
$a \pm b$	a plus minus b
·	times (the multiplication sign)
$a \cdot b$ или ab	1. a times b; 2. a b 3. product of a and b
: или /	the division sign
$a : b$ или a/b	1. a divided by b; 2. a by b 3. ratio of a and b; 4. a over b
$d \equiv h$ или $h \mid d$	1. d is divisible by h 2. h is a divisor of d
=	the equality sign
$a = b$	1. a equals b; 2. a is equal to b
$a \neq b$	a is not equal to b
$a \approx b$	a is approximately equal to b
$\equiv$	the identity sign
$a \equiv b$	a is identically equal to b

$a < b$	a is greater than b
$a > b$	a is less than b
$a \leq b$	a is greater than or equal to b
$a \geq b$	a is less than or equal to b
$\lvert x \rvert$	1. absolute value of x; 2. magnitude of x
$n!$	n factorial
$\blacksquare$	the “end of the proof” sign
правая [левая] часть (уравнения и т.д.)	right-hand [left-hand] side (of equation, etc.)

Brackets

$(\ )$	1. parentheses (ед. число parenthesis) 2. round brackets
$[\ ]$	1. brackets 2. square brackets
$\{\ \}$	braces

Если некоторое выражение стоит в скобках, а к нему применяется какая-либо операция, то в данном случае употребляется слово “quantity”:

$(a+b)c = ac + bc$	a plus b quantity times c equals ac plus bc
$x + a^2$	x plus a squared
$(x+a)^2$	x plus a quantity squared
$a + \frac{b}{c}$	a plus b over c
$\frac{a+b}{c}$	a plus b quantity over c

Также полезными терминами являются следующие:

раскрывать скобки	to expand
выносить за скобки (разлагать на множители)	to factor out (to factor)
приводить подобные слагаемые	to combine like terms

Intervals

(a, b)	open interval from a to b
$[a, b]$	closed interval from a to b
$(a, b]$	1. open from the left interval from a to b 2. closed from the right interval from a to b
$[a, b)$	1. open from the right interval from a to b 2. closed from the left interval from a to b

Some geometric terms

$\bar{a}$	1. a bar; 2. vector a;
$\angle\alpha$	angle alpha
$\triangle ABC$	triangle ABC
$\|\|a\|\|$	norm of a
$a\|\|b$	a is parrallel to b
$a\perp b$	a is perpendicular to b

2. **Set theory.**

Set-theoretic operations.

$A\cup B$	1. A union B 2. union of A and B
$A\cap B$	1. A intersection B 2. intersection of A and B
$A\setminus B$	1. A minus B 2. set difference of A and B
$A \vartriangle B$	symmetric difference of A and B
$\bar{A}$	compliment of A

Operations of containment.

$a \in A$	1. a belongs to A 2. a is an element of A 3. A contains a
$a \notin A$	a does not belong to A
$A \subset B$ или $A \subseteq B$	A is a subset of B
$A \supset B$ или $A \supseteq B$	B is a subset of A
$A \not\subset B$	A is not a subset of B

List of standard sets.

$\varnothing$	the empty set
$\mathbb{N}$	the set of natural numbers
$\mathbb{Z}$	the set of integer numbers
$\mathbb{Q}$	the set of rational numbers
$\mathbb{R}$	the set of real numbers
$\mathbb{R} \setminus \mathbb{Q}$	the set of irrational numbers
$\mathbb{A}$	the set of algebraic numbers
$\mathbb{R} \setminus \mathbb{A}$	the set of transcendental numbers
$\mathbb{R}^n$	the n-dimensional real space
$\mathbb{C}$	the set of complex numbers
$\mathbb{C}^n$	the n-dimensional complex space
$\mathbb{P}^n$	the n-dimensional projective space
2^A	the power ser of A

Operations in topological vector spaces.

$cl(A)$ или $\bar{A}$	closure of A
$\overset{0}{A}$	interior of A

∂A	boundary of A
$A \times B$	1. A cross B 2. direct product of A and B 3. Cartesian product of A and B
$A \oplus B$	1. A plus B 2. direct sum of A and B
$A \wedge B$	1. A wedge B 2. wedge product of A and B 3. interior product of A and B
A/B	1. quotient space A over B 2. factor space A over B

3. **Mathematical logic.**

$A \vee B$	A or B
$A \wedge B$ или $A \& B$	A and B
$\bar{A}$ или $\neg A$	not A
$A \Rightarrow B$	A implies B
$A \sim B$	A is equivalent to B

Quantifiers.

$\forall$	“for any” или “for all”
$\exists$	“there exists”
$:$	“such that”
$\forall r \in \mathbb{R} \exists n \in \mathbb{N} : n > r$	For any real r there exists a positive integer n such that n is greater than r.

4. **Calculus.**

Functions.

$y = f(x)$	1. y equals f of x 2. y is a function of x
$x = f^{-1}(y)$	1. x equals f inverse of y 2. x is an inverse function of y
D_f	domain of the function f

E_f или R_f	range of the function f
$f \circ g$	composition of the functions f and g
сложная функция	composite function
неявная функция	implicit function
график функции	graph of a function

Sequences and series. Convergence.

$\{x_n\}$	sequence x n
$\{x_n\}_{n=1}^{\infty}$	sequence x n as n goes from 1 to infinity
$\sum x_n$	series x n
$\sum\limits_{n=1}^{\infty} x_n = S$	sum of x n as n goes from 1 to infinity is equal to S
$x_n \to A$	1. x n converges to A 2. sequence x n converges to A
$x_n \underset{n\to\infty}{\to} A$	1. x n converges to A as n tends to infinity 2. x n converges to A as n goes to infinity 3. x n converges to A as n approaches infinity
$x_n \to \infty$	1. x n diverges 2. x n diverges to infinity 3. x n goes to infinity 4. x n approaches infinity
$\sum x_n = A < \infty$	series x n converges to A
$\sum x_n = \infty$	series x n diverges
$\sum x_n = \mathrm{DNE}$	1. sum of the series x n does not exist 2. series x n diverges

Limits and convergence.

$\lim\limits_{n\to\infty} x_n = A$	1. limit of x n as n tends to infinity is equal to A 2. x n converges to A as n tends to infinity
$\lim\limits_{x\to a} f(x)$	limit of f of x as x approaches a

$\lim\limits_{x \to a-0} f(x)$	limit of f of x as x approaches a from the left
$\lim\limits_{x \to a+0} f(x)$	limit of f of x as x approaches a from the right
$\lim\limits_{x \to \infty} f(x) = A$ или $f(x) \underset{x \to \infty}{\to} A$	1. limit of f of x as x approaches infinity is equal to A 2. limit of f of x as x goes to infinity is equal to A 3. f of x approaches A as x goes to infinity 4. f of x converges to A as x goes to infinity
$\lim\limits_{x \to a} f(x) = \text{DNE}$	limit of f of x as x approaches a does not exist

Derivatives.

f'	1. f prime; 2. derivative of f
f''	1. f double prime; 2. second derivative of f
f'''	1. f triple prime; 2. third derivative of f
$f^{(n)}$	1. n-th derivative of f 2. derivative of f of the order n
f'_x	1. f prime x 2. derivative of f with respect to x
Δx	1. delta x; 2. increment of x
dx	1. d x; 2. differential ot x
$\frac{df}{dx}$	1. d f by d x 2. derivative of f with respect to x
$\frac{d^2 f}{dx^2}$	1. d two f by d x squared 2. second derivative of f with respect to x
$\frac{\partial f}{\partial x}$	1. partial d f by d y 2. partial derivative of f with respect to y
f''_{xy} или $\frac{\partial^2 f}{\partial y \partial x}$	second partial derivative of f with respect to x and y

Integrals

$\int$	integral
$\iint$	double integral
$\iiint$	triple integral
$\int f(x)\,dx$	1. indefinite integral of f of x d x 2. general antiderivative of f of x
$\int\limits_a^b$	integral from a to b
$\int\limits_a^\infty$	(improper) integral from a to infinity
$\int\limits_\Gamma \omega$	intergral of omega over gamma

Miscellaneous notations and terms.

Δf	1. the Laplace operator of f; 2. the Laplacian of f
∇f	1. gradient of f; 2. nabla f
$\mathbf{grad}$	gradient
$\mathbf{div}$	divergence
$\mathbf{rot}$	rotor
$\mathrm{Im}\, z$	imaginary part of z
$\mathrm{Re}\, z$	real part of z
$\underset{z=a}{res}\, f(z)$	residue of f of z at z equals a
$\underset{x \in A}{min}\, f(x)$	minimum of f of x as x runs over A
$\underset{x \in A}{max}\, f(x)$	maximum of f of x as x runs over A

$\sum_{n=1}^{m} x_n$	sum of x n as n goes from 1 to m
$\sum_{\alpha \in A} x_\alpha$	sum of x alpha as alpha runs over A
$\prod_{t>0} x_t$	product of x t as t is positive

5. **Greek alphabet.**

Α,α	alpha	Ν,ν	nu
Β,β	beta	Ξ,ξ	xi
Γ,γ	gamma	Ο,ο	omicron
Δ,δ	delta	Π,π	pi
Ε,ε	epsilon	Ρ,ρ	rho
Ζ,ζ	zeta	Σ,σ	sigma
Η,η	eta	Τ,τ	tau
Θ,θ	theta	Υ,υ	upsilon
Ι,ι	iota	Φ,φ	phi
Κ,κ	Kappa	Χ,χ	chi
Λ,λ	lambda	Ψ,ψ	psi
Μ,μ	Mu	Ω,ω	omega